

December 1967

Special Technical Report 43

046-469
AD
**ELECTRIC CONSTANTS MEASURED IN VEGETATION
AND IN EARTH AT FIVE SITES IN THAILAND**

Prepared for:

U.S. ARMY ELECTRONICS COMMAND
FORT MONMOUTH, NEW JERSEY 07703

CONTRACT DA 36-039 AMC-00040(E)
ORDER NO. 5384-PM-63-91

By: H. W. PARKER WITHAN MAKARABHIROMYA

SRI Project 4240

Distribution of this document is unlimited.

Approved: E. L. YOUNKER, TECHNICAL DIRECTOR
MRDC Electronics Laboratory, Bangkok

W. R. VINCENT, MANAGER
Communication Laboratory

D. R. SCHEUCH, EXECUTIVE DIRECTOR
Electronics and Radio Sciences

Sponsored by

ADVANCED RESEARCH PROJECTS AGENCY
ARPA ORDER 371
FOR THE
THAI-U.S. MILITARY RESEARCH AND DEVELOPMENT CENTER
SUPREME COMMAND HEADQUARTERS
BANGKOK, THAILAND

ABSTRACT

Balanced two-conductor open transmission line probes were used to measure effective electric constants in vegetation and in the earth. Effective relative permittivity, ϵ_r , and permeability, μ_r , in undergrowth at five dispersed sites were practically unity. The ranges of variation in all results were $0.9 < \epsilon_r < 1.2$ and $0.8 < \mu_r < 1.1$. On the average, ϵ_r was about 1.05, μ_r was about 0.98. Median effective conductivity of the undergrowth varied insignificantly between sites, but showed distinctive variation with frequency, from about $20 \pm 30\%$ at 6 MHz to $300 \pm 30\%$ ($\mu\text{mho/m}$) at 100 MHz. In the few instances where measurements were made among mature trees the results were similar to those obtained for undergrowth.

The most important parameters influencing vegetation constants were stem spacing (related to stem number density) and intrinsic stem conductivity (estimated to be between 0.05 and 0.5 mho/m).

Ground-constant values varied greatly between sites, in a manner consistent with the variation of soil moisture content.

Environmental forestry and soil surveys, summarized in the appendices to this report, are useful in explaining or applying the electric-constant results.

PREFACE

The work described in this report was performed with the support, and using the facilities, of the Military Research and Development Center (MRDC) in Bangkok, Thailand. The MRDC is a joint Thai-U.S. organization established to conduct research and development work in the tropical environment. The overall direction of the U.S. portion of the MRDC has been assigned to the Advanced Research Projects Agency (ARPA) of the U.S. Department of Defense who, in 1962, asked the U.S. Army Electronics Command (USAECOM) and the Stanford Research Institute (SRI) to establish an electronics laboratory in Thailand to facilitate the study of radio communications in the tropics and related topics. The MRDC-Electronics Laboratory (MRDC-EL) began operation in 1963 [under Contract DA 36-039 AMC-00040(E)], and since that time ARPA has actively monitored and directed the efforts of USAECOM and SRI. In Bangkok, this function is carried out by the ARPA Research and Development Field Unit (RDFU-T). The cooperation of the Thai Ministry of Defense and the Thailand and CONUS representatives of ARPA and USAECOM made possible the work presented in this report.

CONTENTS

ABSTRACT.	iii
PREFACE	v
LIST OF ILLUSTRATIONS	ix
LIST OF TABLES.	xiii
ACKNOWLEDGMENTS	xv
I INTRODUCTION	1
A. Background.	1
B. Objectives.	2
II TECHNIQUES USED.	5
A. Theoretical Background.	5
B. Experimental Techniques	7
C. Analytical Procedures	15
D. Environmental Surveys	19
III FIELD MEASUREMENTS	21
A. Muen Chit Results	21
B. Pak Chong Results	27
C. Laem Chabang Results.	33
D. Satun Results	37
E. Chumphon Results.	38
IV DISCUSSION OF RESULTS.	55
A. Applicability of Vegetation-Constant Results.	55
B. Generalized Results	68
RECOMMENDATIONS	77
Appendix A--BIODENSITY EXPERIMENTS.	81
Appendix B--ENVIRONMENTAL SURVEYS	91

Appendix C--ENVIRONMENTAL DESCRIPTION FOR CHUMPHON.	103
Appendix D--ENVIRONMENTAL DESCRIPTION FOR PAK CHONG	119
Appendix E--ENVIRONMENTAL DESCRIPTION FOR LAEM CHABANG. . . .	129
Appendix F--ENVIRONMENTAL DESCRIPTION FOR KUAN KARLONG FOREST IN SATUN.	133
Appendix G--ENVIRONMENTAL DESCRIPTION FOR MUEN CHIT	145
Appendix H--THE OWL COMPUTER PROGRAM.	161
REFERENCES	173
DISTRIBUTION LIST	177

DD Form 1473

ILLUSTRATIONS

Frontispiece	SRI Magnetic-Equator Site near Chumphon (aerial photo).	xvi
Fig. 1	Sites where Vegetation and Earth Electric Constants were Measured	3
Fig. 2	Small Brass-Rod Probe for Earth Measurement	8
Fig. 3	Large Earth Probe for Approximate Technique Only.	9
Fig. 4	Small Earth Probe with Variable Spacing	11
Fig. 5	Small Brass-Tubing Probe for Vegetation Measurements	12
Fig. 6	Large Aluminum-Pipe Probe for Vegetation Measurements.	13
Fig. 7	Large Copper-Wire Probe for Vegetation Measurements	14
Fig. 8	SRI Antenna/Environment Study Site near Muen Chit	22
Fig. 9	Comparison of Vegetation Constants Measured in Three Samples at Muen Chit Site	25
Fig. 10	Comparison of Vegetation Constants Measured in Muen Chit Undergrowth in Different Seasons.	26
Fig. 11	Ground Constants Measured in Forest at Muen Chit Site.	28
Fig. 12	Jansky & Bailey Forest Radio Propagation Study Site near Pak Chong.	29
Fig. 13	Undergrowth Vegetation Constants Measured at Pak Chong Site.	31
Fig. 14	Surface Ground Constants Measured in Forest at Pak Chong Site.	32
Fig. 15	SRI Coastal Brush Radio Propagation Study Site near Laem Chabang	34
Fig. 16	Vegetation Constants Measured at Laem Chabang Site.	35
Fig. 17	Ground Constants Measured at Laem Chabang Site.	36

Fig. 18	Jansky & Bailey Forest Radio Propagation Study Site near Satun.	39
Fig. 19	Undergrowth Vegetation Constants Measured at Satun Site	40
Fig. 20	Surface Ground Constants Measured in Forest at Satun Site.	41
Fig. 21	SRI Antenna/Environment Study Site near Chumphon .	43
Fig. 22	Comparison of Wire Probe and Pipe Probe Results for Tree Boles at Chumphon Sample CIII	44
Fig. 23	Comparison of Undergrowth Vegetation Constants Measured by Two Techniques in Chumphon Sample CII.	46
Fig. 24	Height Profile Results ϵ_r and δ Measured among Trees of Chumphon Sample CV.	48
Fig. 25	Height Profile Results σ and α Measured among Trees of Chumphon Sample CV.	49
Fig. 26	Surface Ground Constants Measured at Chumphon Site	51
Fig. 27	Ground Constants ϵ_r and δ Measured at Several Depths near Chumphon Sample CII.	52
Fig. 28	Ground Conductivity Measured at Several Depths near Chumphon Sample CII	53
Fig. 29	Distribution of Relative Permittivities Measured in Undergrowth at Satun.	57
Fig. 30	Distribution of Conductivities Measured in Undergrowth at Satun	58
Fig. 31	Comparison of ϵ_r and σ Distributions in Gaussian Coordinates.	60
Fig. 32	Distribution of Typical ω_p Results Obtained with Small Probe in Undergrowth at 15 MHz	65
Fig. 33	Comparison of Median ϵ_r and δ Measured in Undergrowth at Five Sites.	67
Fig. 34	Comparison of Median σ and α Measured in Undergrowth at Five Sites.	71
Fig. 35	Median Surface Ground Permittivity Measured at Six Places in Thailand	75

Fig. 36	Median Surface Ground Conductivity Measured at Six Places in Thailand	76
Fig. A-1	Results of Biodensity Experiment Performed on Freshly Cut Undergrowth of Muen Chit Sample MII. .	84
Fig. B-1	Sample Description Spaces for Nearest-Neighbor-Distance Probability Model	96
Fig. B-2	Inverse Cumulative Distribution of Nearest-Neighbor Distances for Undergrowth Sample CII. . .	101
Fig. C-1	Height Distribution for All Trees Surveyed at Chumphon Site.	106
Fig. C-2	Diameter Distribution for All Trees Surveyed at Chumphon Site.	107
Fig. C-3	NND Distribution for All Trees Surveyed at Chumphon Site.	108
Fig. C-4	Height Distribution for Trees in Chumphon Sample CV	109
Fig. C-5	Diameter Distribution for Trees in Chumphon Sample CV.	110
Fig. C-6	NND Distribution for Trees in Chumphon Sample CV .	111
Fig. C-7	Height Distribution for All Plants in Undergrowth Sample CII	112
Fig. C-8	Diameter Distribution for All Plants in Undergrowth Sample CII	113
Fig. C-9	NND Distribution for All Plants in Undergrowth Sample CII	114
Fig. D-1	Height Distribution for All Trees Surveyed at Pak Chong Site	122
Fig. D-2	Diameter Distribution for All Trees Surveyed at Pak Chong Site	123
Fig. D-3	NND Distribution for All Trees Surveyed at Pak Chong Site	124
Fig. D-4	Height Distribution for All Plants in Undergrowth Sample PI.	125
Fig. D-5	Diameter Distribution for All Plants in Undergrowth Sample PI.	126

Fig. D-6	NND Distribution for All Plants in Undergrowth Sample PI.	127
Fig. F-1	Height Distribution for All Trees Surveyed at Satun Site	137
Fig. F-2	Diameter Distribution for All Trees Surveyed at Satun Site	138
Fig. F-3	NND Distribution for All Trees Surveyed at Satun Site	139
Fig. F-4	Height Distribution for All Plants in Undergrowth Sample SI.	140
Fig. F-5	Diameter Distribution for All Plants in Undergrowth Sample SI.	141
Fig. F-6	NND Distribution for All Plants in Undergrowth Sample SI	142
Fig. G-1	Height Distribution for All Trees Surveyed at Muen Chit Site	148
Fig. G-2	Diameter Distribution for All Trees Surveyed at Muen Chit Site	149
Fig. G-3	NND Distribution for All Trees Surveyed at Muen Chit Site	150
Fig. G-4	Height Distribution for All Plants in Undergrowth Sample MII	152
Fig. G-5	Diameter Distribution for All Plants in Undergrowth Sample MII	153
Fig. G-6	NND Distribution for All Plants in Undergrowth Sample MII	154
Fig. H-1	Flow Diagram for Program I	164
Fig. H-2	Flow Diagram for Program II	171

TABLES

Table I	HF Electrical Constants for Samples CIII and CV . . .	47
Table II	Confidence-Interval Estimators for Samples Taken from a Rayleigh Distribution, for Several Confidence Levels, P	63
Table III	Experimental Limits for ϵ_r and μ_r	69
Table IV	Ranges of σ and δ Measured among Trees and Undergrowth at HF	72
Table A-1	Data for Derivation of Intrinsic Conductivity of Vegetation at 50 MHz Estimated Using Weight of Cut Undergrowth	86
Table A-2	Data for Derivation of Intrinsic Conductivity of Vegetation at 50 MHz Estimated Using Only Geometry. .	88
Table C-1	Chumphon Soil Summary--Open Terrain	115
Table C-2	Chumphon Soil Summary--Inside Forest.	116
Table D-1	Soil Summary for Pak Chong Forest near Korat	128
Table E-1	Soil Summary for Vegetated Area near Laem Chabang .	132
Table F-1	Satun Soil Summary.	143
Table G-1	Soil Summary for Muen Chit Forest near Chonburi. . .	155
Table H-1	Input Program I	165
Table H-2	Output of Program I/Input Program II.	167
Table H-3	Output of Program II.	168
Table H-4	Equations in Program I.	169
Table H-5	Equations in Program II	170

ACKNOWLEDGMENTS

The authors wish to acknowledge the cooperation of, and arrangements made by, personnel of the Jansky & Bailey Division of Atlantic Research Corporation regarding our field trips to their sites. We express our appreciation for the use of the environmental descriptions for the sites, which were taken (where available) from survey work done by the MRDC Environmental Sciences Division in concert with the Thai Forestry Department. In particular, we have Donald G. Neal and David V. Vanek, both formerly of MRDC, to thank for the statistical evaluation of vegetation growth characteristics, a subject that, though once far removed from radio engineering, has loomed larger each time we have thought of mathematically modeling the radio environment presented by a forest.



D-4240-1870

FRONTISPIECE SRI MAGNETIC-EQUATOR SITE NEAR CHUMPHON (aerial photo)

I INTRODUCTION

A. Background

The obstacle of jungle vegetation, so obvious to the eye, severely attenuates radio signals. Hence, with the growing needs for radio communication in the tropics, the radio scientist becomes increasingly interested in the effects of tropical forests on radio wave propagation. This special technical report describes part of a continuing investigation of the electromagnetic characteristics and effects of dense forest vegetation begun by Herbstreit and Crichlow^{1*} in Panama during World War II, revived during the Malayan and Indochinese conflicts of the nineteen-fifties² and currently being carried further by Stanford Research Institute (SRI) for the U.S. Advanced Research Projects Agency (ARPA) under its SEACORE program.

The ultimate goal of our vegetation work has been to lay the basis of workable models for radio systems in the tropical environment. Forestry surveys provide distributions of the geometric factors needed for modeling. But since no source of reliable information on electromagnetic factors was known in 1964, SRI developed a probe for measuring the effective complex dielectric constant of living vegetation. This extension of the idea published by Kirkscether³ from ground-constant to vegetation-constant measurement was done at the suggestion of John Taylor, University of South Carolina, and George Hagn, SRI, who postulated that the vegetation would disturb the fields of an open-wire transmission line in a way not unlike that of a homogeneous medium, at least at frequencies below some cutoff frequency. It now appears that that cutoff frequency is above 100 MHz⁴ for dense growth.

The usefulness of these vegetation-constant data has been demonstrated by Sachs,⁵ Sachs and Wyatt,⁶ and Tamir,⁷ who have used initial results in their respective models for predicting the gross variation with

* References are listed at the end of the report.

distance of power in radio waves propagating through dense forest. The earth beneath the forest is of second-order significance in the Sachs/Wyatt model, and entirely neglected by Tamir, but those workers were not including effects of antenna efficiency in their models.

The model for patterns of simple antennas in forests developed by Taylor for SRI⁸ does require that the complex dielectric constant of the earth beneath the forest be known, as well as the variation of complex dielectric constant with height in the vegetation. Further, at low frequency, it requires knowledge of any near-surface layering that exists in the earth. Thus, to complement our vegetation work, we have been taking ground-constant measurements with the probe,⁹ as suggested by Kirkscether,³ and making geophysical resistivity soundings at dc whenever possible at our field sites. Further, the MRDC Environmental Sciences teams have made soil analyses at our sites to supplement our electrical measurements.

B. Objectives

The original purpose of the field work described in the following sections was to provide input information for Taylor's antenna pattern forest model.⁸ At Muen Chit, the Xeledop transmitter,^{10,11,12} was towed in its airborne mode, to measure full-scale antenna patterns¹³ of simple field-type structures erected in clear and forest areas. The results of these measurements can be predicted using Taylor's model and our environmental description, so that the model may be tested and refined.

After the first field trip was planned, to Muen Chit (field-site locations in Thailand are marked on the map, Fig. 1), Sachs and Wyatt⁶ completed a model for propagation in forest (since modified by Tamir⁷). We decided to provide data for testing these models as well as Taylor's. Accordingly, since Sachs and Tamir had used results of Jansky & Bailey¹⁴ (J&B) measurements of path loss to test their models, we decided to include the J & B sites near Pak Chong, and, later Satun, in our field survey of vegetation constants. We also hoped, since the mathematical models approximate a forest by a layered dielectric slab, to take data appropriate to checking them in a truly slab-like environment--the hedgerow of coastal

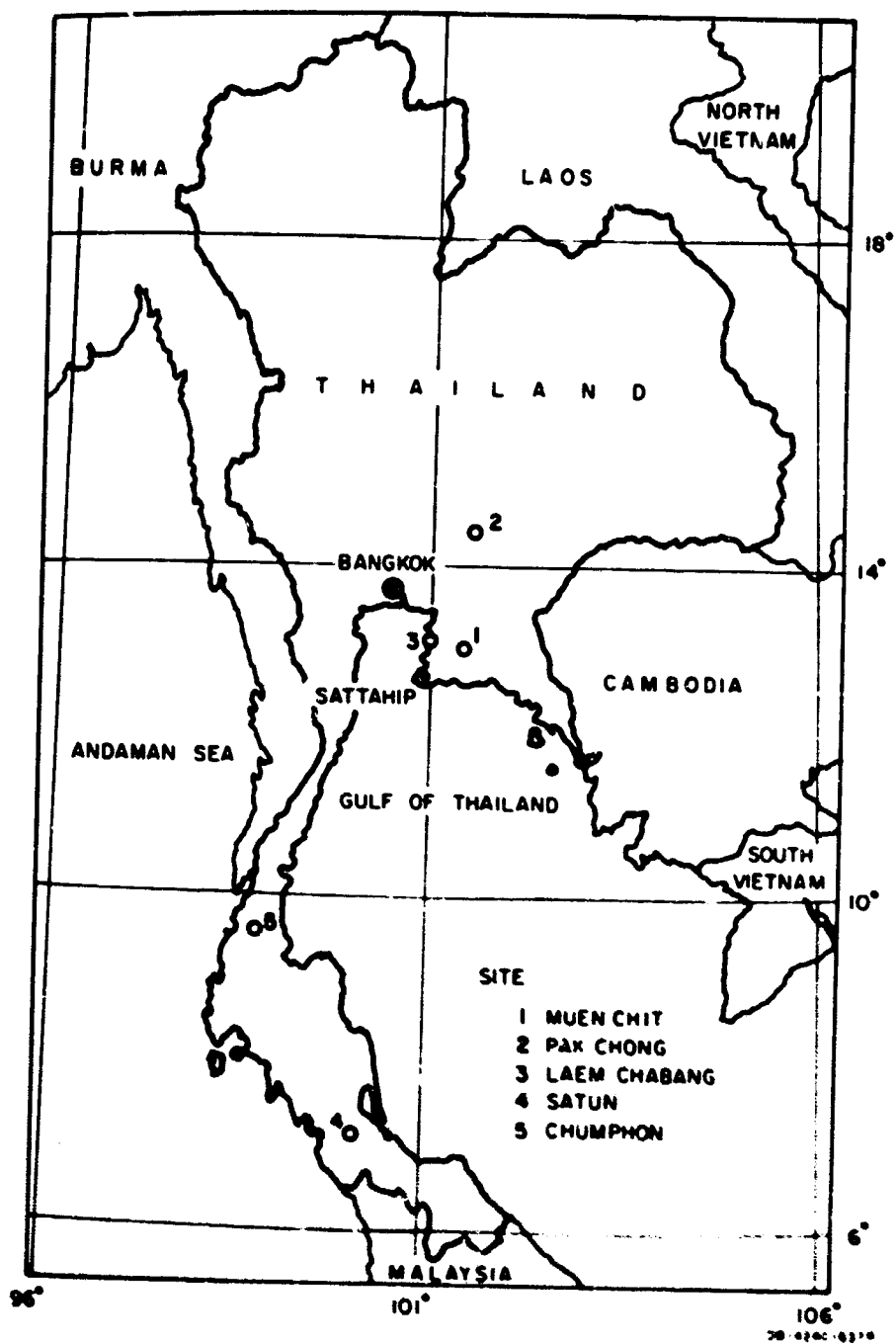


FIG 1 SITES WHERE VEGETATION AND EARTH ELECTRIC CONSTANTS WERE MEASURED

brush near our low-noise site on the beach at Laem Chabang. Data had already been obtained on the variation of signal with distance in the coastal brush,¹⁵ using the Xeledop transmitter carried on a man's back. It should now be possible to use the complete environmental description given in the present report, together with the Sachs/Wyatt model, to predict the results obtained when the Manpack Xeledop was carried through the coastal brush while transmitting a constant signal back to receivers on the beach. A similar test was made using the manpack Xeledop at the Muen Chit site, where the growth was much more irregular; prediction of those Xeledop near range results, using the environmental descriptions given here, should be convincing proof of the usefulness of the Sachs/Wyatt model.

Aside from the direct use of the information contained herein to allow theoretical modeling for radio-propagation studies and antenna studies,¹⁶ and providing data for radio-system design requirements,¹⁷ we hope that the environmental researcher will gain an insight from our work that will allow him to better orient his work toward the requirements of radio physics, for the interface between the botanical and radio sciences is yet a fuzzy one. This area of botanical physics must now be described scientifically; and one important potential use of the techniques (and models) discussed here is the study of plants themselves.

II TECHNIQUES USED

A. Theoretical Background

The probe technique for obtaining the complex dielectric constant in vegetation or earth depends on measurement of the input impedance of a balanced two-conductor open-wire transmission line (OWL) inserted in the test medium.⁴ If the medium is vegetation, the terminal end of the probe can be shorted, and if the impedance measurements are repeated in air for the same conductor spacing, the dielectric permittivity, conductivity, and magnetic permeability of the vegetation, relative to those of air, may be calculated as discussed below.

Symbols used in the equations are:

Z_{oc} = Complex input impedance with OWL termination open

Z_{sc} = Complex input impedance with OWL termination shorted

Γ = Complex propagation constant for TEM waves* on the OWL

Z_o = Complex characteristic impedance of the OWL

ϵ_r = Relative dielectric permittivity of the sample medium

μ_r = Relative magnetic permeability of sample medium

δ = Loss tangent of sample medium

σ = Conductivity of sample medium, mho meter

α = Attenuation rate in sample medium, Neper meter.

f = Radian wave frequency

L = Length of OWL, meters.

First, we find the characteristic impedance of the OWL:

$$Z_o = (Z_{oc} Z_{sc})^{1/2} \quad (1)$$

* The entire development is based on the assumption that the inevitable longitudinal E component of the electromagnetic field is negligibly small.

Next, the propagation constant:

$$\Gamma = \frac{1}{L} \operatorname{arctanh} \frac{Z_o}{Z_{oc}} \text{ or } \Gamma = \frac{1}{L} \operatorname{arctanh} \frac{Z_{sc}}{Z_o} \quad (2)$$

and, using primes to denote air-related symbols,* we can develop

$$\epsilon_r = \frac{\omega'}{\omega} \operatorname{Im} \left\{ \Gamma / Z_o \right\} \div \operatorname{Im} \left\{ \Gamma' / Z_o' \right\} \quad (3)$$

$$\delta = \cot [\operatorname{ARG} \Gamma / Z_o] \quad (4)$$

$$\mu_r = \frac{\omega'}{\omega} \operatorname{Im} \left\{ Z_o \Gamma \right\} \div \operatorname{Im} \left\{ Z_o' \Gamma' \right\} \quad (5)$$

$$\sigma = \omega \epsilon_o \epsilon_r \delta \quad (6)$$

$$\epsilon_o = 8.8542 \times 10^{-12} \text{ Farad/meter}$$

$$\alpha = \frac{\pi}{c} \left[\frac{\mu_r \epsilon_r}{2} (\sqrt{1 + \delta^2} - 1) \right]^{1/2} \quad (7)$$

where c is the velocity of light in vacuum. If $\delta \leq 0.5$ we can approximate

$$\alpha \approx 60 \pi (\mu_r \epsilon_r)^{1/2}$$

It is inconvenient to short the OWL termination when the probe is used in earth, so we obtain the characteristic impedance, not from open and shorted impedance measurements, but from two measurements made with

* Often, a slightly different measurement frequency was used in air (e.g., resonating the system at slightly different ambient temperatures).

different probe lengths.³ If the input impedances Z_1 and Z_2 are measured for the probe lengths L and $2L$, respectively, then we have:

$$Z_o = [Z_1(2Z_2 - Z_1)]^{1/2} \quad (8)$$

and the remainder of the computation can follow Eqs. (2) through (7) if one replaces Z_{oc} by Z_1 . Usually, the permeability μ_r , Eq. (5), is assumed equal to unity.

When $\Gamma L \ll 1$, at low frequency and/or short probe length, the OWL acts as a capacitor, and we can write simple approximations to some of the above expressions. Assuming $\mu_r = 1$, we find that so long as $\Gamma L \ll 1$, we need only measure Z_1 and Z_1' to obtain the electrical constants:

$$\epsilon_r \approx \frac{C}{C'} = \frac{\omega'}{\omega} \left| \frac{Z_1'}{Z_1} \right| \frac{\sin \text{ARG } Z_1}{\sin \text{ARG } Z_1'} \quad (9)$$

$$\delta \approx -\cot [\text{ARG } Z_1] = 1/Q \quad (10)$$

Here, C is the value of the equivalent capacitor and Q is its energy storage/loss ratio. The remaining constants may be found by substitution of the results of Eqs. (9) and (10) in (6) and (7). This approximate technique is the simplest for earth measurement work in situ, and we have used it with confidence below 6 MHz.

B. Experimental Techniques

In obtaining measurements by the OWL technique, Kirkseither³ sacrificed some accuracy by using an unbalanced connection to a General Radio 915-A RF bridge at frequencies up to 10 MHz. The error introduced in ground constants measured in this way is probably not serious if the approximate technique can be used (i.e., assuming the probe is a

³ Or Z_{oc} and Z_{oc}' ; but this variation of the technique is not useful in foliage at frequencies above perhaps 0.5 MHz. We have used it only in measuring ground constants.

capacitor); but we have used balanced connections through coaxial transmission-line baluns* to a GR 1606-A RF bridge at 6 MHz and above, shifting to the GR 1602-B admittance meter at VHF. We have also used the Boonton 250A RX meter, and HP 803A VHF bridge, but they are not as versatile for our purpose.

The contact potentials set up between the probe and earth should be negligible at RF, as Kirkscether has indicated.³ But we have checked this effect by reinserting a probe sprayed with insulation on several occasions, and were unable to detect any significant change in its impedance.

The first versions of the OWL earth probe are shown in Fig. 2. They are made of brass rods spaced 2.5 cm apart for VHF and 5 cm apart for HF, respectively, by a rigid dielectric wafer. Each set consists of

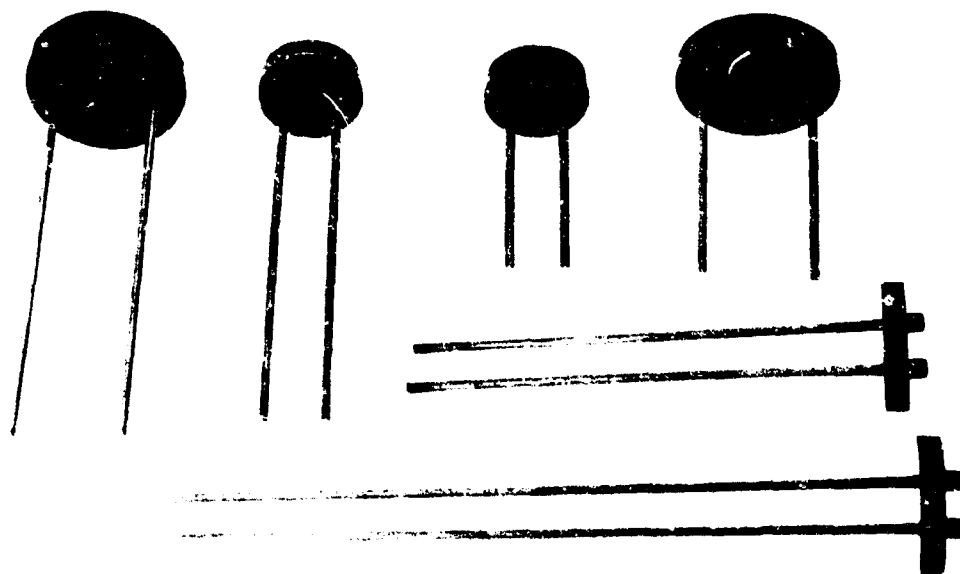


FIG. 2 SMALL BRASS-ROD PROBE FOR EARTH MEASUREMENTS

* Balanced-to-unbalanced transformers.

two such probes, one twice the length of the other. These are 10 and 20 cm long. They have been used at frequencies from 6 to 25 (HF set) and 50 to 200 MHz. Their spacing is not variable. The rods are usually inserted into holes drilled with a wood bit.

Another earth probe, used only for measurement by the approximate method (see Sec. II-A) is shown in Fig. 3. It is made of two large (1.6-cm-diameter) brass rods one meter long, tapped at one end for connection to the impedance bridge leads. No spacer is used, since the approximate technique does not require measurement of characteristic impedance. This probe, used at low HF or MF, is inserted into two holes punched with a steel spike. Their spacing is then measured so the probe can be hung at that spacing in air for control measurement. The bridge connection is usually made unbalanced (e.g., without the use of an external balun).

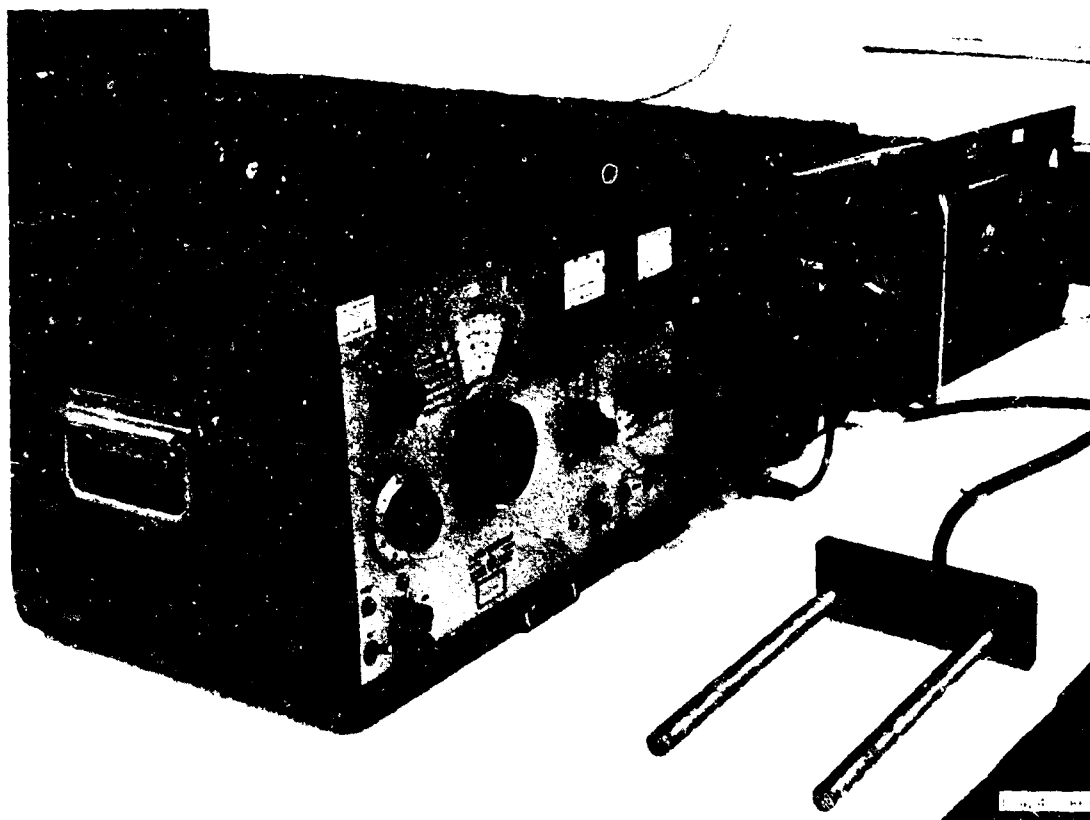


FIG. 3 LARGE EARTH PROBE FOR APPROXIMATE TECHNIQUE ONLY

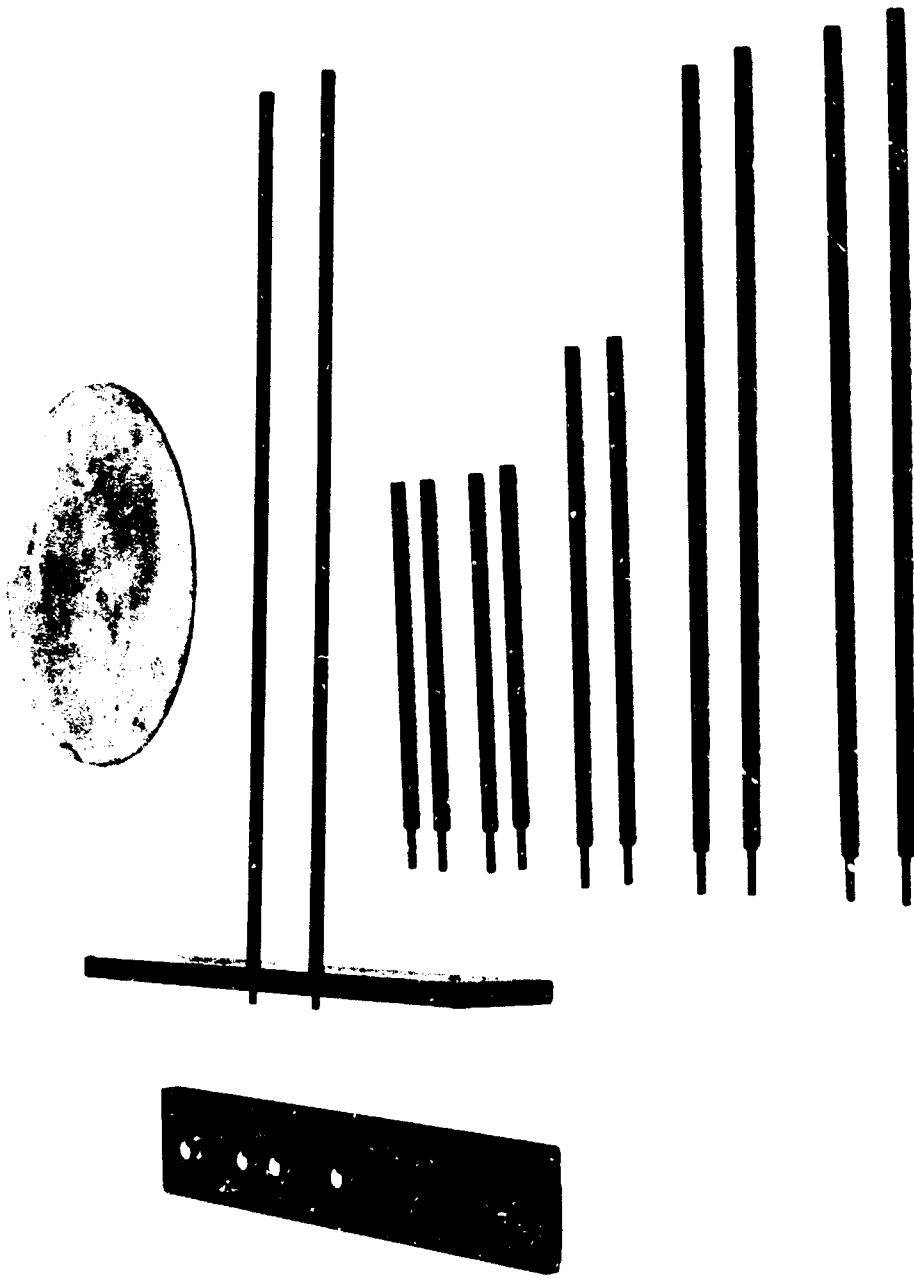
The earth probe shown in Fig. 4 is a refinement of the first one, allowing variable spacing. It has been used at HF and VHF. Varying the spacing allows us to adapt our impedance-measuring capabilities to various types of earth over a wide frequency range.

The small vegetation probe shown in Fig. 5 is made of 1.6-cm-diameter brass tubing plated with silver. These tubes can be connected in sets 1 meter long to form a probe of any desired length up to 6.5 meters, since the terminal section is designed like a trombone slide. The spacers that support the tubing allow a choice of conductor spacing--7.6, 15.2, or 22.9 cm. We use a 38-cm-diameter aluminum disc when shorting the probe termination. This probe has been found satisfactory for balanced measurements in dense vegetation at frequencies between 6 and 100 MHz.

The large vegetation probe shown in Fig. 6 is made of 10-cm-diameter aluminum drainage pipe coated to inhibit corrosion. It may be assembled in lengths up to 30.5 meters from 6.1-meter sections fitted with friction joints. Since the conductors are supported on poles, their spacing could be varied at the expense of some effort, but we have always set them one meter apart. We have chosen operating frequencies between 3 to 30 MHz for which this probe is nearly an odd integral number of eighth wavelengths long, and we have cut coaxial baluns accordingly. We use a bar made of the aluminum drainage pipe when shorting the probe termination.

The latest OWL probe innovation is shown in Fig. 7. We string number 12 copper wire between two posts or trees and use it in the same way we would use the aluminum pipe, except that the short termination is made with a clip lead. We were able to do this successfully at 6, 12.5, and 15 MHz with a 2-meter conductor spacing and wire lengths up to 31.5 meters. The wire lengths are chosen to make the probe approximately an odd integral number of eighth wavelengths long at the three operating frequencies.

Of the OWL probe configurations shown in Figs. 2 through 7, those allowing variability of spacing proved the most useful, because they were adaptable to both physical and electrical properties of the sample. The copper wire probe (Fig. 7) is most convenient for height-profile



1 4740-1367

FIG. 4 SMALL EARTH PROBE WITH VARIABLE SPACING

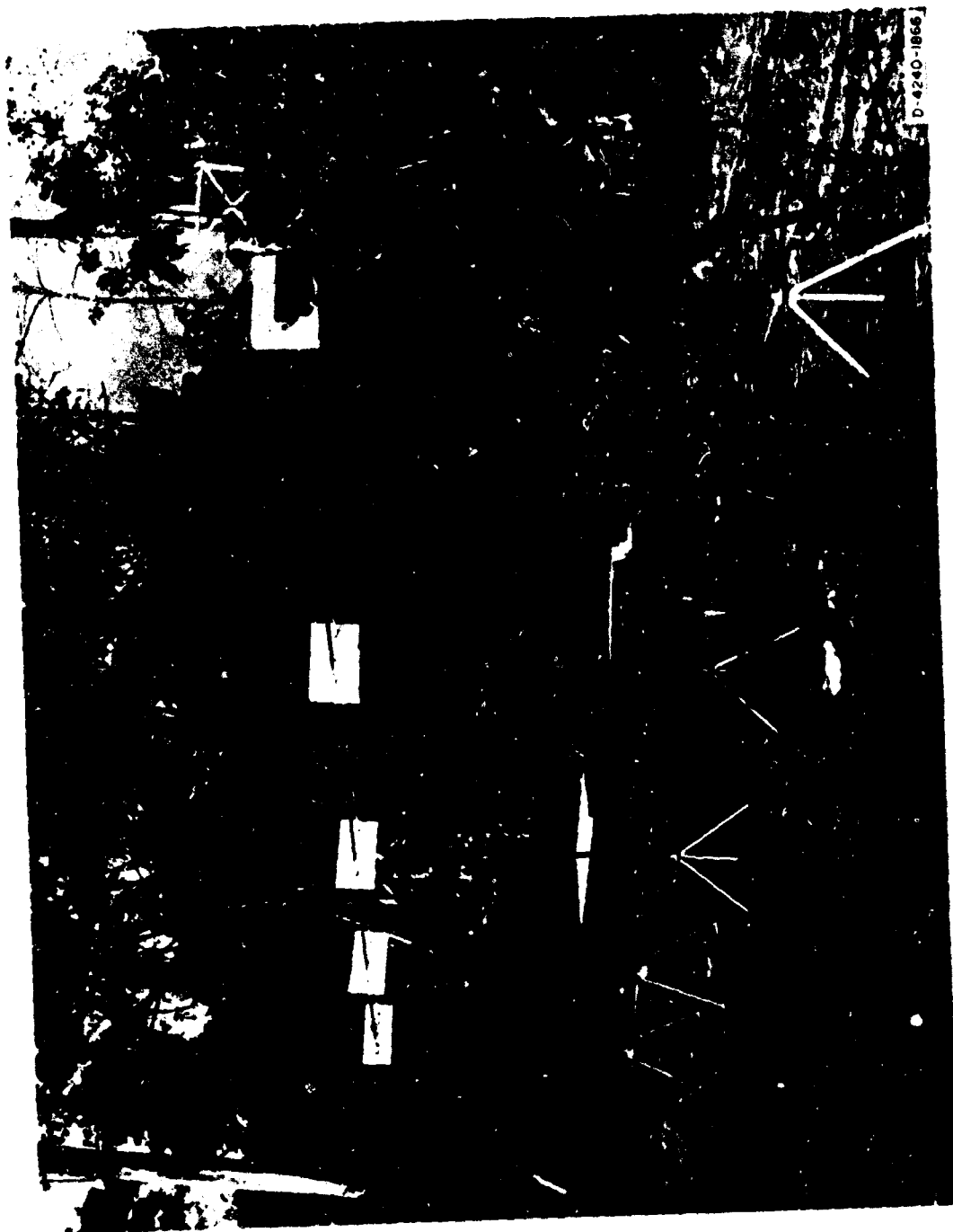


FIG. 5 SMALL BRASS-TUBING PROBE FOR VEGETATION MEASUREMENTS

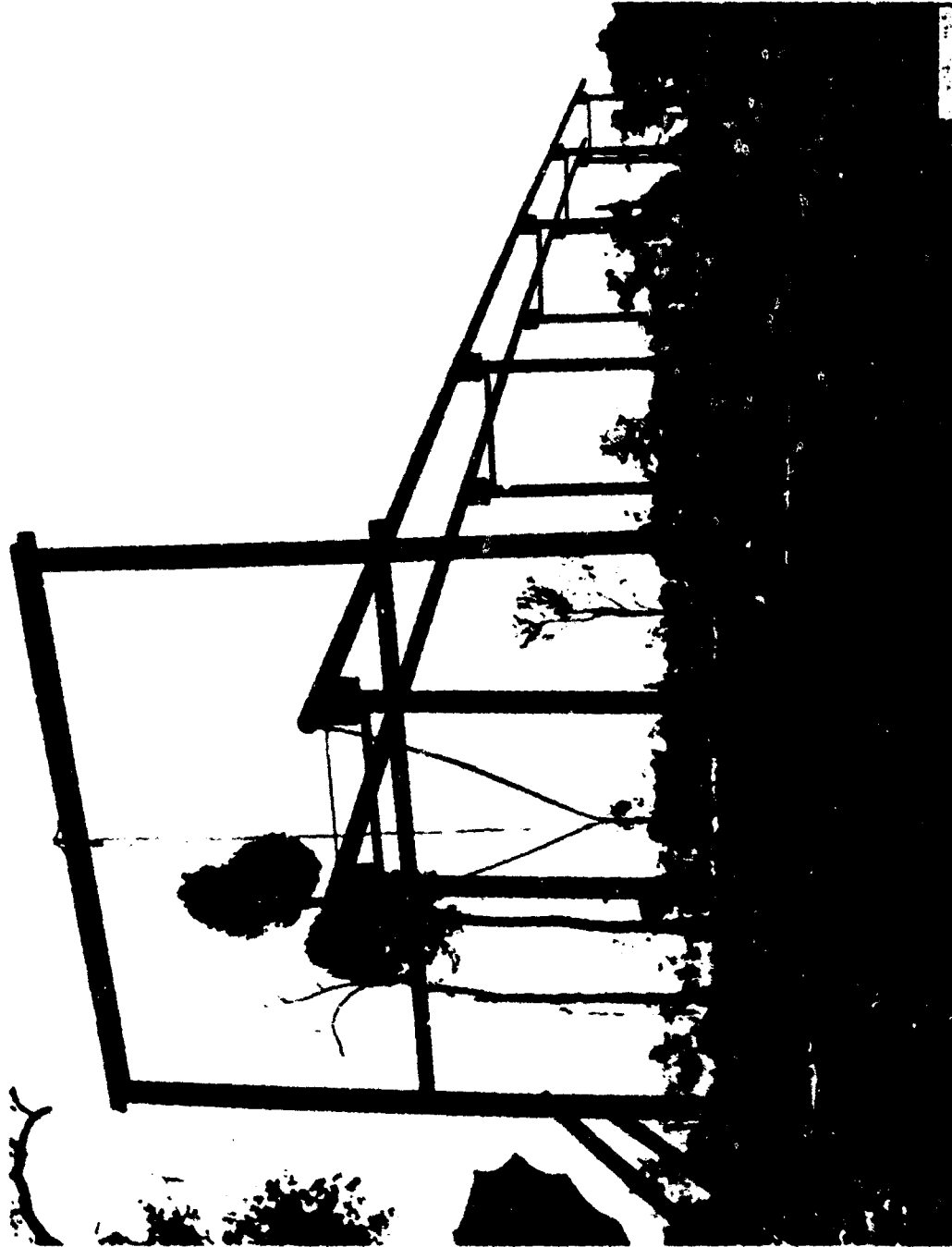


FIG. 6 LARGE ALUMINUM-PIPE PROBE FOR VEGETATION MEASUREMENTS



FIG. 7 LARGE COPPER-WIRE PROBE FOR VEGETATION MEASUREMENTS

work among trees above the undergrowth; the aluminum pipe (Fig. 6) is handy for very dense growth including trees, but the small brass vegetation probe (Fig. 5) is the easiest to use since its length is continuously variable and it can be placed in any vegetation with 3 degrees of freedom. The spacing of all three vegetation probes can be varied within reasonable limits, but only small-spacing probes are efficient at VHF. We have relied heavily on the use of the small vegetation probe, depending on a statistical sampling approach to make the values obtained with it more nearly representative of the growth in a region or forest.

When obtaining probe measurements in vegetation, we have faced the problems caused by heterogeneity in the sample by careful orientation of the probe and multiple measurement, often pairing results of measurements with the probe input and termination interchanged, or with an axial probe shift of about one-quarter wavelength to help overcome the effect of heterogeneity of the sample along the probe's long axis. Even so, a large number of single measurements is required to describe a sample of vegetation, and we usually mark off the vegetation into stations in a matrix pattern, and try to base our statistics on at least 20 measurements per sample per frequency.

We now have computer programs for transforming bridge readings to OWL input impedance, and then calculating all the constants and listing results in tabular form. From these, clerks plotted (on standardized graph paper) the medians and quartiles of the measurement value distributions, from which the figures were drawn. However, we have continued to spot-check by sliderule calculation in the field.

C. Analytical Procedures

A large quantity of raw electric-constant data was collected from the forest sites in different parts of Thailand. These data were obtained as impedances of open-wire transmission-line probes inserted in vegetation, ground, and air. Some results were computed by sliderule in the field,

* The air measurements were used as a control to which the sample measurements were normalized, assuming ϵ_r for air = 1.00 and σ for air = 0.

and rough analysis was made to give guidance for the field crew. Then all field data were sent to Bangkok for processing. The IBM 1620 computer at the Thai Land Department or the IBM 360 at the National Statistical Organization was used to work out the data, several thousand problem sets in total.

The field data were grouped according to site, type of sample, operating frequency, probe dimension, and measured station. They were encoded in computer format on punch cards. Before running the computer, the data had to be sorted to relate the sample medium and the air (control) data at each probe dimension, frequency, length, and experimental condition or time period.

The computer program consists of two parts, called Program I and Program II. The field data were entered in the appropriate format of Program I for computing the open and short-circuit impedances of the vegetation probes or the open impedance at lengths L and $2L$ for the ground probes. Computer Program I transforms the raw data from four types of impedance measurements [parallel, series, polar, and inverse (admittance) bridges] to obtain the impedances as they appear at the input of the probe. It also computes Z_0 and Phase Constant β from either of two measurement techniques: open-short-ended probe or Kirkscether's L , $2L$ method (Sec. II-A). The outputs of Program I are listed, and punched into file cards. The file-card outputs from Program I, grouped as to corresponding sample and control (air) results, are the input data for Computer Program II. The flow diagrams for both programs are given in Appendix H.

The separation of Programs I and II allows one to check the experimental data, especially to see whether the approximate method should be used in computing ground constants. Also, extra measurements were often taken in each probe position, since it is not feasible to pick up the best value from raw data. The quantity of data is so great that the sliderule cannot keep pace. The Program I output listing was studied for reasonable results according to the criteria, that, for a probe in an effectively homogeneous dielectric medium, $Z_0 < Z_0'$ and

$\text{ARG } Z_o > \text{ARG } Z_o'$.^{*} Thus, the possibility of obtaining $\epsilon_r < 1.0$ was avoided in the results.

These criteria are explained by the following argument taken from Ref. 4.

In terms of its distributed resistance R , conductance g , capacitance C , and inductance l , the characteristic impedance of the probe is

$$Z_o = \left[\frac{R + j\omega l}{g + j\omega C} \right]^{1/2} \quad (11)$$

If the probe was placed in a lossless medium such as air,

$$\epsilon_r \approx 1.0$$

$$g \approx 0$$

$$R \approx 0$$

$$l = l'$$

$$C = C'$$

and

$$Z_o' = (l' C')^{1/2} \quad (12)$$

When the probe is placed in a lossy medium such as foliage, having effective permittivity ϵ_r and effective conductivity σ , then

* Here again, the primes denote air-related quantities.

It now appears that, for vegetation, $Z_o < Z_o'$ hence $\epsilon_r < 1.0$, may be a valid result, since the conducting stems might occasionally form a phase-advancing lens (see Sec. IV-A). The criterion for $\epsilon_r < 1.0$ was applied for all results shown in this report except those in Fig. 21. We have discontinued its use at HF but do not find that the inclusion of $\epsilon_r < 1.0$ would significantly change our results.

$$C = \epsilon_r C'$$

$$g = \frac{\sigma C'}{\epsilon_0}$$

so that

$$Z_0 \approx \left[\frac{\omega \epsilon_0 l' (\omega \epsilon + j\sigma)}{C' (\omega^2 \epsilon^2 + \sigma^2)} \right]^{1/2} \quad (13)$$

where $\epsilon = \epsilon_r \epsilon_0$. Since $\delta = \sigma/\omega\epsilon$, we can simplify, using Eq. (12), to:

$$Z_0 \approx Z'_0 \left(\frac{1 + j\delta \frac{1}{\epsilon_r}}{1 + \delta^2 \frac{1}{\epsilon_r}} \right)^{1/2} \quad (14)$$

Then,

$$\left| \frac{Z_0}{Z'_0} \right| \approx \left(\epsilon_r \sqrt{1 + \delta^2} \right)^{-1/2} \quad (15)$$

and we see that $|Z_0| < |Z'_0|$ unless δ is small and ϵ_r is less than 1.0. Further, from Eq. (14), we can develop, using complex algebra

$$\text{ARG } Z_0 - \text{ARG } Z'_0 \approx 1/2 \text{ Arctan } \delta \quad (16)$$

from which it follows that for any lossy dielectric,

$$\text{ARG } Z_0 > \text{ARG } Z'_0 \quad (17)$$

For ground constant results at low frequency the lossy-capacitor approach (see Sec. II-A) may be valid.* This can be judged from the

* Often, it is the more reliable, since, when Z_1 and Z_2 in Eq. (8) are both large, errors in the impedance measurements greatly influence the value of Z_0 from which the ground constants are obtained by Kirkcether's L, ZL method.

negative arguments of the input impedances of the open-ended probe in ground at lengths L and $2L$. If the arguments of those two impedances were nearly equal, the approximation formula was applied to compute the ϵ_r , σ , and δ from the single-input impedance data by sliderule (assuming μ_r is unity).

The impedance data not subjected to approximation or rejection were entered in Computer Program II for computing the electrical parameters such as the relative permittivity (ϵ_r), the conductivity (σ), the relative permeability (μ_r), the loss tangent (δ), the attenuation constant (α), the phase constant (β), and the propagation constant (γ) of the medium. Since, by use of Eqs. (3) through (7), any of the desired parameters of a lossy dielectric medium can be found from knowledge of ϵ_r , σ , and μ_r , we choose to publish only those used directly in the current propagation models. These are ϵ_r and σ (Sachs/Wyatt/Tamir) and ϵ_r and δ (Taylor). We continue to assume $\mu_r = 1.0$, since the models do so, although there is justification for making it a variable, as we shall see from Sec. IV-A.

D. Environmental Surveys

The work of the Military Research and Development Center's Environmental Sciences Division (MRDC-ES) in forestry surveying and soil analysis has been supplementary to our own. At the sites where we made electromagnetic measurements of vegetation and ground constants (except Laem Chabang), MRDC-ES survey teams helped choose special volumes of undergrowth foliage that seemed representative of an area or were at least representative of natural growth. The survey teams took descriptions, counts, and measurements of height and diameter at some reference height and nearest-neighbor distance (NND), of all trees, vines, and shrubs within these volumes. These special volumes were then marked off into matrix stations, and the vegetation constants were measured with the small probe. In two instances, at Muen Chit and Chumphon, the entire volume of foliage was then cut down and weighed for biodensity studies (see Appendix A).

In addition to the special volumes, the MRDC-ES surveyed several standard 10-by-40 meter forest plots at each of our sites, which they have described in full^{*}--from species names to cumulative distributions of growth parameters--for all trees having breast-height diameter (DBH) greater than 5 cm. They also tabulated soil data, analyzed by MRDC-ES and Southeast Asia Treaty Organization (SEATO) laboratories. Excerpts from these environmental descriptions are given in Appendices C (Chumphon), D (Pak Chong), E (Laem Chabang), F (Satun), and G (Muen Chit). Methods involved in forest surveying are given in Appendix B.

^{*}Except Laem Chabang.

III FIELD MEASUREMENTS

A. Muen Chit Results

An SRI search for an alternate forest area similar to that used by Jansky & Bailey near Pak Chong located a forest near the village (ban) of Muen Chit, about 25 km southeast of Chon Buri, in the province of the same name. There, in conjunction with airborne and manpack Xeledop experiments, we began our first foliage measurement series in Thailand. Figure 8 is a map of the test area and its surroundings showing the locations of the OWL test plots relative to selected Xeledop receiving antennas and the MRDC-ES survey plots.

A detailed description of the site, based on the environmental survey done by the MRDC-ES, is included in Appendix G. Briefly, there were about ten square kilometers of trees, bordered on the southwest by the tapioca fields where much of the control measurement was done for the several experimental programs in progress at the site. The grove had been subject to selective logging for many years, so that the remaining older trees of the population were interspersed with second-growth members, and there was dense undergrowth everywhere, rising often as high as 7 meters, where it merged with the lower story of tree crowns. The tree-crown canopy in this dry evergreen forest was often three-storied. Then the upper story, quite discontinuous, grew between 25 and 34 meters high. The middle story, containing more species, grew from 15 to 24 meters high. The lowest story was of young trees that had attained heights between 6 and 14 meters. In many places, especially the areas bordering the tapioca field,* the forest canopy was two-storied. Here, the upper story lay between 15 and 30 meters, the lower between 6 and 15. Vertical projection of the canopy system for all the 10-by-40-meter plots surveyed would cover only 67 percent of the total plot area.

* Where VHF antennas for the Xeledop experiments were set up.

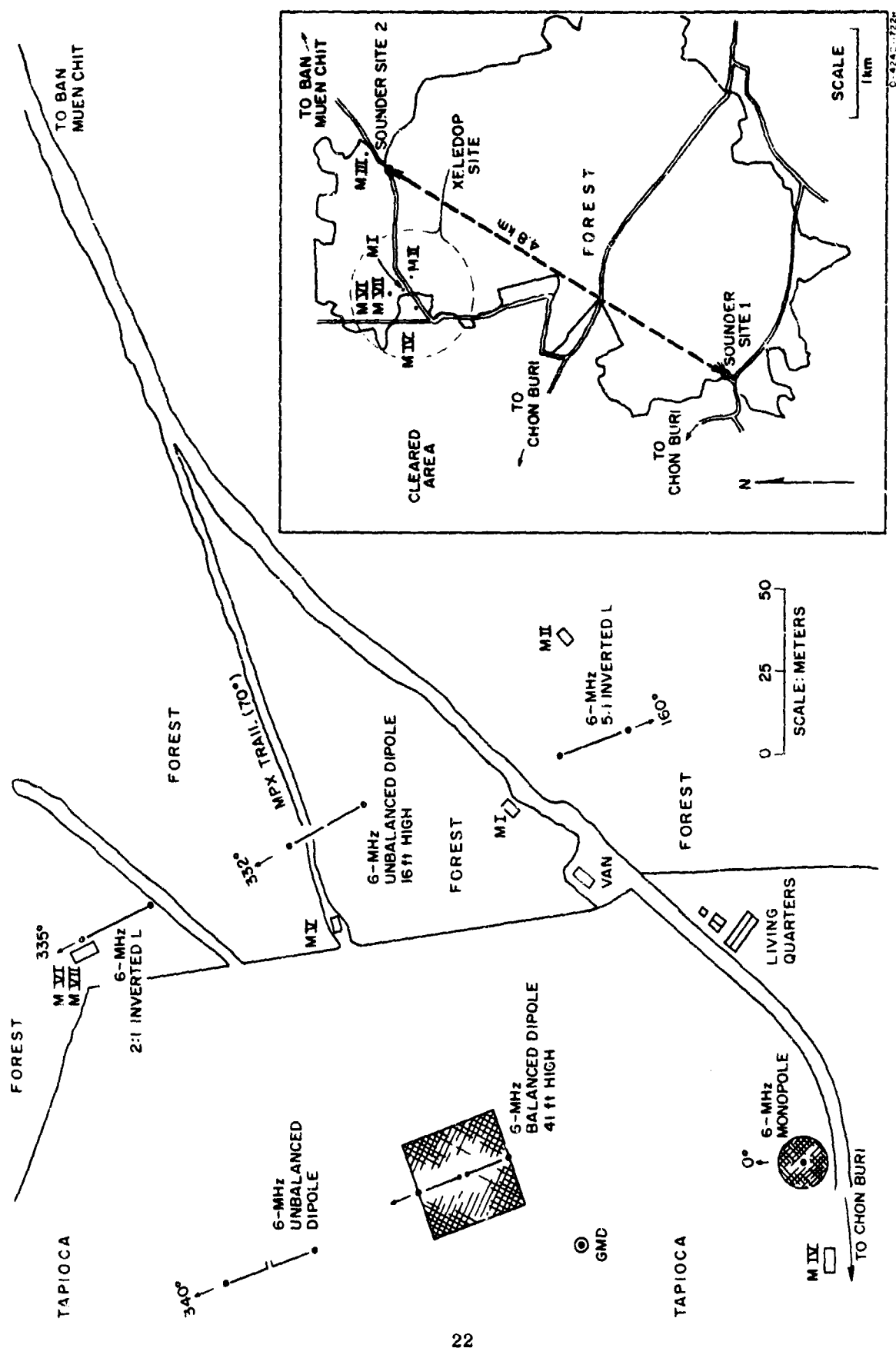


FIG. 8 SRI ANTENNA/ENVIRONMENT STUDY SITE NEAR MUEN CHIT

We chose four experimental areas for the measurement of vegetation electrical constants during our first visit to the site in June of 1966. These areas are marked on Fig. 8 as Samples MI, MII, MIII, and MIV. Sample MI was a dense undergrowth along a forest trail, where we perfected our measurement techniques. We used the small vegetation probe there, translating its position in a regular pattern. Sample MII was selected (with the help of MRDC-ES personnel) to be typical of undisturbed undergrowth in that forest area. It was found deep in a thicket, all of which was later cleared save the sample itself,* a volume on a 3-meter-square base, and about 3 meters maximum height, the "cube" thus formed being marked off with nylon cord into stations 0.6 meter apart in a matrix pattern for convenient measurements with the small vegetation probe. We inserted the probe from two sides and from the top "face" of Sample MII, hoping to obtain a statistical measurement population sufficient to describe the vegetation despite its heterogeneous growth habit.

We picked Sample MIII in the canopy of a small tree of the lowest story, inserting the small probe at random about a point 7 meters above ground. Here, we tried to orient the probe so that the vegetation near the conductors was symmetrical about their long axis, but the presence of limbs larger than the probe hampered successful measurement, and we decided that another type of probe would be required for use in canopy foliage. The number of results that appeared to reflect Sample MIII as a "homogeneous medium"† was not great enough to represent the lowest-story canopy well. We may estimate $\epsilon_r \approx 1.02$, $\sigma \approx 10 \mu\text{mho/meter}$, and $\delta \approx 0.01$ at HF for the canopy, but cannot place high confidence in these values.

*The entire sample was cut, following these electric measurements, and packed in a hopper containing the small vegetation probe, whence the variations of its electric constants and weight were measured for several days. This biodensity experiment is reported in Appendix A.

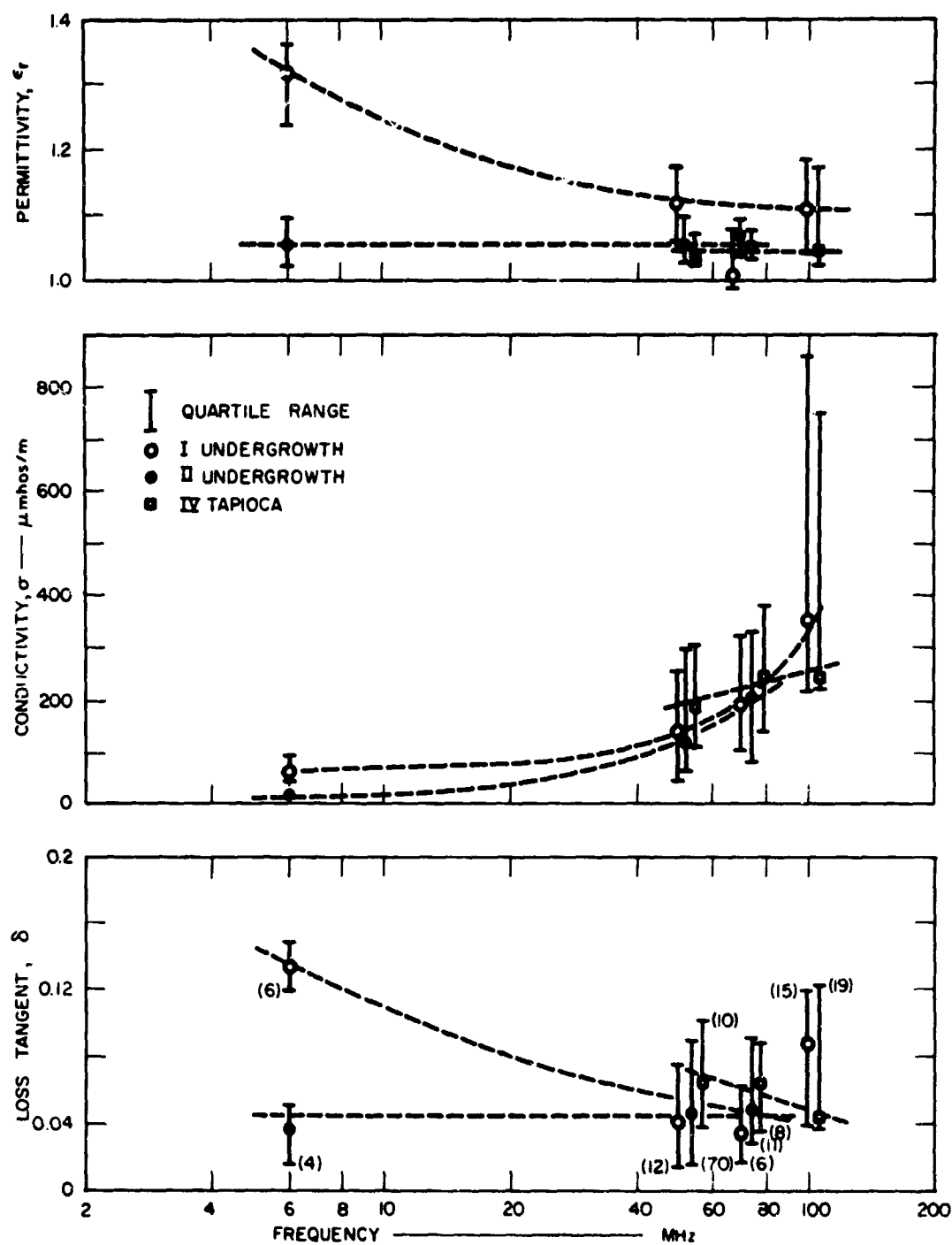
†The presence of a few large limbs in the volume sensed by the small-scale probe often unbalanced it seriously, causing an impossible-looking effective electric constant to result.

Sample MIV was in a volume containing tapioca plants. These plants in the "open" field southwest of the forest, negligible in April when the antenna pattern measurements began, grew up to about 4.5 meters by mid-July, so that we feared they might be affecting some of the antenna-pattern control measurements.

The results from Samples MI, MII, and MIV are compared in the graphs of Fig. 9, where medians and quartile bounds (including half the population of values) obtained for effective ϵ_r , δ , and σ are plotted as functions of frequency. The dashed curves are the result of attempting to fit, by eye, a monotonic function of frequency to the data. The population sizes for each frequency are shown in parentheses near the loss-tangent values. Where the populations had fewer than five members, we used the entire population range instead of its quartile bounds. The undergrowth of Sample MI was visibly the most dense, and we are not surprised to find that the volume containing it had higher effective σ than that of undergrowth MII, or the sparsely-grown tapioca of Sample MIV. But the similarities apparent between the electric constants of Samples MII and MIV would not seem probable to the observer who based his guess on visual appearances of the growth.

Six months after we began our field work at the Much Chit site, we revisited that site in order to obtain vegetation constants with the large aluminum-pipe probe in dense undergrowth (Sample MVI) similar to that of Sample MII. We also wished to compare results obtained with that probe to the distributions of values measured with the small vegetation probe in the same volume, which we called Sample MVII.* This comparison of December 1966 results is shown in the graphs of Fig. 10, where we also show lumped results from Samples MI and MII, labeled June 1966. Notice that there was usually a factor of 2 difference between the results obtained with the large and small probes, and that there was also a difference between June and December results. The

* Although a sample area MV is indicated on Fig. 8, no data were obtained there. Samples MVI and MVII were near, but not within MRDC-ES survey plot No. 391.



DB-4740-641

FIG. 9 COMPARISON OF VEGETATION CONSTANTS MEASURED IN THREE SAMPLES AT MUEN CHIT SITE

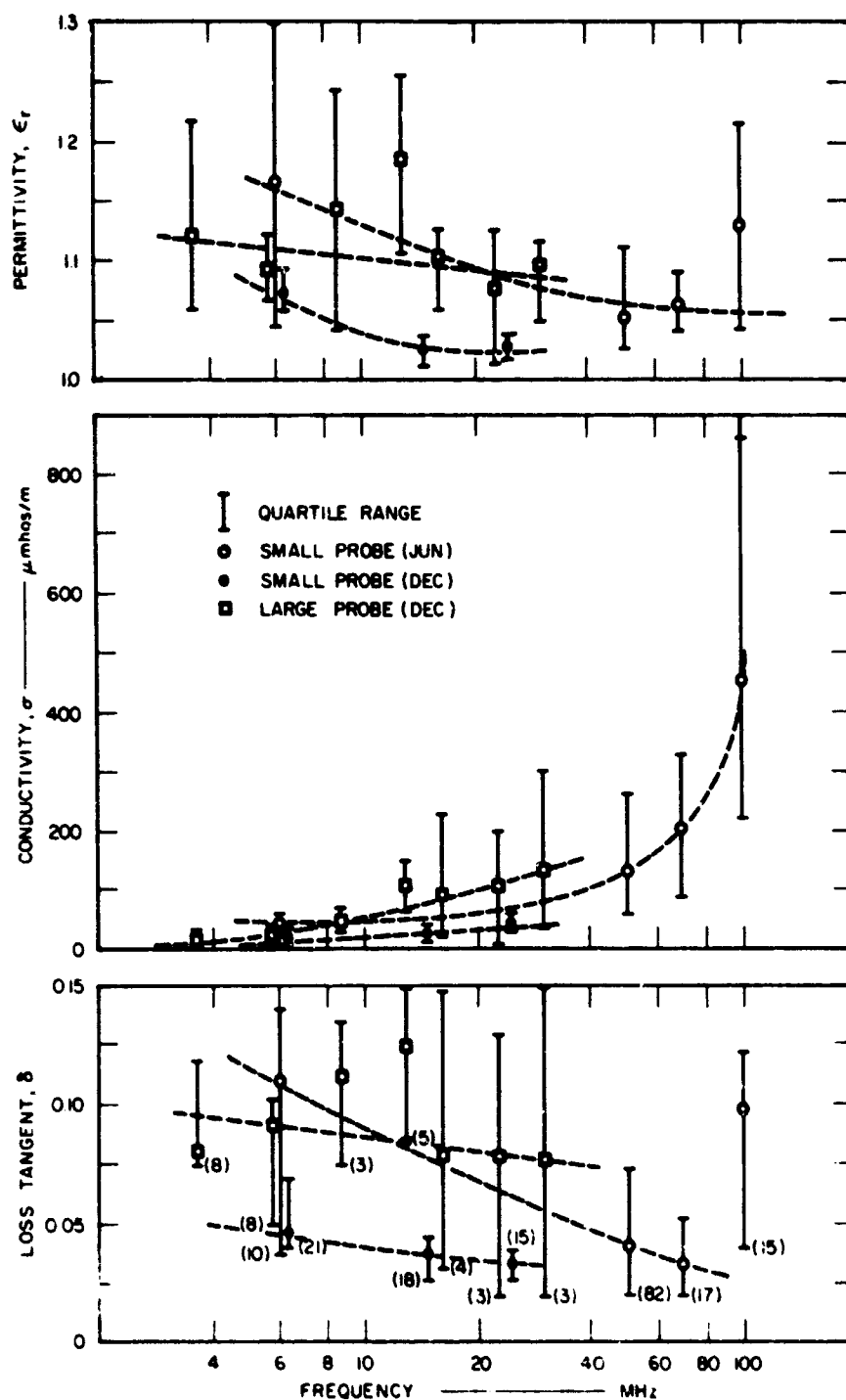


FIG. 10 COMPARISON OF VEGETATION CONSTANTS MEASURED IN MUEN CHIT UNDERGROWTH IN DIFFERENT SEASONS

latter could arise from a seasonal cause, but the tests were not well designed to show purely seasonal variation, since the June and December samples were not the same, but similar in appearance. The position of Sample MVI, marked on Fig. 8, was near that of the SRI 6-MHz inverted-L antenna, about 400 meters north of Sample MII.

We measured electric constants of the earth near Samples MI and MII in the forest. Results of these measurements are shown in Fig. 11. The RF ground constants were found not to vary with depth, at least to 2 meters.

Results of earth-resistivity measurements (dc) made in the forest along trails between Samples MI and MII give an indication of the sub-surface conductivity stratification at the site. Together with results of a soil survey done there under the direction of the MRDC-ES, they show that the earth was heterogeneous near the surface, which was mostly brown sand, having an average moisture content of about 10 percent by weight and dc conductivity of 1.7 to 3.4 mmho/meter down to about 3 meters, where a deeper stratum having higher dc conductivity (perhaps 100 mmho/m) seems to begin.

B. Pak Chong Results

The Jansky & Bailey forest site near Pak Chong is described in detail in Refs. 18 and 19, parts of which are reprinted in Appendix D. The main camp is in a large valley supporting dry evergreen forest similar in many respects to the forest at Muen Chit. Since our time at the site was very limited, we chose to measure vegetation constants with the small probe, and chose only two samples near the first J & B trail marker on Trail B, designated FP B-1. This sample spot was chosen with the help of MRDC-ES personnel, and it happened to be within MRDC-ES Plot No. 43, surveyed by the group two years before.² Other former MRDC-ES plots nearby were Nos. 44 and 82 (see Fig. 12).

The forest at this J & B site usually had its crown canopy in two stories: the lower between 1.5 and 18 meters and the upper between 6 and 41 meters. Vertical projection of all canopy cover surveyed indicates that it covered 60 percent of the ground area. This is quite similar to

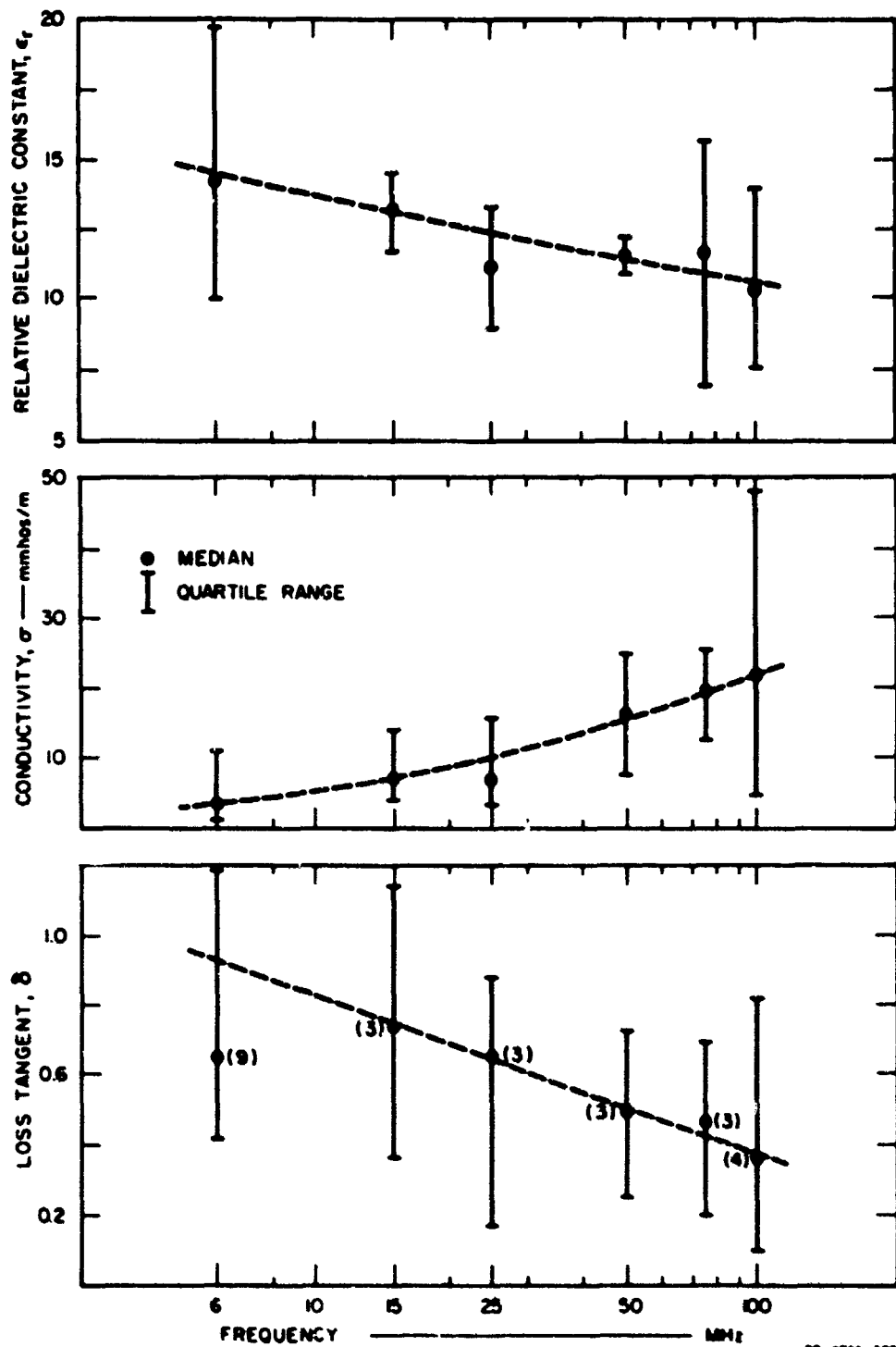


FIG. 11 GROUND CONSTANTS MEASURED IN FOREST AT MUEN CHIT SITE

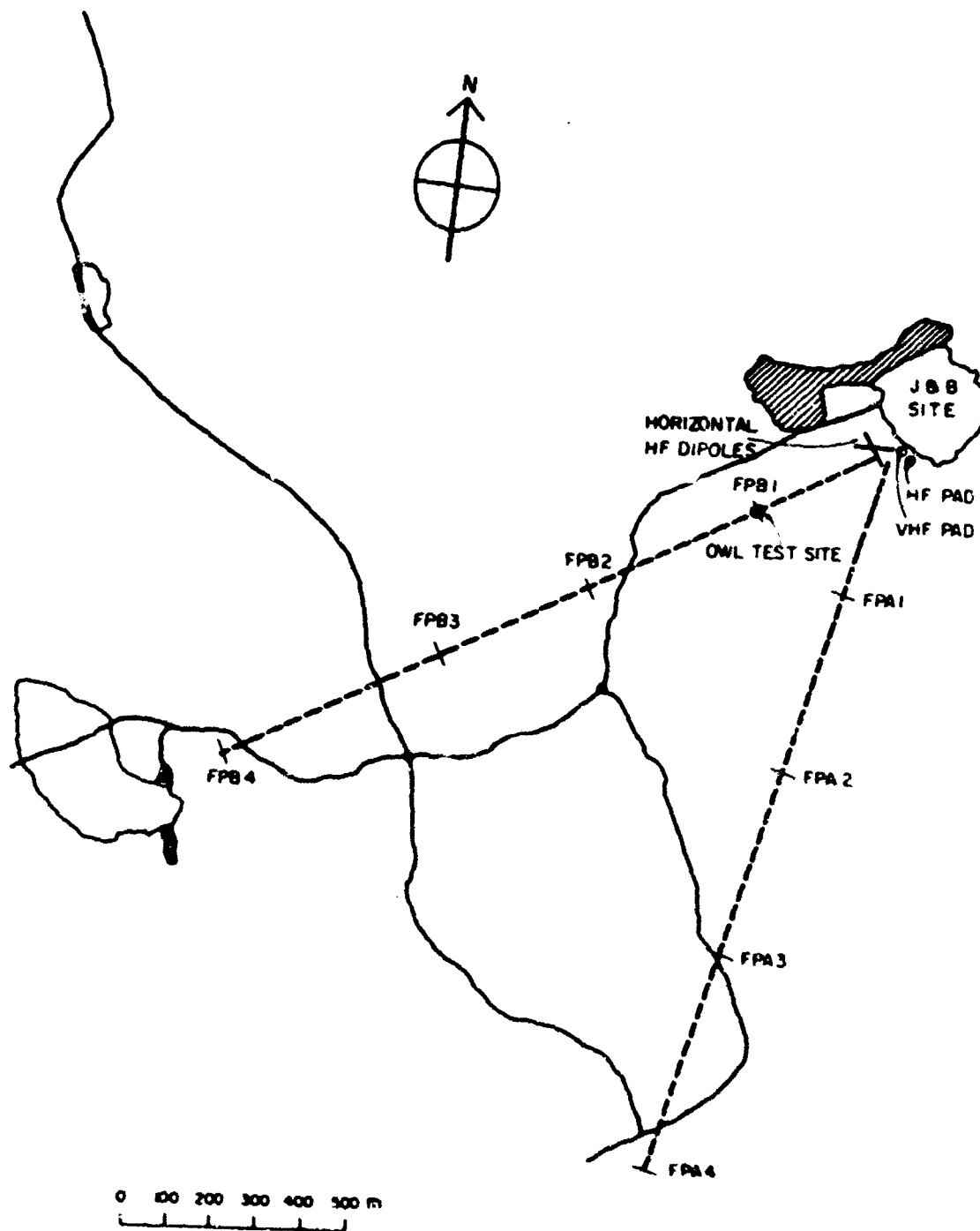


FIG 12 JANSKY & BAILEY FOREST RADIO PROPAGATION STUDY SITE NEAR
PAK CHONG

the canopy coverage estimated for the forest near Muen Chit. However, since the lower canopy at the Pak Chong site was closer to the ground, it blocked more light, and the undergrowth at this site, though dense, was not so luxuriant as that at the Muen Chit site. We were able to walk about at Pak Chong without cutting a path. As with the forest at Muen Chit, much of the Khao Yai forest at Pak Chong was secondary growth, not virgin stand.

We marked off a cubic volume (27 m^3) in the undergrowth about 20 meters from J & B fixed point marker FP B-1, using nylon cord to define stations 0.6 m apart in a cubic matrix, and called the volume of vegetation enclosed Sample PI. We inserted the small vegetation probe into this cube from two adjacent sides to obtain a distribution of the effective vegetation constants there. We then took a random distribution of similar measurements in the vegetation surrounding Sample PI, calling this distribution Sample PII. The medians and quartile bounds of the measurement populations for each sample are shown in Fig. 13. The population sizes for each frequency are shown in parentheses. If the population numbered less than 5, we used its total range instead of its quartile bounds.

We also used the probe to measure electric constants of the ground beneath Sample PI. The results, which apply for the surface only (to ≈ 30 cm depth), are given in Fig. 14. We did not check their variation with depth.

Earth resistivity measurements (at dc) were made in the open near the J & B transmitter tower for estimation of subsurface conductivity stratification at the site. Together with results of a soil survey done there under the direction of the MRDC-ES, they show that the earth conductivity decreased uniformly with depth, from a surface value of about 8 mmho/m (dc) to less than one mmho/m (dc) at 3 meters down; that the soil moisture content above a depth of one meter was between 24 and 33 percent by weight; and that the surface in the vicinity of FP B-1 was composed of either silty or sandy clay (USCS terminology) containing fragments of red stone.*

* It should be emphasized that the soil moisture content data (obtained two years before) do not seem compatible with the electrical-constant data--which indicate a soil moisture content of 5 to 10 percent.

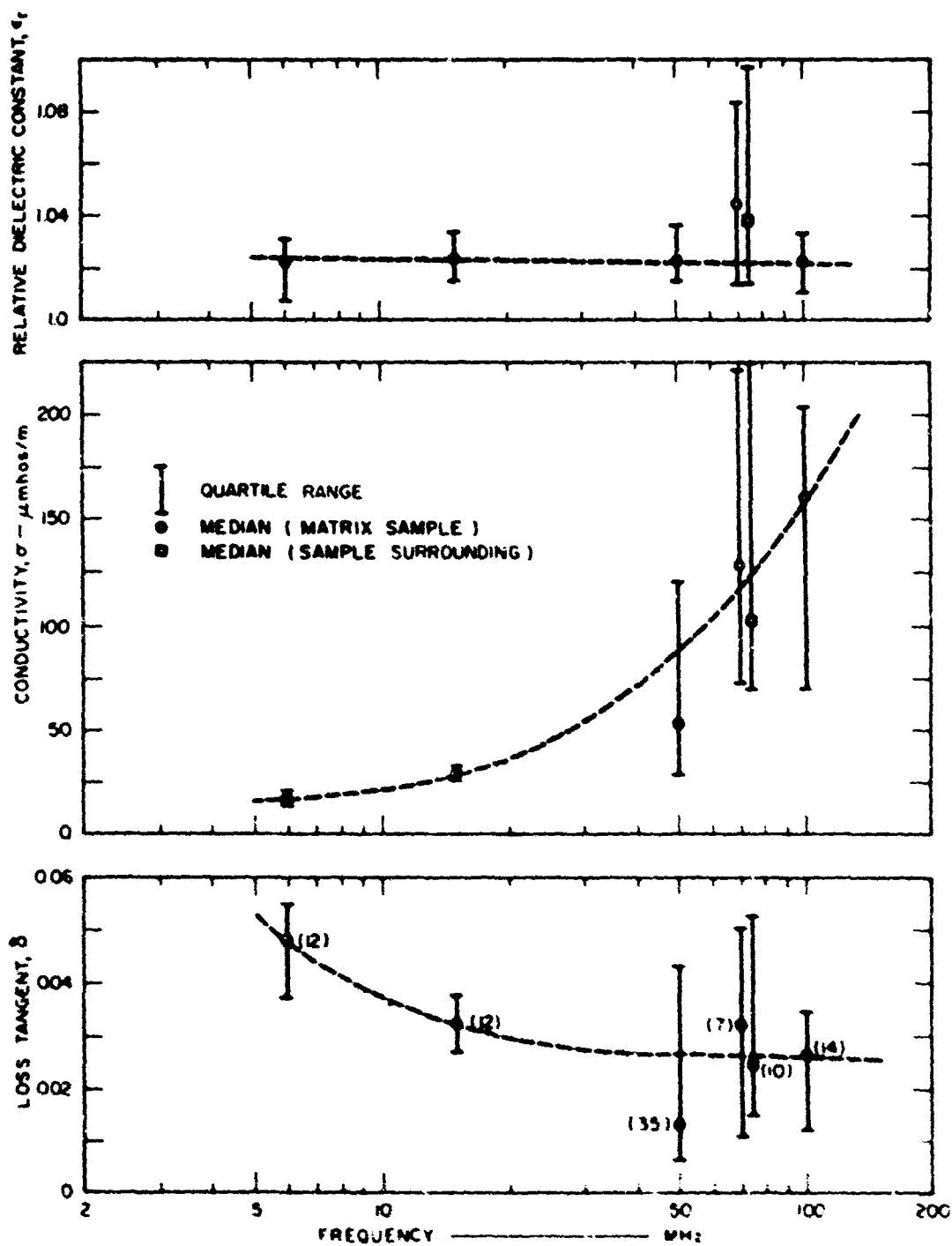


FIG 13 UNDERGROWTH VEGETATION CONSTANTS MEASURED AT PAK CHONG SITE

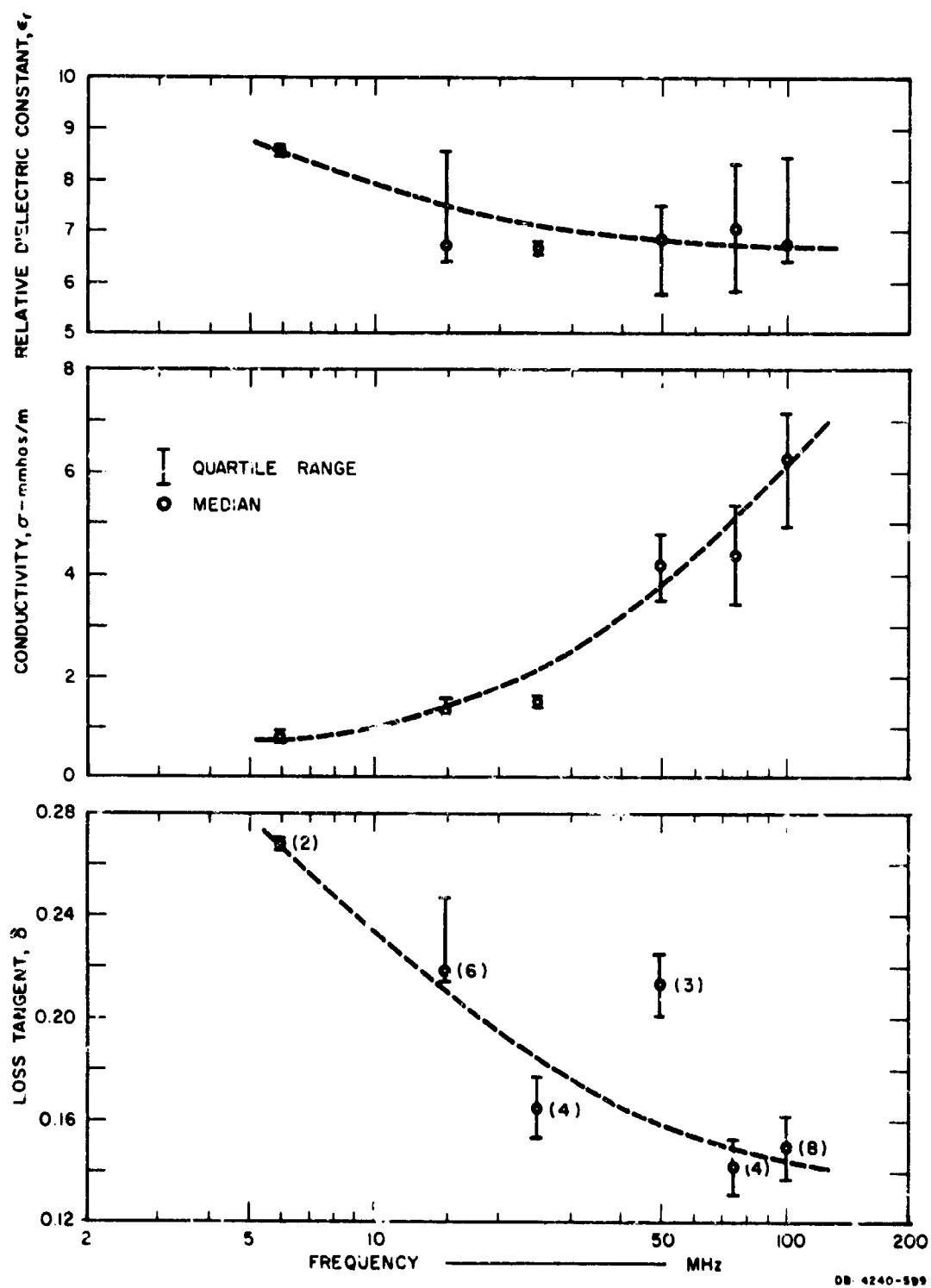


FIG 14 SURFACE GROUND CONSTANTS MEASURED IN FOREST AT PAK CHONG SITE

C. Laem Chabang Results

The coastal brush and other environment on the beach near the SRI Laem Chabang low-noise site have been described in Ref. 15 from which we have reprinted excerpts in Appendix E. True trees are scarce at that location, and none taller than 10 meters was found there. The vegetation is mostly scrub growth classified as evergreen beach forest though its composition of shrubs, bushes, climbers, and thorny herbs (including cactus) led us to call it coastal brush. This growth presents a dense tangled mass that provides poor penetration and visibility. It is quite similar to what we have called undergrowth at other sites, usually growing up to at least 2.5 meters and sometimes as much as 6. The median growth height is about 3.5 meters. The growth is quite evenly distributed, as one may see from Fig. 15.

We marked off a matrix with nylon cord in the coastal brush, at a spot near MRDC-ES Plot No. 307 and called the 27-m^3 volume enclosed Sample LII (see Fig. 15). Here, we used the small vegetation probe to obtain the distribution of electric constants whose medians and quartile bounds are graphed as a function of frequency in Fig. 16. The numbers of valid measurements comprising the populations presented for each frequency are in parentheses. Note the abscissa has a linear frequency scale. Figure 16 represents results of two slightly different measurement techniques. At 50 and 75 MHz, a GR 16023 admittance meter was used, but at 100 MHz the Boonton 250A RX-meter was used. The use of the former allows us to reduce the effect of axial inhomogeneity in the growth sample by optimizing probe length. We would have expected the 100-MHz σ results to fall near the dashed line if the admittance meter had been used at that frequency.

Similarly, the electric constants measured with the probe repeatedly inserted into the earth near Sample LII are shown in Fig. 17, compared with ground constants measured 200 meters to the west, on the open beach. (The latter site was well above the sea. It was about 50 meters from the tide line.) The near-surface soil in both places--in the brush and in the open--was classified as well-graded sand (USDA), which was mostly

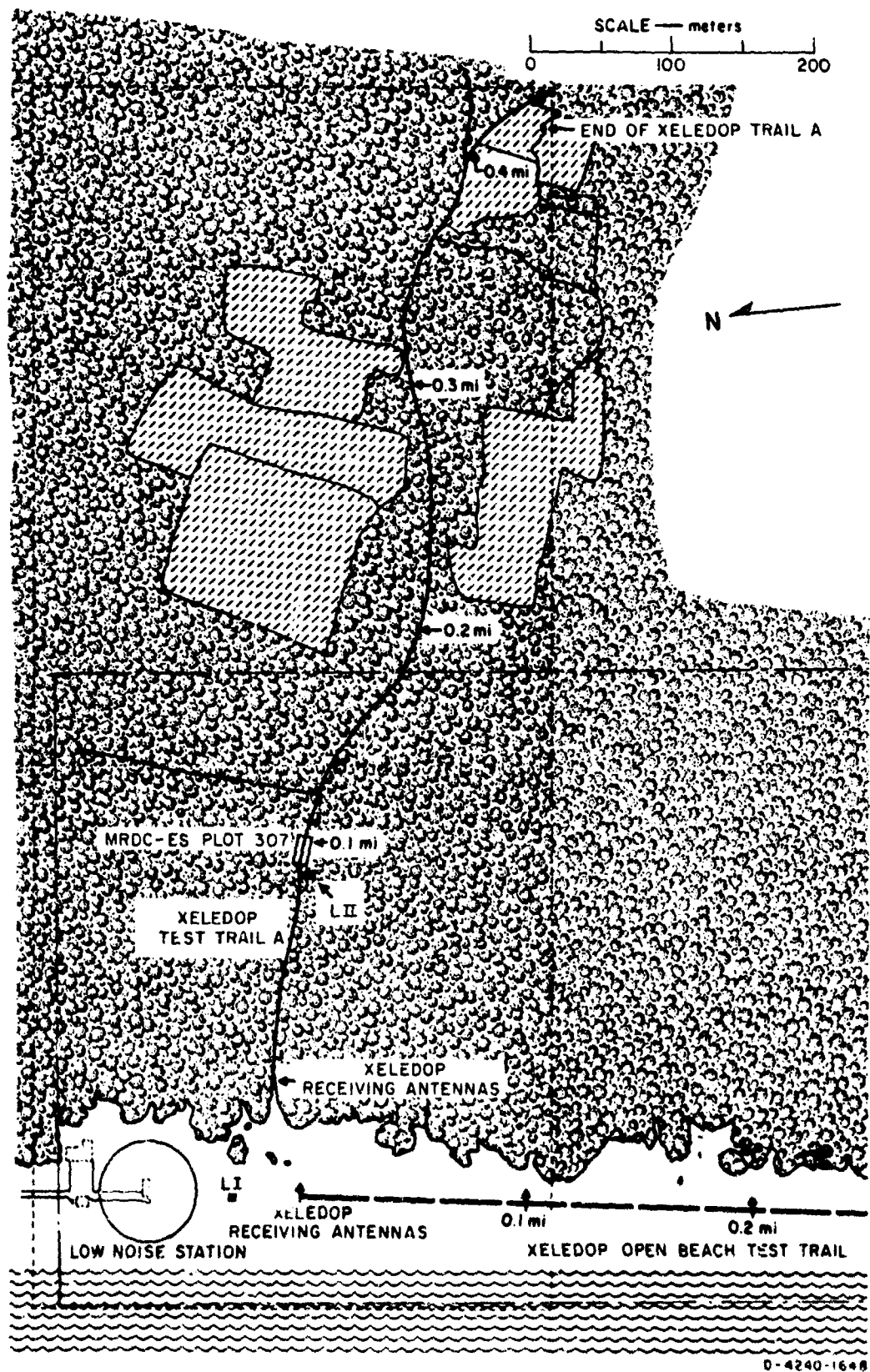


FIG. 15 SRI COASTAL BRUSH RADIO PROPAGATION STUDY SITE NEAR L&EM CHABANG

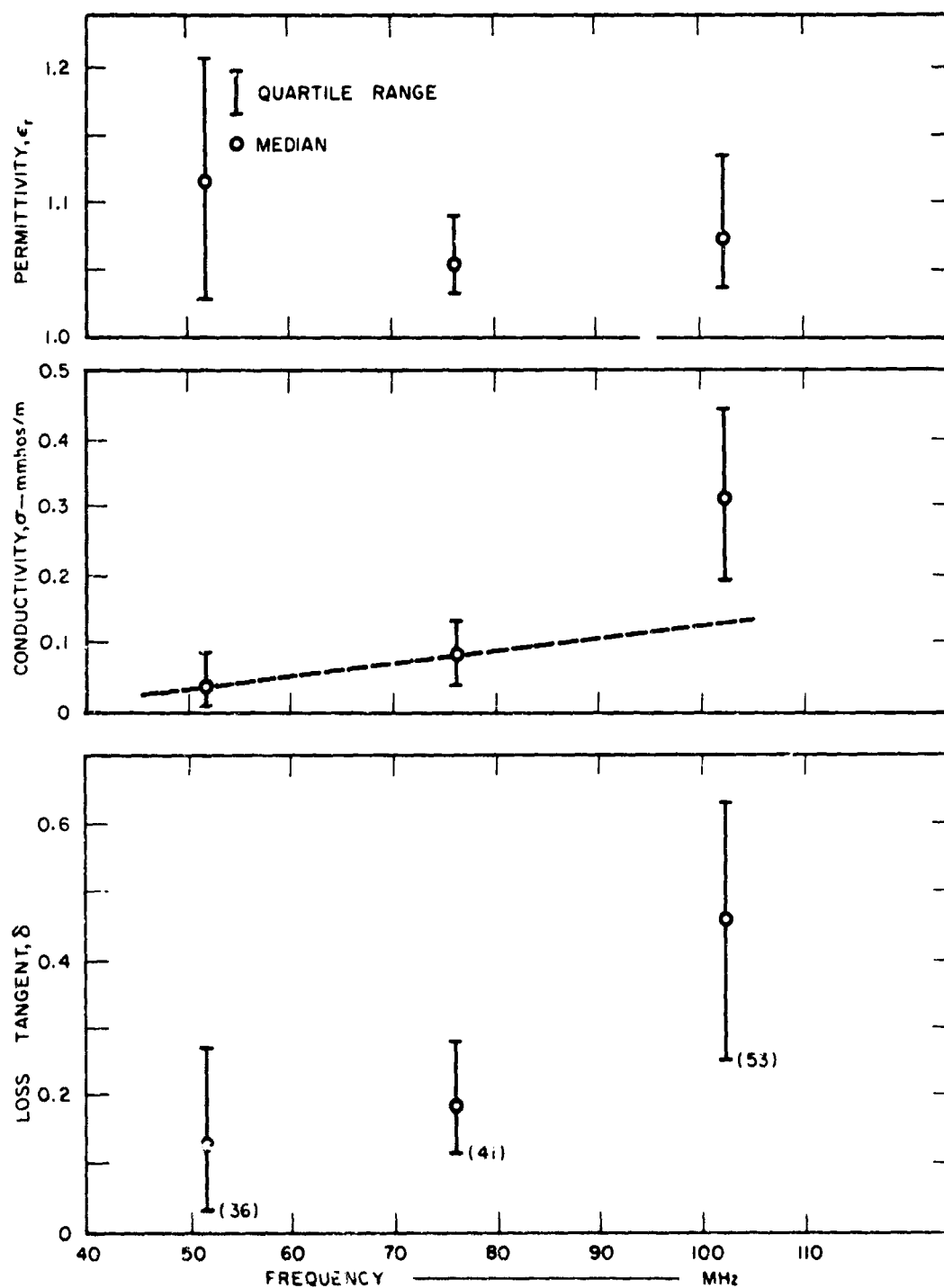


FIG 16 VEGETATION CONSTANTS MEASURED AT LAEM CHABANG SITE

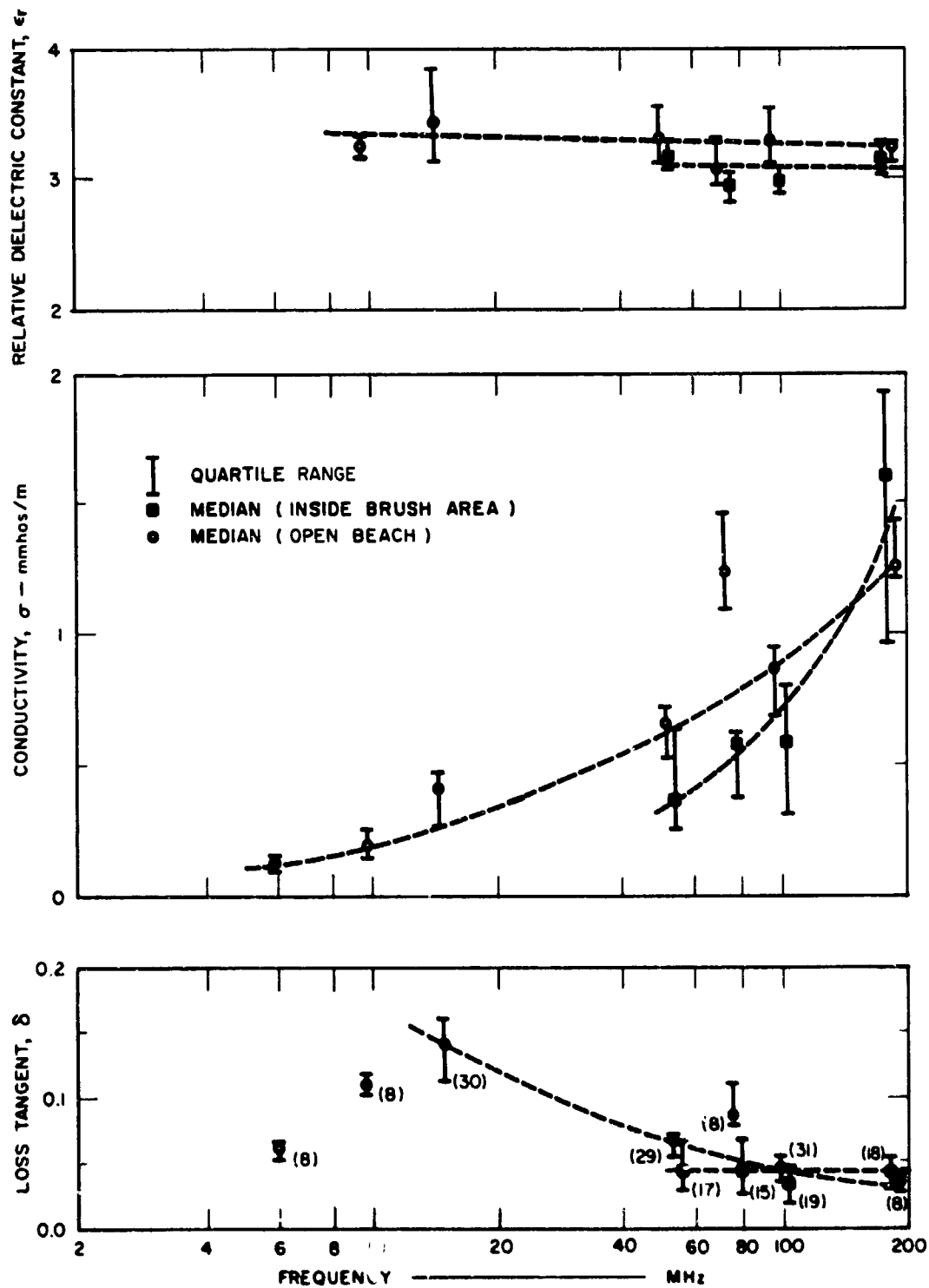


FIG 17 GROUND CONSTANTS MEASURED AT LAEM CHABANG SITE

coarse and dry--witness the presence of cactus. Thus it should provide a poor electrical ground, and we were not surprised to find that our standard technique of dc resistivity sounding would not work without some wetting of the soil near the electrodes, a technique that produced results of doubtful value. The natural moisture content of this soil was less than five percent above a depth of 2 meters; it varied slightly from place to place. These factors are reflected in the results shown in Fig. 17: ϵ_r does not vary appreciably with frequency when soil moisture is low, but σ does. The greater slope of the conductivity variation in sand beneath brush indicates that was the drier soil.

The values for 6 MHz (there is an ϵ_r median of 5 at 6 MHz, not shown in Fig. 17) were measured by the approximate method discussed in Sec. II-A, using a 10-cm probe only. Obviously, this method did not always produce believable results even though the approximation involved should be best for short probes in this type of dry soil. The fault here, we think, lies not with technique itself, but with the use of physically large coaxial baluns to connect the bridge to the small probe, and the need for choosing a bridge that is well-suited to the measurement of Z in the range occurring in this case.

There was no significant variation of electric ground constants with depth (to 2 meters) at the site. The ranges of values at each frequency in Fig. 17 represent probings at each of 5 levels--surface, 0.5, 1.0, 1.5, and 2.0 meters depth.

D. Satun Results

The J & B test site on the Malay Peninsula is near Satun on the western coast, in an evergreen tropical rain forest (see Appendix F for detail). Thunderstorms are prevalent in this area, usually being heard on more than 100 days each year, and bringing torrential rain that produces the succulent growth northerners associate with the word jungle. Indeed, the Khuan Karlong forest at the site is the last stand of a once-rich wilderness: but it has lost many of its valuable trees to the ax, so that its upper-canopy story is now discontinuous, though regular in height, having trees between 24 and 30 meters tall.

The greatest numbers of trees form the middle-story canopy, 15 to 23 meters high, in a seemingly continuous horizontal layer. There is a lower-canopy story composed of young trees between 8 and 14 or more meters high that forms a sort of height continuum with the middle story; the result is complete canopy coverage of the ground beneath this forest. The irregular undergrowth must live on filtered light except where rare breaks occur in the cover. There, in the direct sunlight, the undergrowth resembles what we saw at the other sites: dense shrubs, climbers, and herbs reaching up between 3 and 7 meters, barely penetrable on foot.

We selected, with the advice of MRDC-ES field personnel, a typical undisturbed volume of undergrowth on a base of 9 square meters, tied it off into stations for insertion of the small vegetation probe, and obtained a population of measurements of the effective electric constants of that volume containing undergrowth, which we called Sample SI. The position of our sample may be located with respect to the J & B reference point Z2 on the map in Fig. 18. The medians, quartile bounds, and numbers of that population of vegetation results are shown in Fig. 19.

The similar process of measurement of effective ground constants in the earth beneath Sample SI produced the results shown in Fig. 20. The variation of ground constants with depth was not checked.

Results of earth resistivity measurements (at dc) made in the middle of the clearing, along the airstrip, indicated subsurface conductivity stratification at the site. They show that the earth conductivity varied markedly with depth: there was a 0.3-meter-thick surface layer of conductivity 2 mmho/meter (dc), a 4.3-meter-thick mid layer of conductivity 0.4 mmho/meter (dc), and a region below that having dc conductivity 15 mmho/meter. Results of a soil survey done there under the direction of the MRDC-ES show the average moisture content of the sandy soil above 2 meters was 29 percent by weight.

E. Chumphon Results

The 'RI test site on the isthmus of Kra southwest of Chumphon (Fig. 1) is in a low valley inundated by water during the tireless rains, often to a depth of 30 cm. Some types of vegetation thrive under these

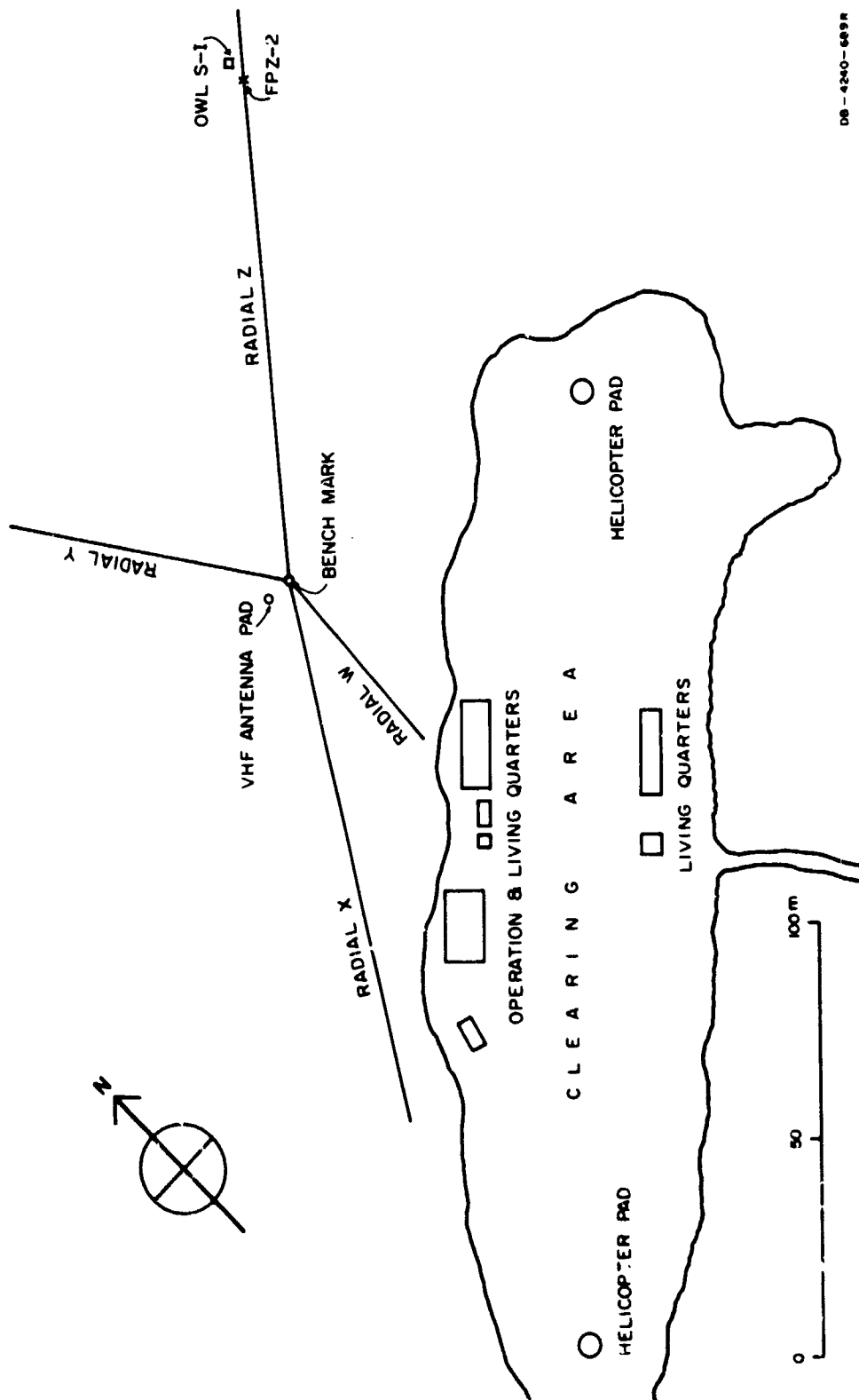
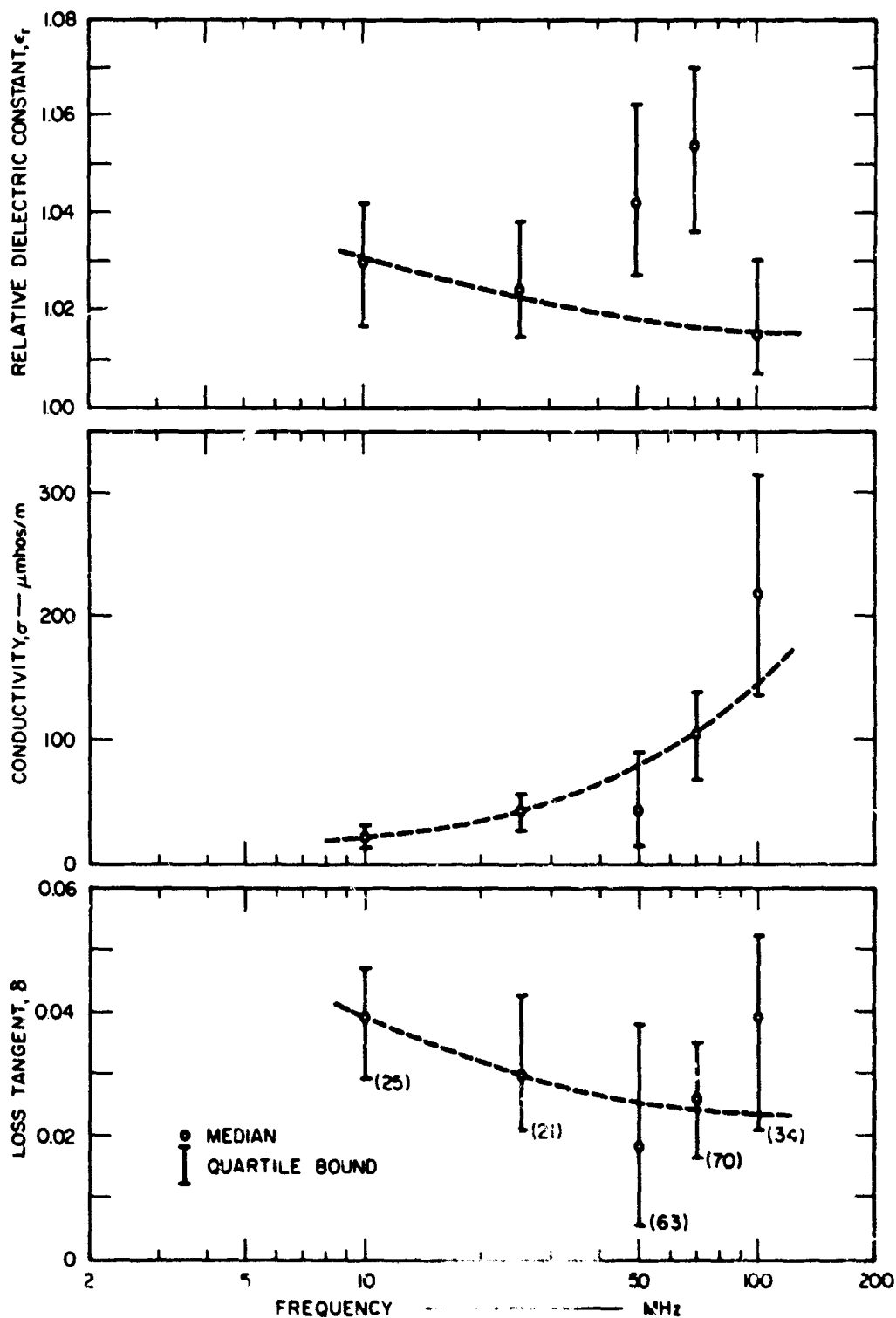


FIG. 18 JANSKY & BAILEY FOREST RADIO PROPAGATION STUDY SITE NEAR SATUN



DB-4240-546H

FIG 19 UNDERGROWTH VEGETATION PARAMETERS MEASURED AT SATUN SITE

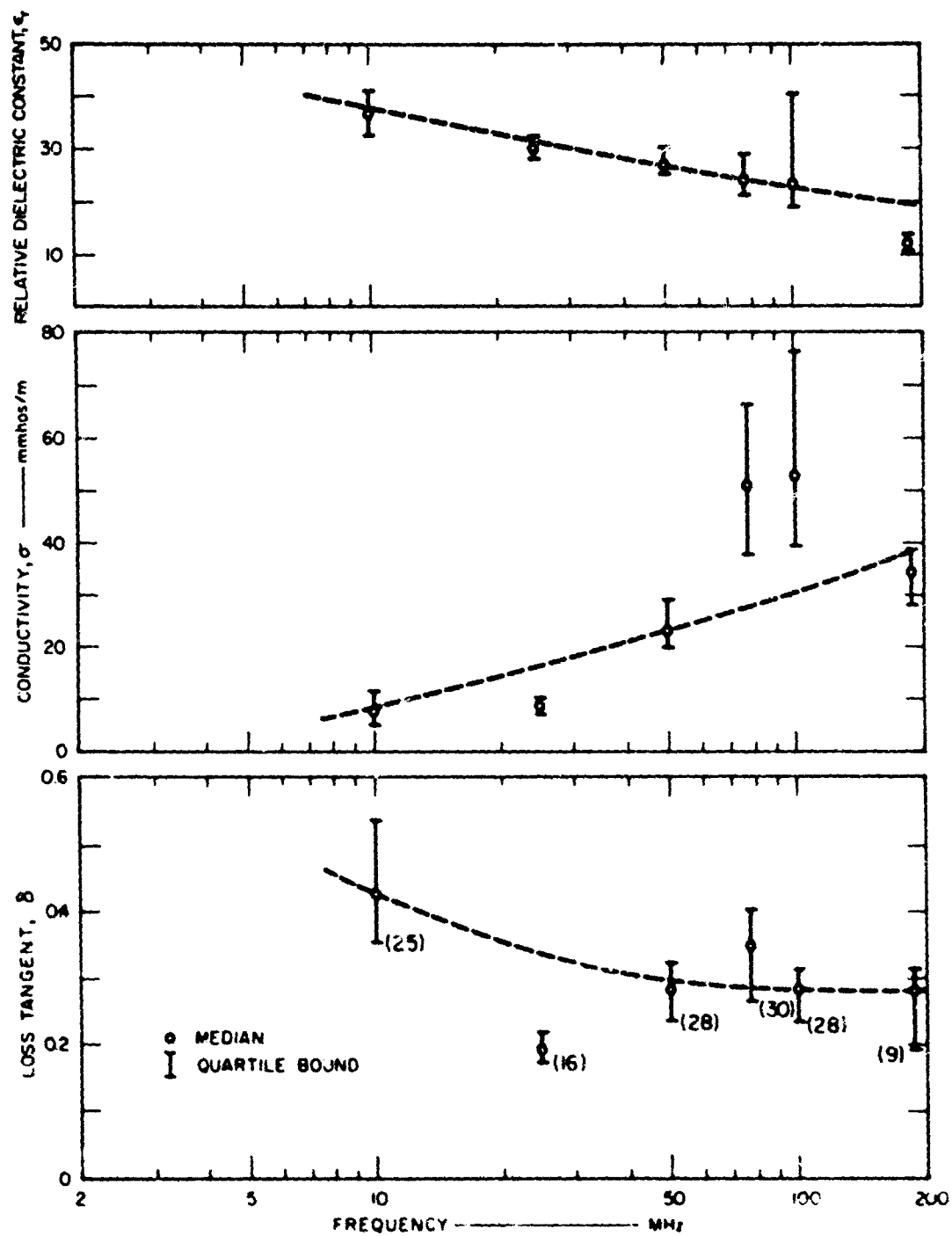


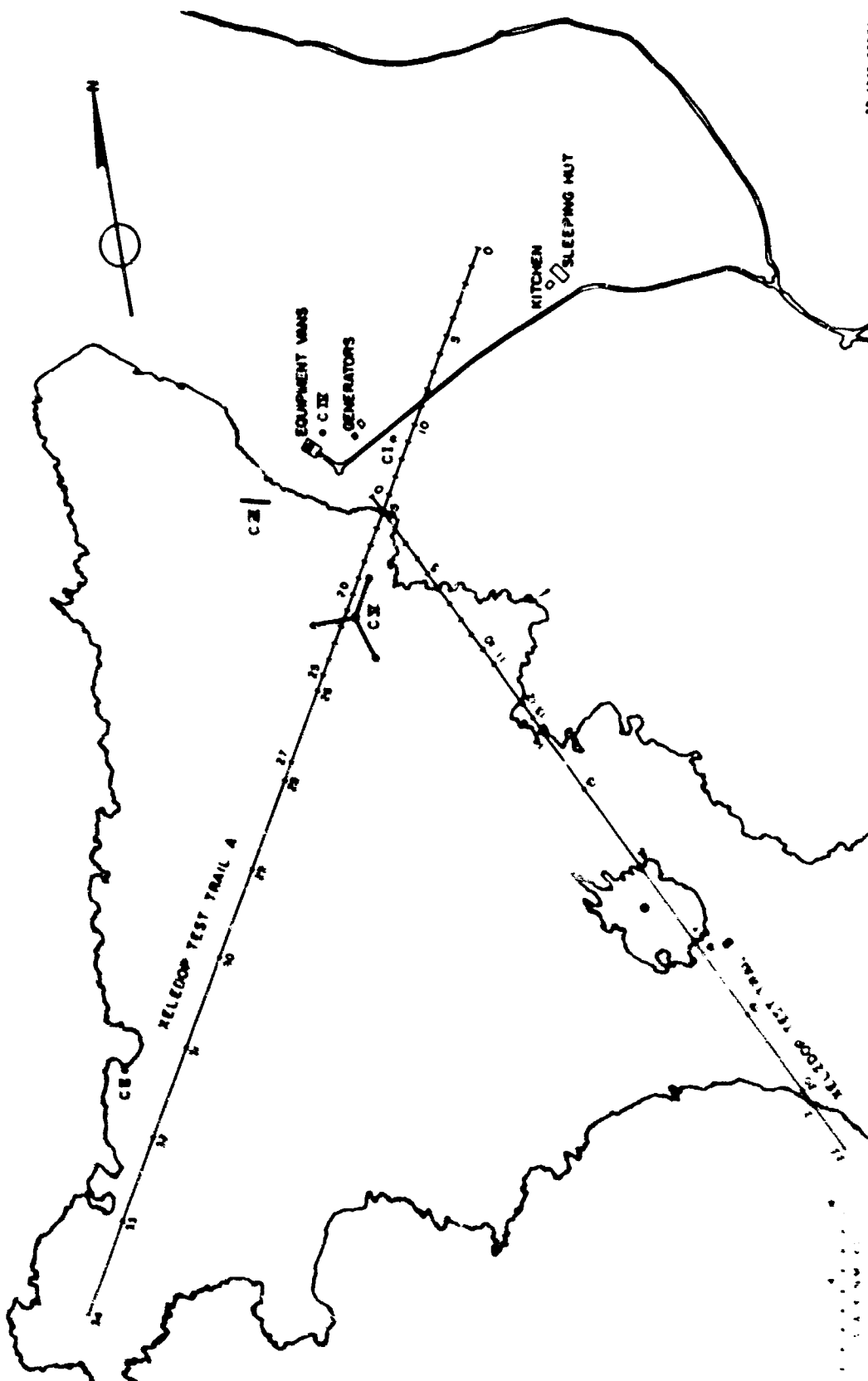
FIG. 20 SURFACE GROUND CONSTANTS MEASURED IN FOREST AT SATUN SITE

conditions (see Appendix C for detail), forming a fresh-water swamp forest such as the Wisai Nua forest we studied. The tree growth there is almost uniform throughout the forest stand. Its canopy is three-storied as usual, but here the upper story is almost horizontally continuous, between 25 and 36 meters high. The middle story is 15 to 24 meters high. The lowest story contains about 60 percent of the trees, these between 7 and 14 meters high. The lowest trees are heavily suppressed by the continuous canopy above them, yet there is considerable undergrowth present.

The undergrowth is quite uniform, in two layers, the upper composed of tree seedlings and shrubs growing to 4 meters; the lower layer, only 0.3 meters high, has mostly herbs. Below these, the soft, muddy forest floor is covered with a layer of humus several centimeters thick.

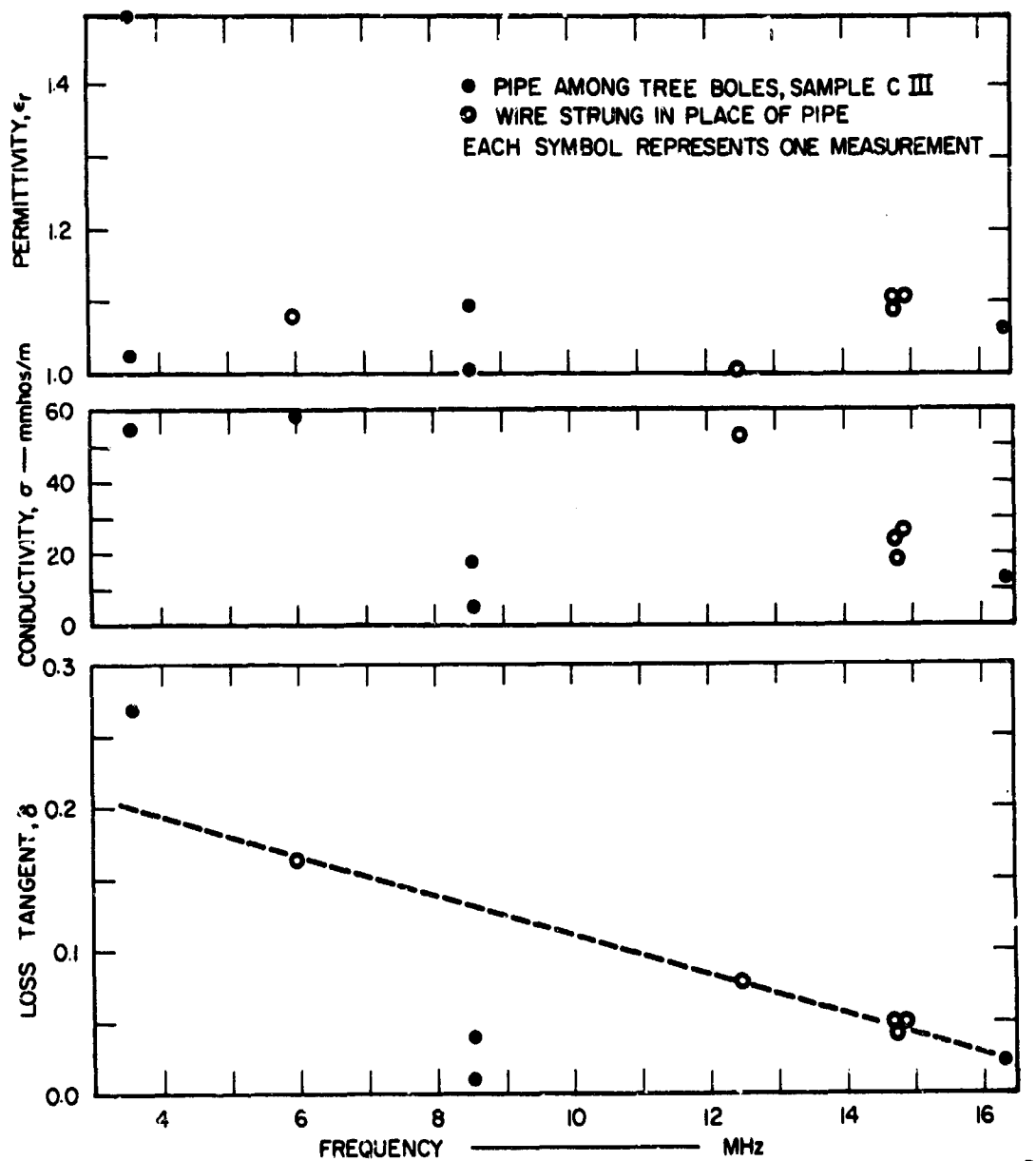
Following the advice of forestry experts on vegetation sample selection, we made extensive measurements in this forest to study electric constants in undergrowth (CI. and among large trees in absence of undergrowth (CIII), and the height profiles of the electrical constants among large trees (CV). These experimental sites and two others where we measured ground constants in the clearing (CI and CIV) are marked on Fig. 21.

To compare the measurement capability of the recently developed wire vegetation probe with that of its ancestor, the pipe probe, at HF, we inserted the two in sequence among large tree boles of Sample CIII. The results are shown in Fig. 22, where their scatter, seemingly associated with this type of sample, is obvious. Since the values of loss tangent obtained with the wire followed a more reasonable trend with increasing frequency than did those measured with the pipe probe, and since the ranges of all constants obtained were not dissimilar, we decided to use the wire later in taking height profiles at HF. We did not expect the wire- and pipe-probe results to be identical, since the wire spacing (2 meters) was twice that of the latter probe, and it was (at 20.8 m) 2.5 meters longer. The tendency of the wire to produce higher conductivity results than the pipe may owe to its enclosing more trees, none of them smaller than 5 cm in diameter at breast height.



DB 4240 58882

FIG 21 SRI ANTENNA ENVIRONMENT STUDY SITE NEAR CHUMPHON



DB-4240-644 R

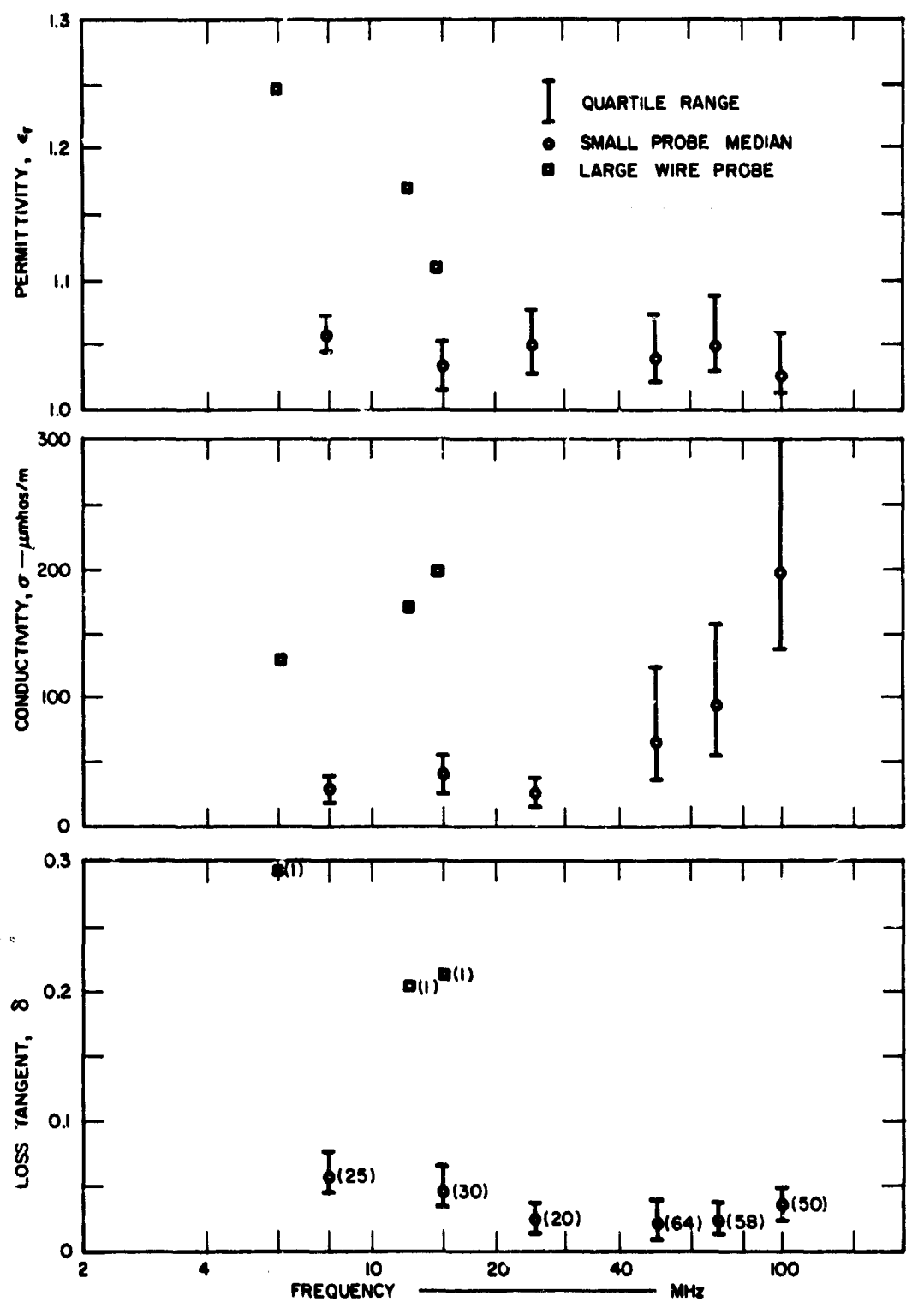
FIG. 22 COMPARISON OF WIRE PROBE AND PIPE PROBE RESULTS FOR TREE BOLES AT CHUMPHON SAMPLE CIII

In the undergrowth sample, CII, we used both the large-spacing-wire probe in one position (8 m long) and the small-scale-probe in multiple insertions as discussed for the other sites. The characteristics of this sample are described in Appendix C; it was more dense than Muen Chit undergrowth MII, and larger. Its base was $3.5 \times 7.5 \text{ m}^2$. The results of our vegetation-constant measurements there are shown in Fig. 23. Note that those obtained statistically with the small probe show reasonable behavior with increasing frequency through 75 MHz.* The wire-probe results were neither similar to those nor reasonable, by comparison, probably because the larger spacing-to-length (in wavelengths) ratio of the wire allowed it to radiate more in the presence of undergrowth. We decided that the wire must be made several times longer and inserted at more positions in samples measured in the future, which would of course have to be much larger.

We chose to make vegetation-constant height-profile measurements in the vicinity of the HF antenna test site, where several forestry plots had been surveyed. From a trio of tall trees in the center of Sample CV, we strung three sets of wire probes radially at each of three levels. The lowest of these sets was in the region of tree boles only; the second was midway in the lower tree canopy; the highest was just within the middle canopy, above about 70 percent of the trees. At the hub of this network of 3 sets of wire probes we erected two working platforms, one just above the mud, the other 16 meters high in the swaying trees.

Initially, each wire was 31.6 meters long. We later trimmed those we could reach easily to 28 and then 21 meters to obtain a larger population of measurements. We also shifted two of the probes horizontally, but did not continue this laborious process, as time was short. All wire probes above the lowest level ended at large trees laddered with spars for the climbers who changed the probe terminations.

*The loss tangent of a dielectric medium should decrease hyperbolically except in the frequency band where ϵ_r has a resonant peak related to polarizability of constituents of the medium.



DB-4240-636

FIG. 23 COMPARISON OF UNDERGROWTH VEGETATION CONSTANTS MEASURED BY TWO TECHNIQUES IN CHUMPHON SAMPLE CII

We were forced to make several measurements and average these for each position of the probe because the swaying of the trees in the persistent wind caused widely ranging impedance readings. Even so, the results,* especially for σ and δ , covered more than one order of magnitude (see Figs. 24 and 25). Referring to the results for δ , one may see that dispersion of the sample range increased with both height and frequency, and note that above 9 m and 6 MHz no δ values occurred between 0.01 and 0.04. This curious grouping of the δ results (it is not so obvious in the σ graph) seems to be related to the branching of the trees, as there were no branches below about 9 m, and undergrowth had been cleared from the entire area. Obviously, with this much dispersion occurring in the results, we will require many more measurements than we took in order to describe the electric constants of a tree canopy region. It may be premature to bound ϵ_r between 0.96 and 1.14, and δ between 0.004 and 0.16 in the canopy, or σ for canopy foliage between 2 and 200 mmho/m at HF. The limits seem both too high and too low. There is no evident central tendency in this measurement population of 3 to 5 members per frequency per height, even for the region having no branches.

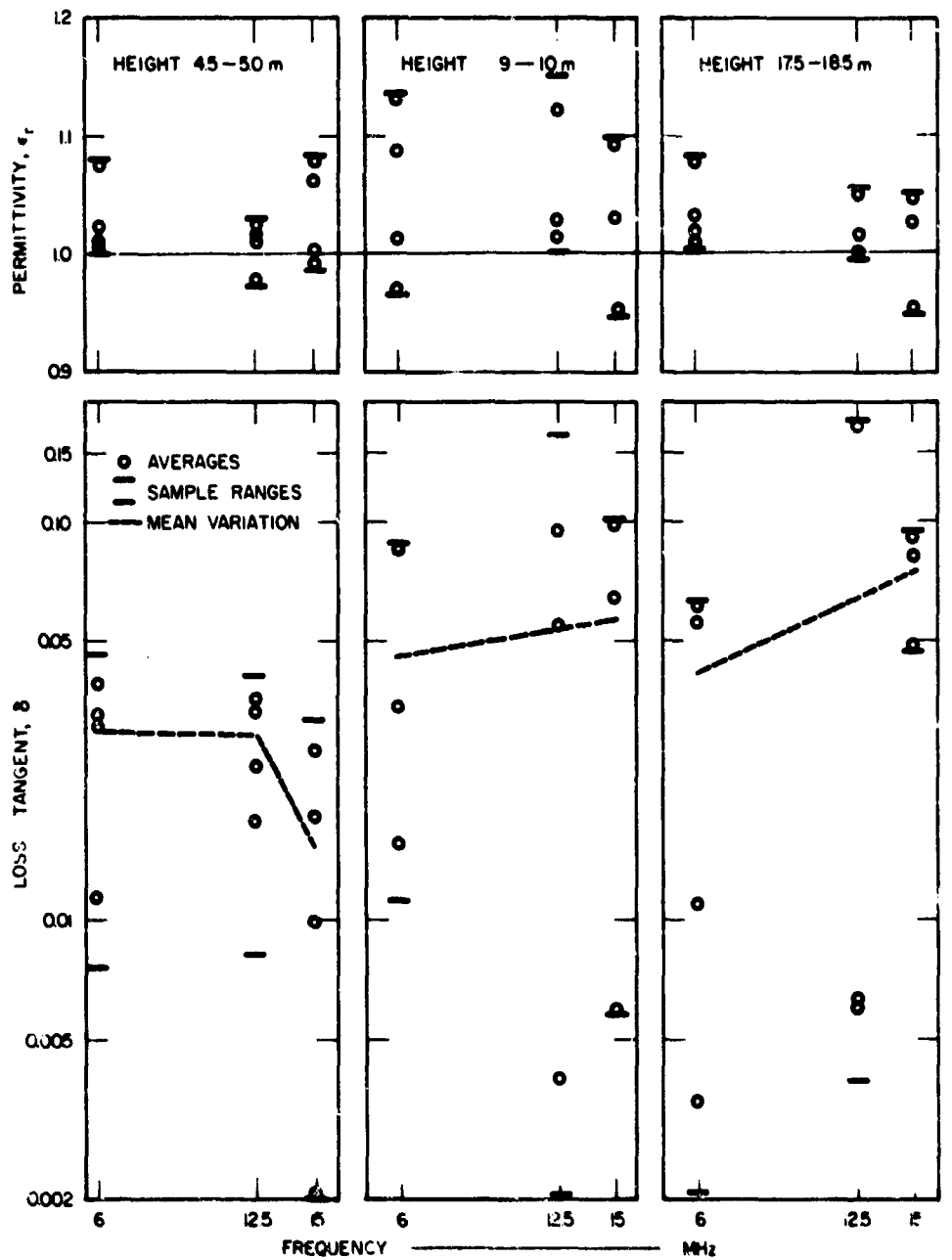
We can compare results for the lowest region with those obtained at a similar height in Sample CIII (Fig. 22). Table I will suffice.

Table I

HF ELECTRICAL CONSTANTS FOR SAMPLES CIII AND CV

Frequency (MHz)	Dielectric Constant		Loss Tangent		Conductivity	
	ϵ_r		δ		σ (mmho/m)	
	CIII	CV	CIII	CV	CIII	CV
6 - 8.5	1.0 - 1.1	1.01 - 1.08	.01 - .15	.075 - .45	5 - 60	2 - 18
12.5	.08	.98 - 1.04	.08	.08 - .04	54	6 - 26
12 - 16	1.06 - 1.1	.99 - 1.09	.025 - .15	.002 - .027	14 - 28	1 - 28

* In Figs. 24 and 25 the circles represent spatially independent measurements, usually averages for a single probe position.



DB-4740-6489

FIG. 24 HEIGHT PROFILE RESULTS ϵ_r AND δ MEASURED AMONG TREES OF CHUMPHON SAMPLE CV

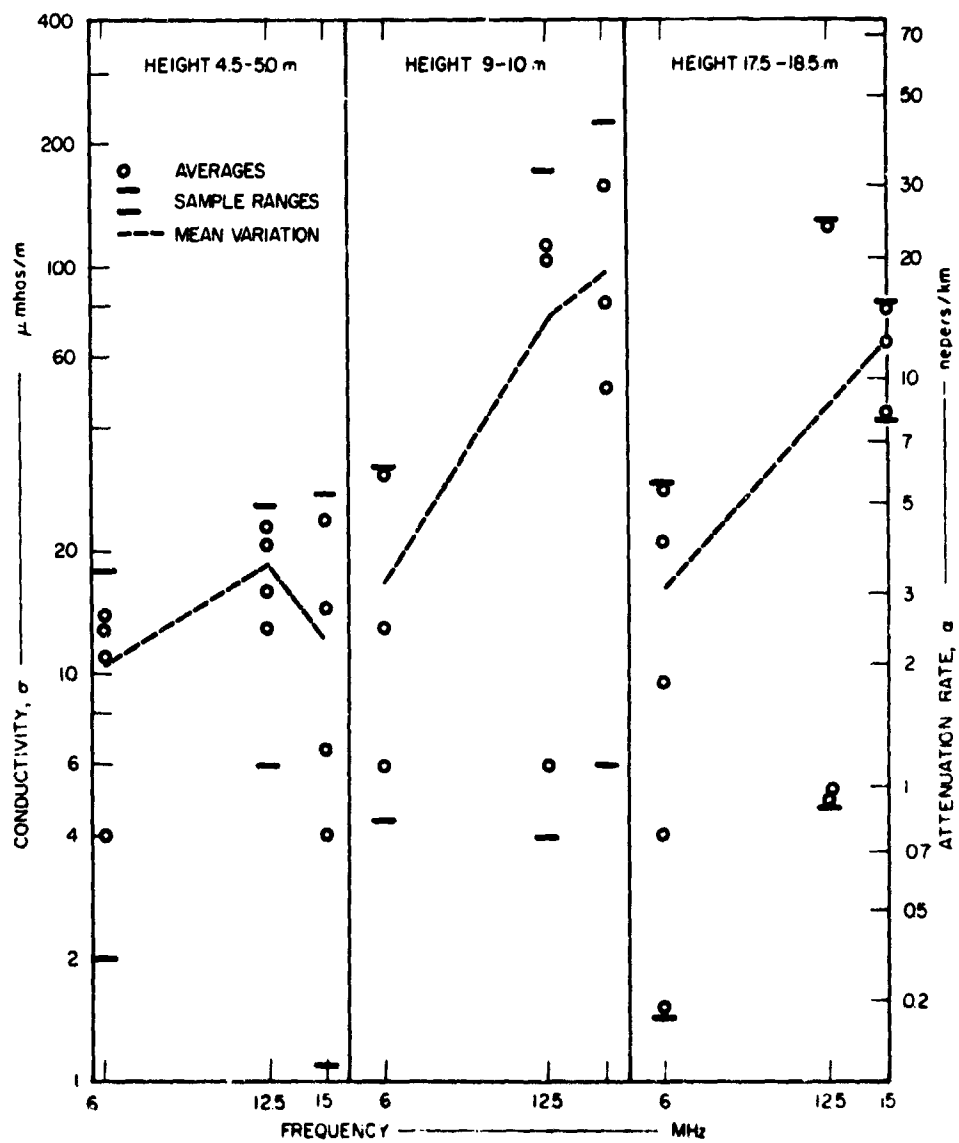


FIG. 25 HEIGHT PROFILE RESULTS σ AND α MEASURED AMONG TREES OF CHUMPHON SAMPLE CV

Notice that if CIII results were added in with those from CV, they would cause an upward bias in most cases. Now, if we look back to Fig. 24, we see that there are more values of δ occurring near the upper limits than near the lower. This trend toward high (or lossy) values is based on a very few measurements, though, and does not seem reasonable in light of the distributions of the undergrowth results.

We measured electric constants of the surface earth in the forest near Samples CII and CV, and in the clearing took ground-constant Samples CI and CIV, over a period of two months. The surface measurement results are compared in Fig. 26. Of these, CII was apparently in the least lossy earth, being on a raised part of the valley that was not flooded by the rains. The wide scatter in the VHF results from CI may also have been caused by the heavy rains. Samples CIV and CV were in continually swampy areas.

We also measured the variation of ground constants with depth near Sample CII (Figs. 27 and 28). We simply dug a large hole and inserted the ground probes in its sides, shaving away, just before each insertion, the earth that had been exposed to air. It is evident that the earth there became more lossy with increasing depth to 2 meters, the limit of our dig. Earth-resistivity sounding measurements at dc, done at the same place two months earlier than the probe work, indicate the presence of a 0.3-m surface layer (σ at dc \approx 2 mmho/m) resting on a 1-m-thick middle layer (σ at dc \approx 120 mmho/m) with a semi-infinite region below that (σ at dc \approx 2 mmho/m). Basing conjecture on this interpretation of the dc soundings, we expected σ at HF to fall between 2 and 10 mmho/m, as it does, for the upper region; but for the middle and lower regions probed we did not find the expected sixty-fold increase followed by a return to conductivity similar to that of the surface.

The soil at Chumphon site is silty clay with gravel interspersed. The clay in forest is grey, having a mixture of humus that improves its water-holding capability (average surface moisture content 70 percent); most of the clay in the clearing was reddish, and often dried at the surface between rains (average surface moisture content 25.4 percent).

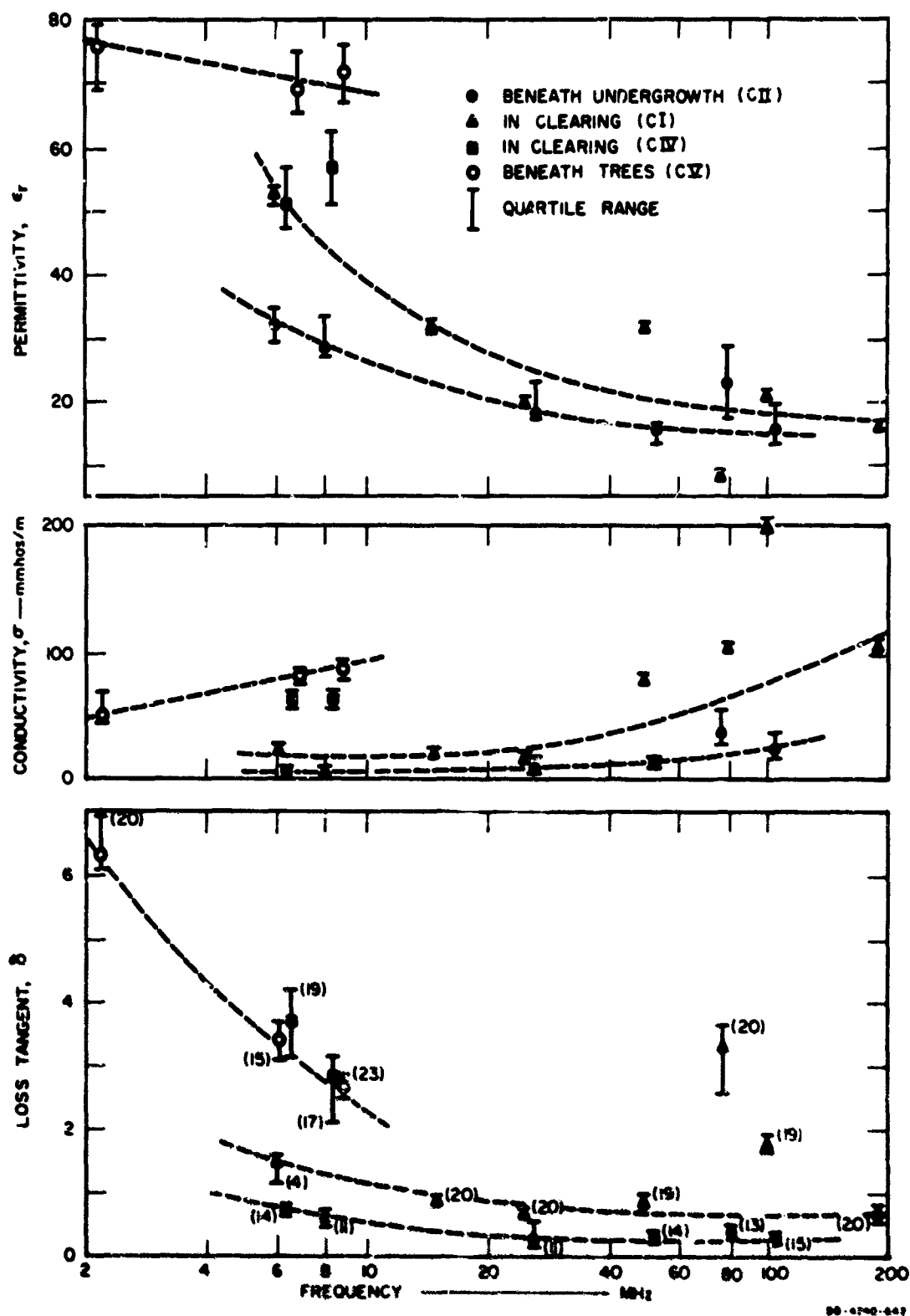
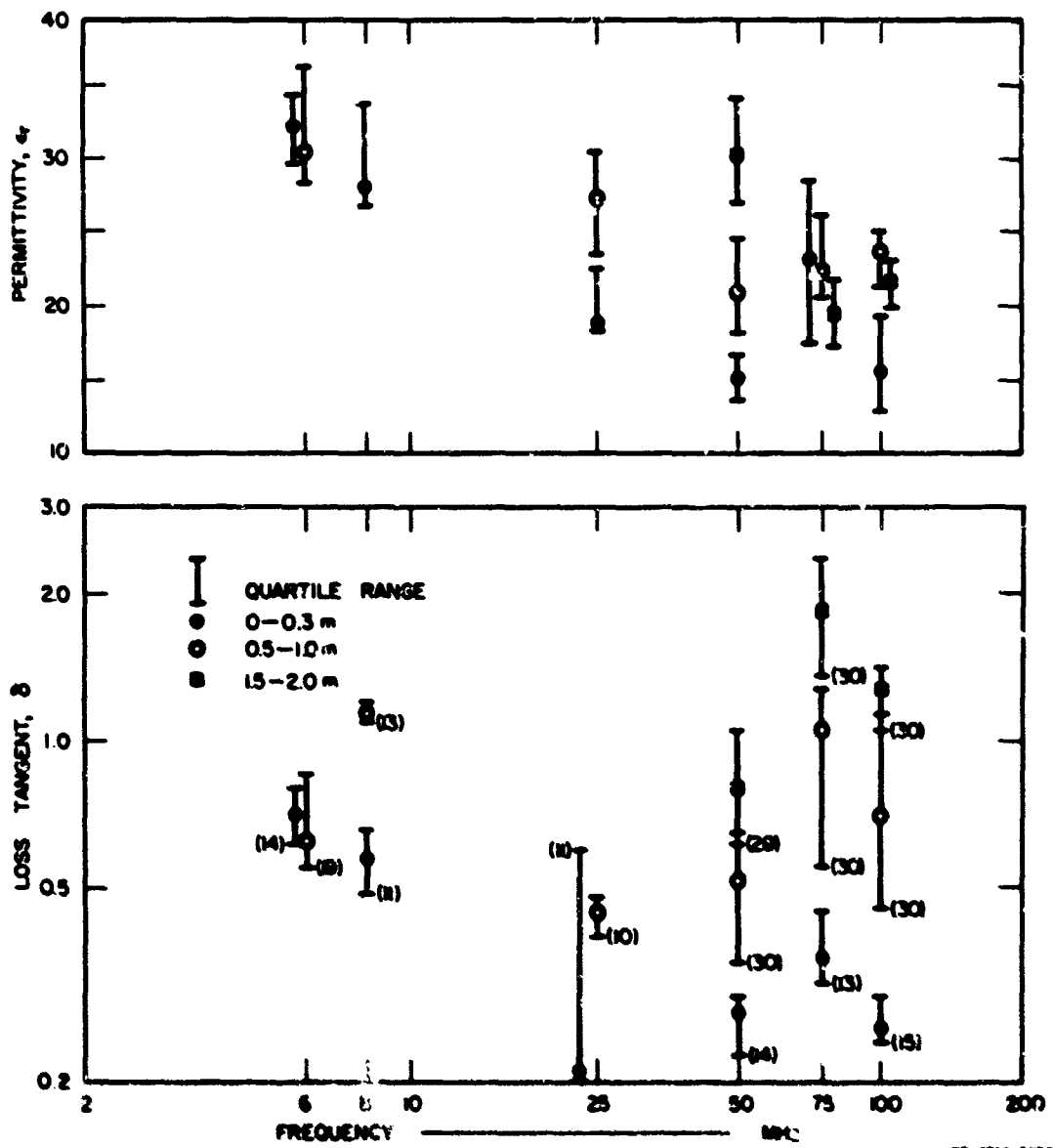


FIG 26 SURFACE GROUND CONSTANTS MEASURED AT CHUMPHON SITE



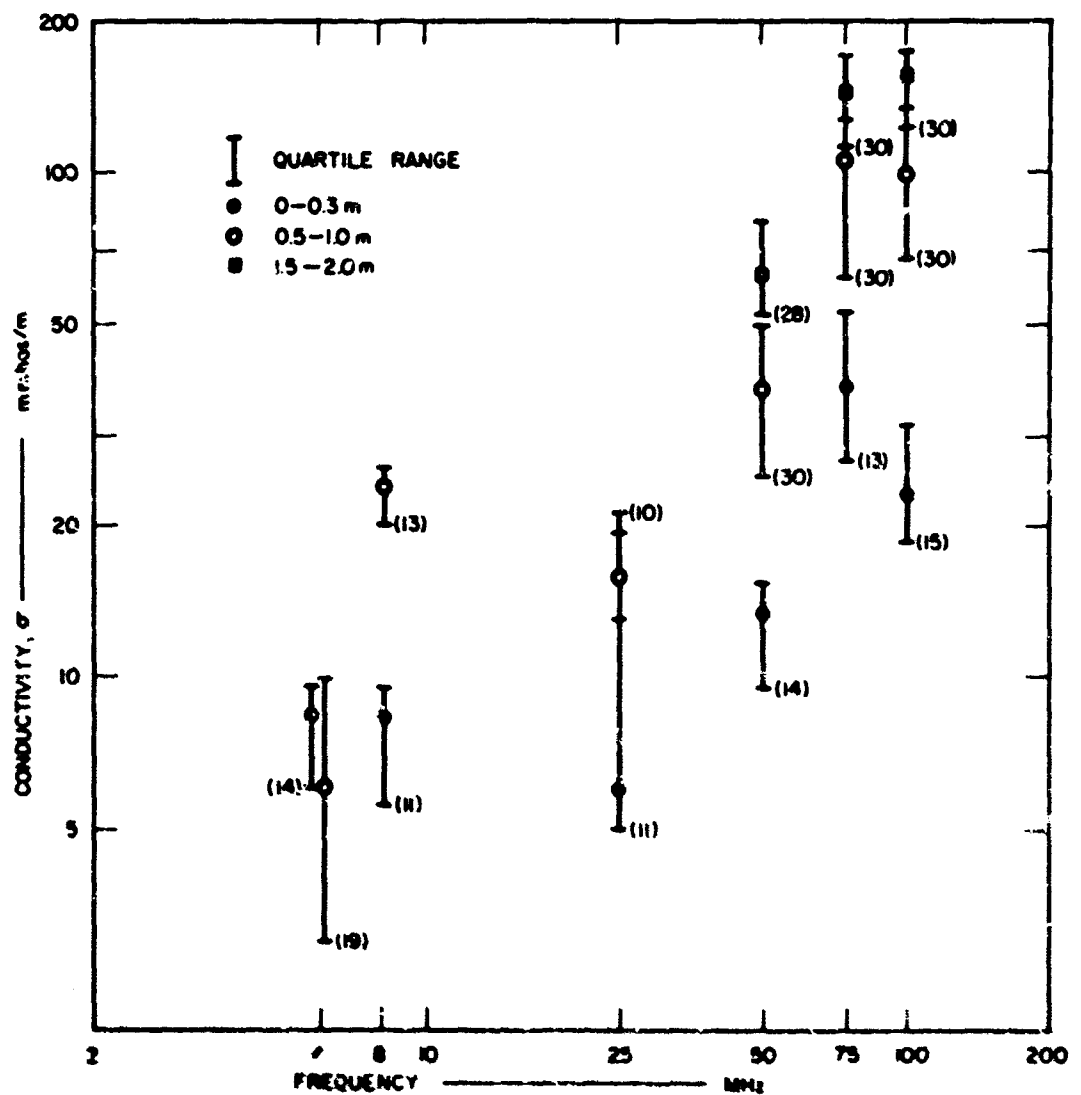


FIG 28 GROUND CONDUCTIVITY MEASURED AT SEVERAL DEPTHS NEAR CHUMPHON SAMPLE C1

At a depth of 15 cm in the clearing, and about 2 m at CII, the soil was water-saturated at all times. The surface soil at Samples CIV and CV remained saturated with water during the entire summer, being low-lying areas fed by a stream.

IV DISCUSSION OF RESULTS

A. Applicability of Vegetation-Constant Results

How well do our results, reflected as medians, represent the true populations of effective electric constants that we presume must exist for a volume of air containing living vegetation? In preparing an answer, we would like to be able to define the intrinsic distribution underlying our measurements.

Now if the number of stems on any horizontal area has a Poisson distribution,²⁰ the distribution of those stems with respect to any stem at random (or with respect to some point on the OWL inserted among them) should be Rayleigh.* In particular, the nearest-neighbor distances between stems are distributed according to Rayleigh's distribution. We can deduce that the probability of finding any stem within the sensing region of the horizontal OWL has the same distribution. And if we can assume that insertion of the OWL in planes other than the horizontal merely increases the parameter of that distribution, we should expect to find that the measurement populations for effective values of ϵ_r^\dagger and σ are approximating, for large populations, the cumulative distribution function

$$\begin{aligned} F(r) &= \int_0^r \frac{r}{S^2} \exp(-r^2/2S^2) dr \\ &= 1 - \exp(-r^2/2S^2) \end{aligned}$$

where r is the variable and S is its standard deviation[§] in the underlying distribution.

* This is developed in Appendix B.

[†] We actually use $\epsilon_r - 1$ to allow a more usual variation range.

[§] In these cases, S^2 is perhaps more properly called the parameter of the distribution.

This surmise is supported by the results, as shown by the inverse distribution for $F(r) = g(\epsilon_r - 1)$ in Fig. 29, using the same coordinates as in Appendix B in order to graph $F(r)$ as a straight line. The dashed line shown in that figure is the Rayleigh function for $S = 0.0454$, corresponding to a mean of 0.057 on the $\epsilon_r - 1$ scale, and having median 0.054. The measurement population itself has the mean $\epsilon_r - 1 = 0.058$ and median 0.056; it contains 71 values whose standard deviation is 0.034. It seems biased upward a bit, but is well represented by the Rayleigh distribution. Matters seem worse when we consider conductivity in a similar fashion, as in Fig. 30. The obvious bias of σ toward the higher values seems enough to invalidate our Rayleigh approximation. We noted that all the values for $\sigma > 270$ $\mu\text{mho/m}$ came from three stations in the Satun vegetation-sampling matrix, and surmise that unusual growth patterns in those sub-volumes caused the bias. If we ignore that 10 percent of the measurement population, we can easily fit a straight line to the other 90 percent. The dashed line in Fig. 30 represents a Rayleigh distribution having median 102, mean 109, and standard deviation 87 $\mu\text{mho/m}$. It approximates the population fairly well: the measured values had median 97.3, mean 121, and standard deviation 81 $\mu\text{mho/m}$. Obviously, we must choose the medians rather than the means of our measurement populations to reduce the effect of upward bias.

A word on the accuracy of measurement is required here, for if the members of the measured population were subject to significant error arising from the technique of measurement, their distribution might show characteristics unrelated to the environment. On the distributions of results obtained for repeated measurement with the OWL in a single position, the total range of variation has been less than 2 percent. Further, if the length of the OWL was varied by a few hundredths of a wavelength while in a given station, the results never varied by more than 10 percent about their median values. Thus variations arising from the measurements themselves, or from slight differences in positioning of the OWL, are likely to be insignificant compared with the effects obtained when the OWL is moved from station to station in vegetation. As we have shown above, the standard deviation that arises in the latter case is

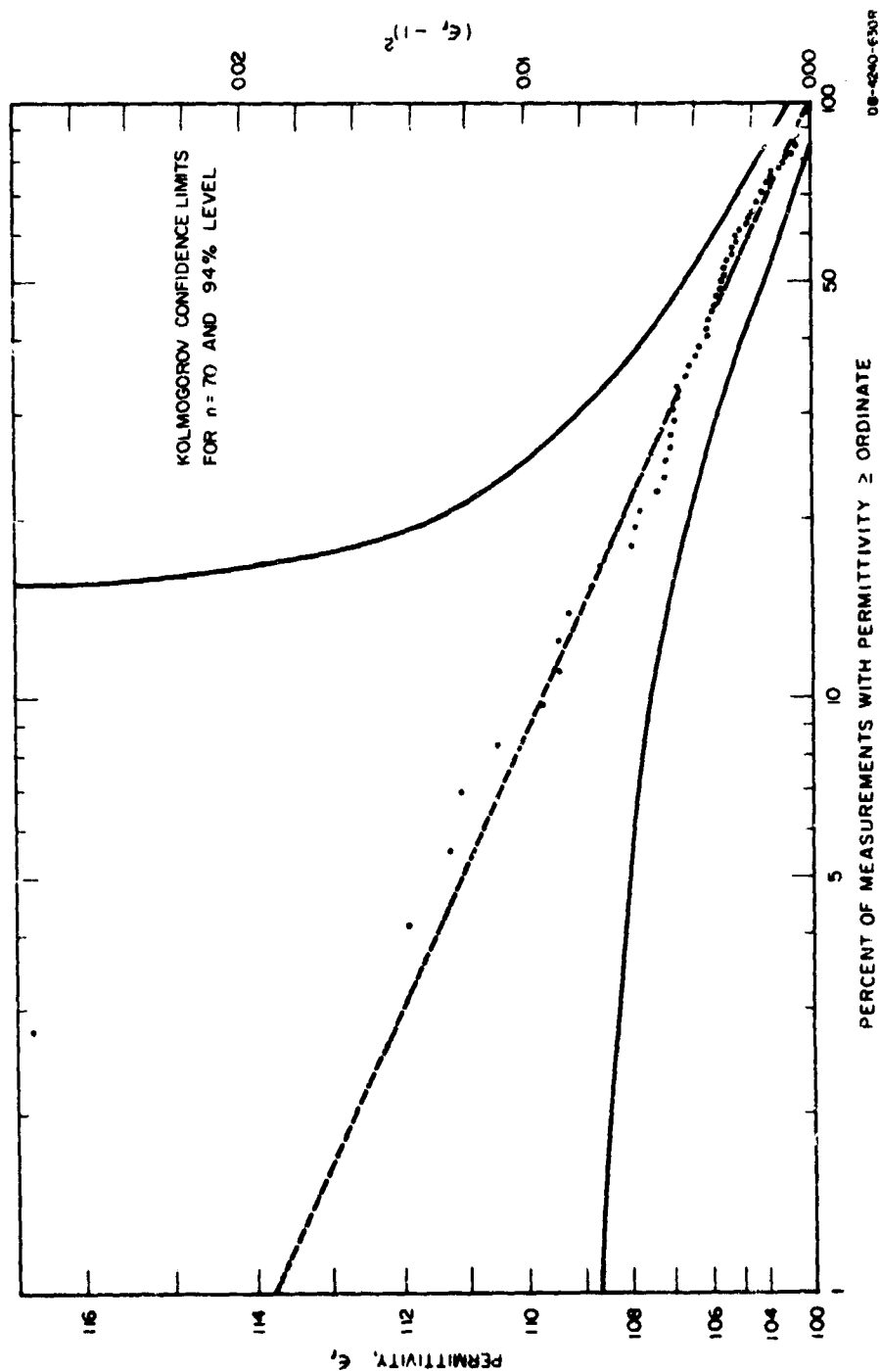


FIG. 29 DISTRIBUTION OF RELATIVE PERMITTIVITIES MEASURED IN UNDERGROWTH AT SATUN

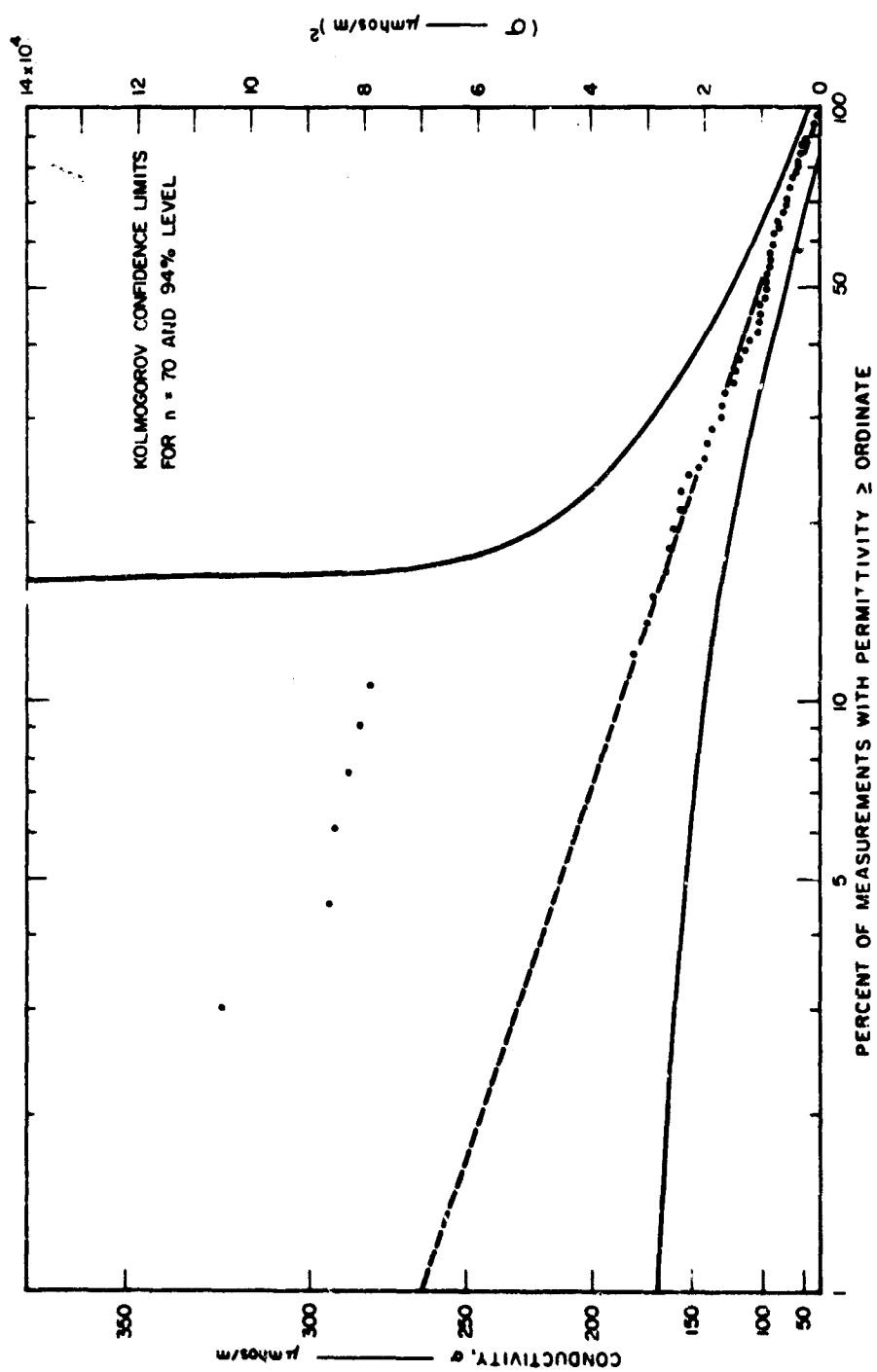


FIG. 30 DISTRIBUTION OF CONDUCTIVITIES MEASURED IN UNDERGROWTH AT SATUN

about 85 percent about the median.* It seems safe to assume that this large variation is essentially characteristic of the vegetation medium and that true errors in measurement little alter the form of a distribution of vegetation constants. If the measurement error were as great as ± 5 percent, it would account for much of the scatter of the results about the dashed lines in Figs. 29 and 30, which is obviously not great enough to preclude representing the measurement population by a Rayleigh distribution.

We also applied Kolmogorov's hypothesis test for the fit of a sample population to any known cumulative distribution²¹ to see if we could estimate the true distribution function by using confidence limits. For 94 percent confidence and 70 in the population, the width of the confidence interval for this test is quite large--32 percentiles. It is necessary to have $n \approx 500$ to obtain more useful confidence limits of ± 6 percentiles about the test distribution. We had no such large samples available. Thus we are not able to define the distributions of our vegetation constant results with any rigor. We show Kolmogorov confidence limits at the 94-percent confidence level for the Rayleigh distribution on Figs. 29 and 30 to demonstrate that there is no good reason to reject a Rayleigh distribution as an approximation of our results. It follows, however, that there is no more reason to reject other likely distributions. In Fig. 31 we show the same (70 MHz, Saturn) results plotted in Gaussian coordinates, with the same Kolmogorov limits about the dashed line. (The line represents a Gaussian distribution that could approximate the middle 50 percent of the measurements.) The Gaussian distribution also passes Kolmogorov's test,[†] but we prefer to use the Rayleigh to analyze our results because it appears to be a better approximation, it has a basis in the environment, and it has only one parameter.

* A characteristic of the Rayleigh distribution: see Appendix B, equation (B-21).

† As does the Chi-Square distribution, whose several parameters can be manipulated to give the closest fit of the three to the measurement populations.

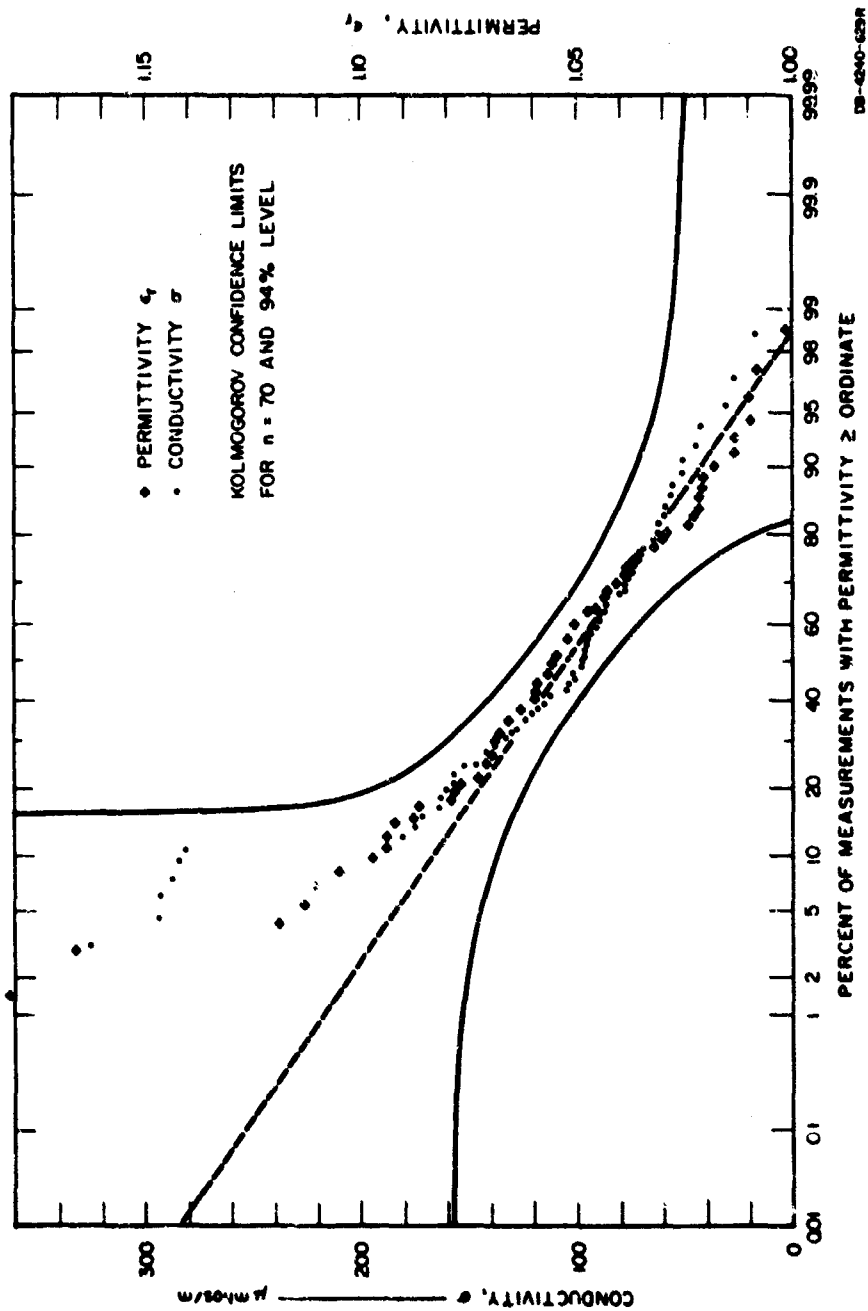


FIG. 31 COMPARISON OF ϵ , AND σ DISTRIBUTIONS IN GAUSSIAN COORDINATES

From study of Fig. 31, one may conclude that between their quartiles the measurement populations of ϵ_r and σ can be well represented by a normal distribution. Certainly it is probable that for n large, by Lyapunov's condition for the central-limit theorem of probability,²² the means, $\bar{\epsilon}_r$ and $\bar{\sigma}$, of our measurement populations will be approximately Gaussian in distribution. (This is often assumed for n greater than 4--see Ref. 23.) This will allow us to calculate, following the work of W. S. Gossett,²⁴ the number, n , of measurements required in order to have probability P that $\bar{\sigma}$ (or $\bar{\epsilon}_r$) is within some confidence interval of width W about the true mean \bar{M} of the underlying distribution from which the n measurements were taken.

The quantity*

$$t = (\bar{\sigma} - \bar{M}) \left[\sum_{i=1}^n (\sigma_i - \bar{\sigma})^2 / n (n - 1) \right]^{-1/2}$$

involves the comparison we want to make, and has Gossett's t distribution with $n - 1$ degrees of freedom.²⁴ It may be rewritten as

$$t = (\bar{\sigma} - \bar{M}) \sqrt{n}/s$$

where s is the standard deviation of the sample of n measurements. Now it is possible to find a number t_j (the value in j^{th} percentile of the cumulative t distribution) for which the probability we seek may be obtained from

$$P \left[\bar{\sigma} - t_j s / \sqrt{n} < \bar{M} < \bar{\sigma} + t_j s / \sqrt{n} \right] = 1 - 0.2j$$

which is often called the $(100 - 20j)$ percent confidence level. The width of the confidence interval is

* We have used σ in the example development to avoid compounding notation. Of course, it may be replaced by $(\epsilon_r - 1)$ or ϵ , if the sub- and super-scripts are retained.

$$W = 2 t_j s / \sqrt{n}$$

The equations for P and W may be applied to any set of measurements; but for convenience we wish to write them in terms of the medians, σ_m , of the measurements, taken together with their numbers. Using the assumption that the measurements are Rayleigh distributed, we may write*

$$P \left[(\sigma_m - W/2) < M < (\sigma_m + W/2) \right] = 100 - 20j \text{ percent},$$

where

$$W \approx 1.35 t_j \sigma_m / \sqrt{n}$$

and M is the median of the underlying Rayleigh distribution. A tabulation of the fractional widths W/σ_m of the confidence interval for sample sizes $n = 5$ to 201 and several confidence levels is presented in Table II.

This information may be used to estimate the confidence to be placed in any of the results of measurement of electric constants of vegetation presented in this report. To read the table, enter under the desired confidence level and read, opposite the sample size, the factor W/σ_m . Then the true median should lie (with probability P) within $\pm \sigma_m (W/2\sigma_m)$ about the measured median σ_m of the n samples. Note that we may be 90 percent confident that the true median lies within ± 65 percent of the measured median of a sample of only 5 values.

One may also use Table II to estimate n for the Gaussian distribution if he multiplies the tabulated values by 1.40. Then he can relate W/s to n , where s is the desired standard deviation of the Gaussian sample and W is the width of the confidence interval centered on the Gaussian mean or median. The confidence levels, of course, do not change.

* See Appendix B, Eqs. B-19 through B-23.

Table II

CONFIDENCE-INTERVAL ESTIMATORS FOR SAMPLES TAKEN FROM A
RAYLEIGH DISTRIBUTION, FOR SEVERAL CONFIDENCE LEVELS, P

Sample Size, n	Confidence-Interval Estimators				
	P = 99%	P = 95%	P = 90%	P = 80%	P = 60%
4	—	—	1.59	1.11	0.66
5	—	1.68	1.29	0.90	0.57
6	1.86	1.42	1.10	0.82	0.51
7	1.61	1.25	1.0	0.74	0.46
8	1.43	1.13	0.90	0.68	0.43
9	1.30	1.04	0.84	0.63	0.40
10	1.21	0.97	0.79	0.59	0.38
11	1.13	0.91	0.74	0.56	0.36
12	1.07	0.86	0.70	0.53	0.34
13	1.01	0.82	0.66	0.51	0.33
14	0.96	0.78	0.64	0.49	0.31
15	0.88	0.75	0.62	0.47	0.30
17	0.85	0.70	0.57	0.44	0.28
20	0.77	0.63	0.52	0.40	0.26
25	0.68	0.56	0.46	0.36	0.23
30	0.61	0.50	0.42	0.32	0.21
41	0.52	0.43	0.36	0.27	0.18
51	0.45	0.38	0.32	0.25	0.16
61	0.43	0.35	0.29	0.22	0.15
81	0.36	0.30	0.25	0.19	0.13
101	0.32	0.27	0.22	0.17	0.11
201	0.22	0.19	0.16	0.12	0.08

Note: The width of the confidence interval centered on the sample median is given approximately by the product of that median and the factor from the table.

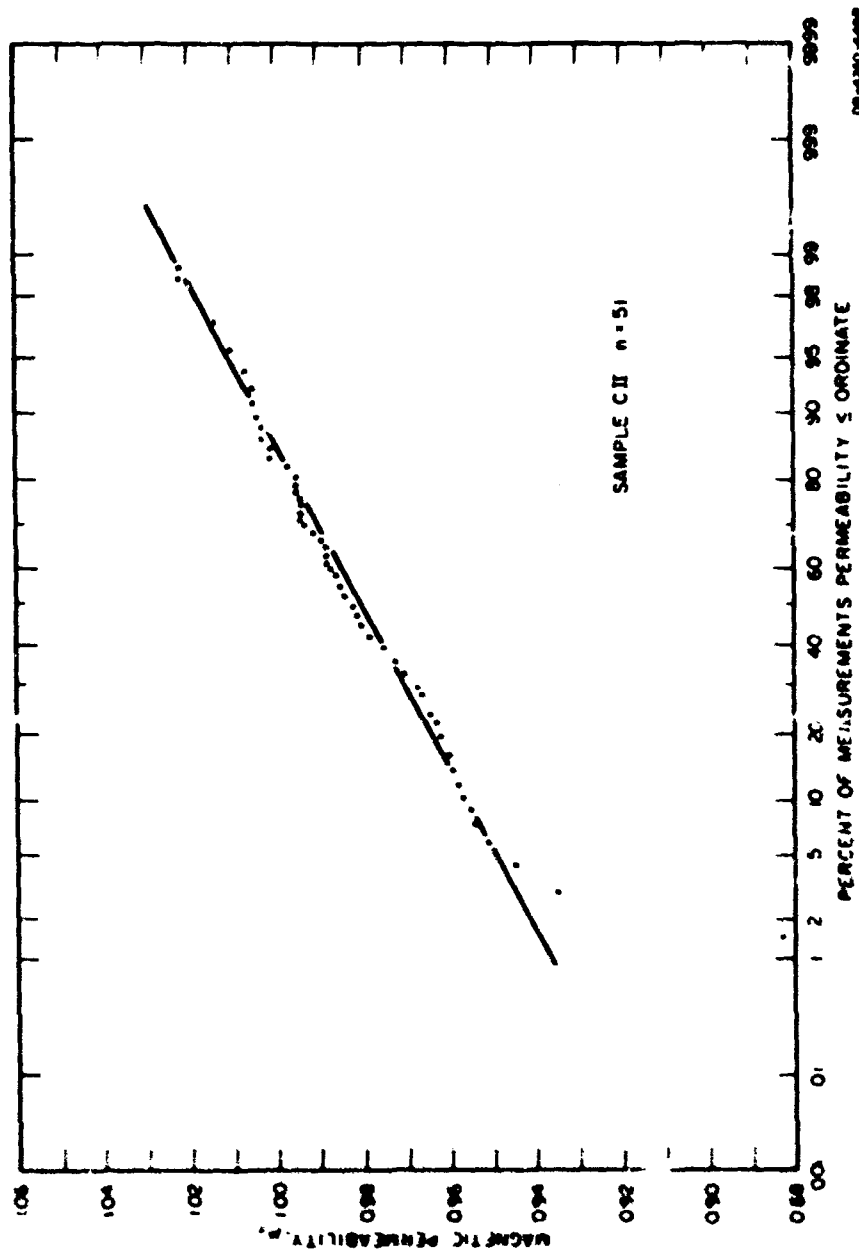
Another distribution of interest to us is that of the magnetic permeability results for vegetation. Initially, we had assumed that μ_r must be 1.0 for vegetation, with some Gaussian scatter (involving true measurement error) about that as a mean. But our results have consistently indicated mean μ_r (see Fig. 32) less than 1.0, especially for the lower frequencies where the probes and the approximations made about the medium should be at their best. Now we are forced to conclude that, if our measurement techniques are not introducing bias, the structure of the vegetation medium gives rise to a magnetic effect. This latter idea is not far fetched; it is well known that microwave delay lenses made up of regular arrays of conducting cylinders act as an artificial dielectric²⁵ whose properties are well-behaved for element spacings less than about 0.1λ . At HF, the random spacing (NND) of stems in undergrowth or forest may be a secondary effect, so that the stems or tree boles could be treated as conducting* cylinders in an array whose effective element spacing was the average NND. Such a "regular" array would be anisotropic, dielectric, and diamagnetic, as the following equations²⁶ indicate:

$$\begin{aligned} \epsilon_r(\perp) &\approx 1 + \frac{\pi d^2 \rho}{2} & \epsilon_r(\parallel) &\approx 1 + \frac{\pi d^2 \rho}{4} \\ \mu_r(\parallel) &\approx 1 - \frac{\pi d^2 \rho}{2} & \mu_r(\perp) &\approx 1 - \frac{\pi d^2 \rho}{4}, \quad \text{NND} < \lambda \end{aligned}$$

where d is the cylinder diameter (or average stem diameter at breast height) and ρ is the number of cylinders (or trees) per unit area perpendicular to cylinder length. The parenthetical symbols indicate whether the primary E field is parallel to the cylinder's length. Unfortunately, we have no good way of testing the applicability of these equations for our results, since the probes cannot resolve anisotropy well.[†] We can

* Lossy, but conducting--their intrinsic conductivity may be as high as 0.44 mho/m. See Appendix A.

† The ratio of orthogonal components in the E field of the 300-M. probes is ≈ 2 . (See Reference 38.)



DB-4340-4444

FIG. 32 DISTRIBUTION OF TYPICAL " , RESULTS OBTAINED WITH SMALL PROBE IN UNDERGROWTH
AT 15 MHz

bound the constants, however. By using the relations above, and forestry survey data for the Chumphon undergrowth CII (Appendix C), we can estimate the effective values that the probe should have measured:

$$1.01 < \epsilon_r < 1.02$$

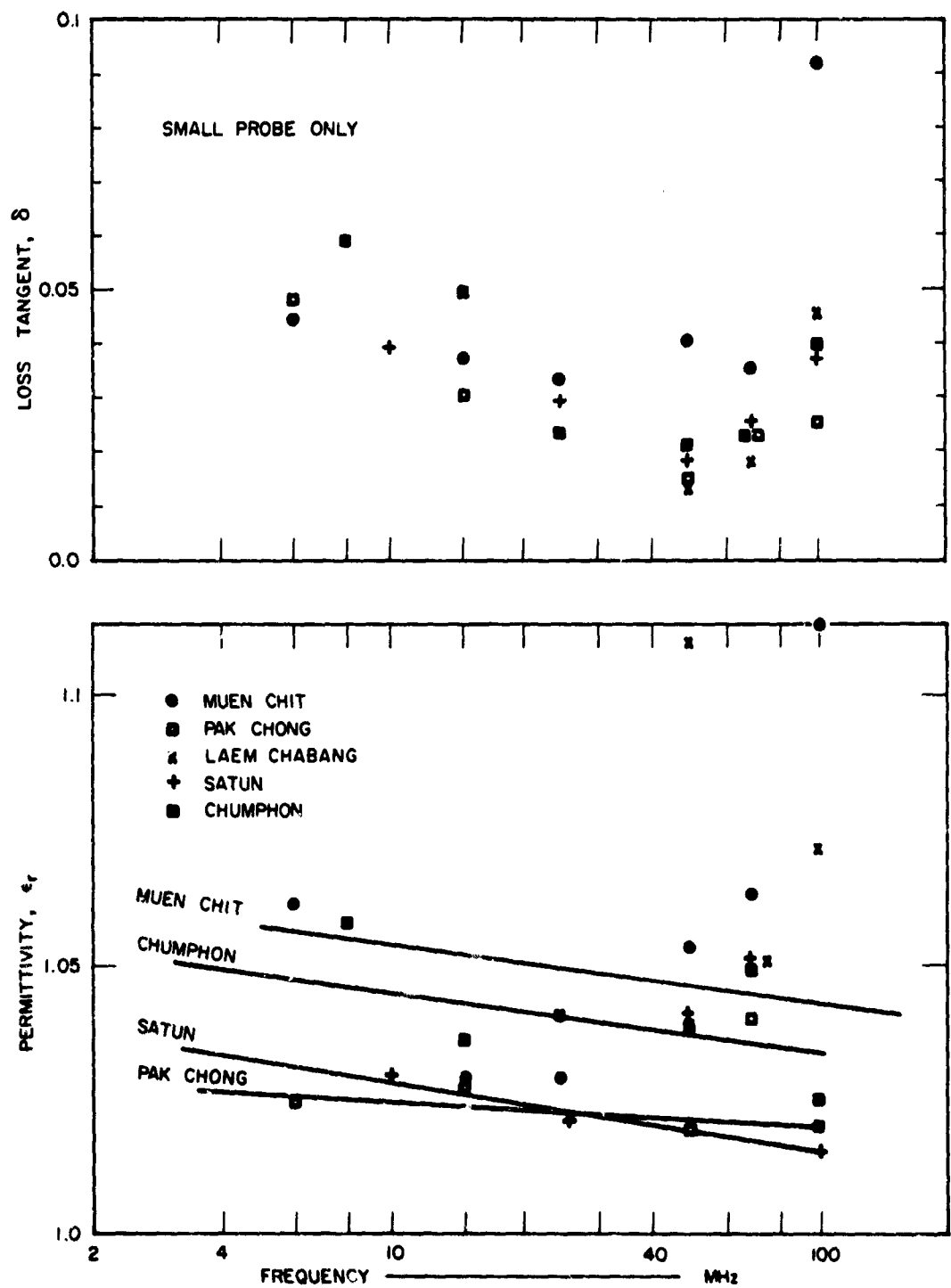
$$0.98 < \mu_r < 0.99$$

These are only slightly similar to the measured results (see Figs. 32 and 33) for Chumphon CII--the bounds are much too tight, and their medians are not nearly so different from 1.0 as those indicated by the measurements. An increase in the effective diameter of the constituent cylinders or a change to some other shape (perhaps a tapered cylinder or ellipsoid) seems indicated for better prediction of the results. Actually, too, the equations given for ϵ_r are obviously crude because they neglect the direction of propagation, for wave guiding may occur among stems viewed from a favorable orientation (as in an orchard), causing their effective ϵ_r to be less than unity. This is the phase-advancing effect of some waveguide modes. That it does seem to occur is evident from Fig. 24. At present the best we can do is to specify the ranges over which effective μ_r and ϵ_r may be expected to vary in forests, so that checks can be made on the variance those effects may cause in propagation-model predictions. We have rarely found ϵ_r or μ_r to fall outside the following experimental bounds:

$$0.9 < \epsilon_r < 1.2$$

$$0.8 < \mu_r < 1.1$$

The simple model of the vegetation viewed as a collection of cylinders scattered randomly over an area perpendicular to their lengths has also been used in Appendix A to illustrate a possible scheme for obtaining effective vegetation conductivity if the intrinsic conductivity of stems is known together with their average diameter and spacing. The



DB-4240-639A

FIG. 33 COMPARISON OF MEDIAN ϵ_r AND δ MEASURED IN UNDERGROWTH AT FIVE SITES

relation derived for σ does not have a frequency dependence, and is given only for illustration. We are not yet prepared to define a frequency law for the effective conductivity (or loss tangent) of vegetation.

One aspect of the use of a cylindrical-constituent artificial-dielectric vegetation model is the simplification that results from using ρ instead of constituent spacing. Of course, ρ can be derived from spacing for a regular array; but what about a random array? When spacing is Rayleigh distributed, the problem of relating ρ to spacing is quite simple, as shown in Appendix B, so that we should hope that tree or stem or branch spacing distributions found in nature can always be approximated by a Rayleigh formula.

One further comment must be made on the nature of living vegetation. In spite of the fact that, for both undergrowth and mature forest trees, NND are approximately Rayleigh distributed, and height and diameter are approximately log-normally distributed,* there is usually no scalar relationship between the two types of growth. Undergrowth cannot be used as a radio-propagation scale model of a forest because the mean spacing-to-diameter ratio in natural undergrowth is too large. If scaled up in diameter, undergrowth would be spread out like trees in a park. If we can develop rules for scaling with frequency, this may allow us to infer effects for man-made but not natural forests.

B. Generalized Results

Although our ideas about the way in which a forest acts as a medium for radio-wave propagation may be changing, we can draw useful inferences from a view of the OWL measurement results in the context of a forest slab model. True, the parameters μ_r and ϵ_r could not vary over the ranges found experimentally if the forest were actually slab-like, but the expected values of these constants in all distributions of our results have been very near unity. The occurrence of ϵ_r or μ_r at the limits shown in Table III is rare enough so that the slab-model approach will be a good

* See Ref. 26 and Appendices to this report.

approximation for most purposes, at frequencies below that for which the mean stem or branch spacing (or NND) is $\lambda/10$ --that is, at HF (30 MHz) and below, if we take only tree boles into account.

Table III

EXPERIMENTAL LIMITS FOR ϵ_r AND μ_r

	HF	VHF \leq 100 MHz
ϵ_r	0.9 to 1.2	1.0 to 1.1
μ_r	0.8 to 1.1	0.8 to 1.1

At these frequencies the fact that ϵ_r and μ_r may be anisotropic probably has little significance for the slab modelist. The use of values near unity and invariant with frequency should suffice. But inversion of slab models has shown^{*5,6} that they require quite different horizontal (σ_H) and vertical (σ_V) forest conductivities to allow that good predictions of path loss measurements be made for polarizations so directed.

The OWL probes are not well suited to separating anisotropic effects of the vegetation. The results shown in this report are biased somewhat toward a representation of horizontal effects, since the probes were usually in the horizontal plane and their horizontal E-fields in that position contain more energy than do the vertical. (Recall that the ratio is 3/2 for a 300- Ω OWL.) The OWL probe results usually lie between σ_H and σ_V obtained from model inversion,^{*5} and show a frequency dependence similar to that of σ_H . Thus our results might be taken as approximate upper limits for vegetation effective conductivities to be used in modeling for horizontally polarized wave propagation.

* Private communication from Dr. J. E. Spence, Jansky & Bailey Division of Atlantic Research Corporation.

* Although we have few results based on tree growth rather than undergrowth, we have no reason to distinguish between the electromagnetic effects of the two types of vegetation at HF (see Table IV).

A word of caution is in order, however. At 100 MHz we are scattering significant energy out of the transmission line mode unless the growth is extremely dense. The effect on our results which may be seen in many of the σ graphs, is the opposite of the scattering effect of the medium on freely propagating waves. As frequency is increased the forward-scatter cross section of the medium should increase, allowing one to approximate the medium by a slab having a negative $d^2\sigma/df^2$. But our curves of $\sigma(f)$ often increase slope as f approaches 100 MHz (see Laem Chabang, Muen Chit, Satun on Fig. 34), an indication that our measurement technique may be breaking down above 75 MHz.

Realistic ranges of δ and σ may be taken from Figs. 33 and 34 which show median results obtained for undergrowth at all the sites we visited in Thailand. We added, on Fig. 34, results obtained in the most dense patch of undergrowth we have ever found, in order to place an upper limit on attenuation of RF energy passing through living vegetation. The attenuation rate scale on that figure applies strictly to that which would be effectively encountered in a vegetation medium of infinite extent. In usual practice, the existence of boundaries allows for wave propagation via surface modes that suffer less attenuation with increasing distance than these results indicate. But for the case of an air-rescue beacon, for example, the maximum or probable power losses for transmission through undergrowth can be estimated from the figure.

A further discussion on the range of variation of σ (and hence δ) is necessary because, while we gave realistic limits for ϵ_r and μ_r above, based on all our measurements, we have only discussed effective σ (and δ) of undergrowth. In speaking of the effects among larger trees, we must restrict ourselves to the frequency range (3-16 MHz) of the results obtained with the large probes and presented in Figs. 22, 24, and 25. We can compare the effective conductivity ranges measured among tree boles and canopy foliage with those obtained at HF undergrowth as in Table IV.

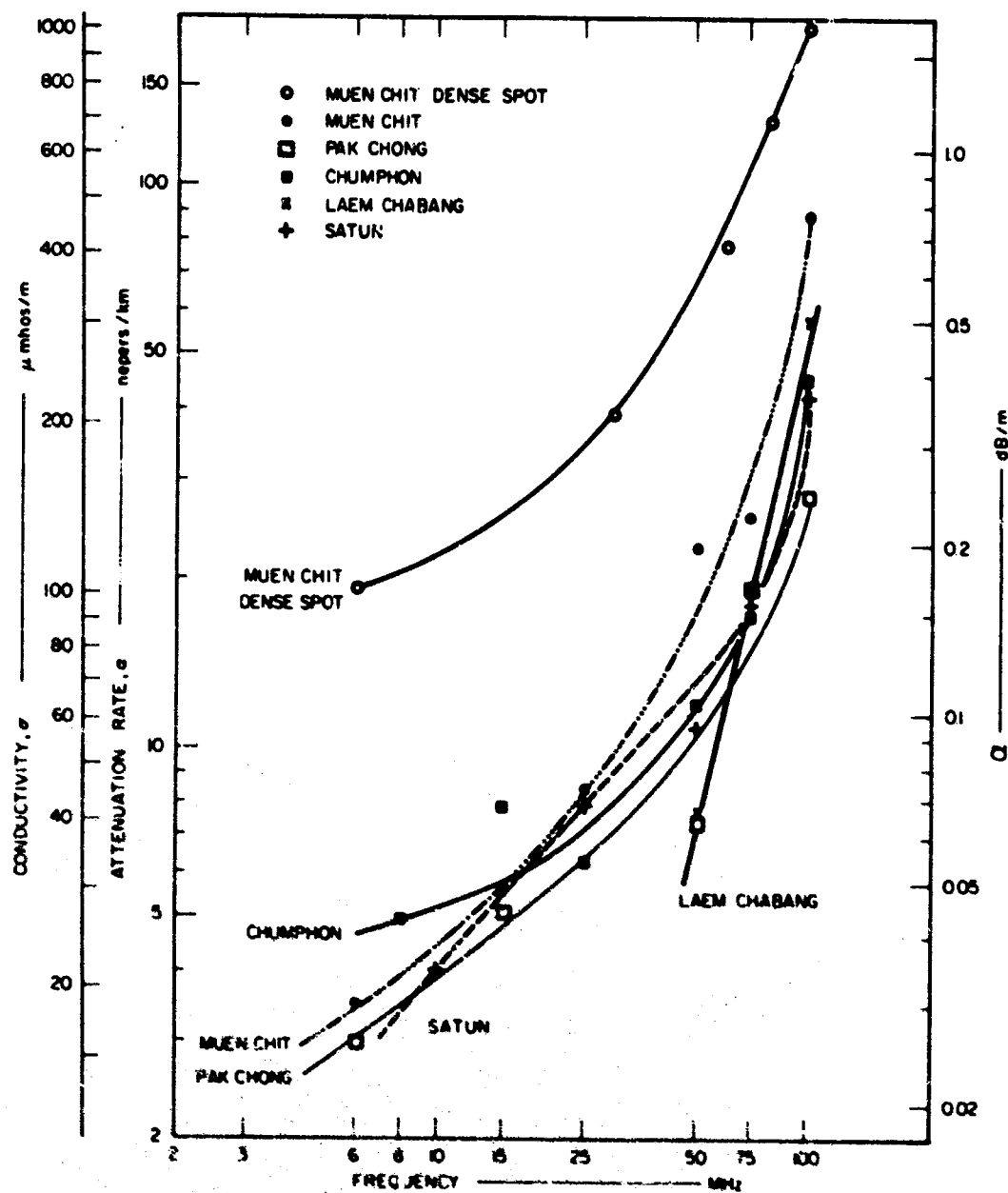


FIG. 34 COMPARISON OF MEDIAN α AND σ MEASURED IN UNDERGROWTH AT FIVE SITES

Table IV

RANGE OF σ AND δ MEASURED AMONG TREES AND UNDERGROWTH AT HF

Frequency (MHz)	Undergrowth*		Tree Boles†		Tree Canopy†	
	σ	δ	σ	δ	σ	δ
6 - 8	5 - 60	0.02 - 0.15	2 - 60	0.008 - 0.15	1.5 - 32	0.02 - 0.09
12 - 16	15 - 200	0.02 - 0.15	1 - 54	0.008 - 0.15	4.0 - 230	0.02 - 0.16

* Quartile Ranges

† Sample Ranges

The undergrowth limits are taken from quartile ranges of all samples obtained with both large and small probes except the wire-probe results for Sample CII shown in Fig. 23. We decided the wire probe was too short, compared with its spacing, to work well in that instance. The Laem Chabang results, obtained only at VHF Xelelop frequencies, do not apply either; we suppose that, had we HF results for Sample LII, they would have decreased the lower limits shown for undergrowth in Table IV. The limits for tree boles came from Figs. 22, 24, and 25; those for canopy include results for the middle and upper regions shown in Figs. 24 and 25.

The significance of Table IV is immediately felt: the sample ranges for the tree measurements indicate nearly the same loss (or less) as do the quartile ranges of the undergrowth measurements. We have no more than six independent measurements among the trees in any one case: often there were only three, as in the highest canopy. But probably, if we had as many canopy measurements as we have for undergrowth, the effective (or median) σ and δ for all these regions would be similar. The absence of a central tendency in the canopy and bole results goes against this statement, however, and it must be tested by making a large enough number of measurements to show the shape of the distribution for effective σ and δ of trees. If the undergrowth and tree constants were

as similar as Table IV indicates, the similarity would explain why model predictions* based on undergrowth measurements^{7,27} seem to be valid for an entire forest.

Although the effective values of the undergrowth constants (Figs. 33 and 34) could sometimes be said to increase with greater growth density, from Satun ($\rho = 2.4 \text{ stems/m}^2$) through Muen Chit (3.4) and Chumphon (5.25), the Pak Chong undergrowth, which was the most dense ($\rho = 6.8 \text{ stems/m}^2$), caused lowest loss. The correlation between ϵ_r , δ , and σ on the one hand, and ρ , d , and λ on the other, is not yet clear. The most significant aspects of Figs. 33 and 34 for the radio engineer or botanist-physicist are the grouping trends, which indicate that various species of plants, growing in widely separated areas of the tropics, seem to have electromagnetic effects much in common. Even at 100 MHz, where the greatest scatter occurred and the usefulness of the vegetation-slab medium concept seems to come into question, the spread in median results was only about one-half order of magnitude for δ and σ . This may not be an unrealistic tolerance for a communication-system model. Thus it may be that in many cases radio engineering design tolerances can be set without recourse to specific knowledge about a forest environment. Further, this comparison by sites indicates that there is something similar in the makeup of the plants (probably their intrinsic conductivity),[†] that, coupled with a relatively invariant growth habit at least for the places we visited, constrains their effective electromagnetic behavior as a wave medium to such a small range. It is quite small compared with the relatively large variations of the electric constants of the earth in which these plants were growing.

We have compared median electric ground constants from eight types of soil that we measured at six sites in Thailand--the five discussed in this report, plus a sampling taken in an open rice paddy near the

* Horizontal polarization only.

† See Appendix A for a discussion of intrinsic conductivity.

MRDC-EL in Bangkok. These are presented in Figs. 35 and 36. They tell a consistent story based on water content. The driest soil has the least ϵ_r and σ ; the change of ϵ_r with frequency is slight, of σ quite high. The Bangkok rice paddy and the Chumphon IV and V (swamp) samples held the most water; Satun soil was also very wet. These four samples had the highest ϵ_r values, and typically for very wet soil, the greatest change of ϵ_r with frequency. They also had the highest conductivities, for the most part, but the least rate of change of σ with frequency. Pak Chong soil, which was rocky, and Muen Chit soil (sandy) had constants lying between these extremes of magnitude and slope. The frequency dependence of conductivity suggests a law of the form

$$\sigma = Af^u$$

where A depends on soil porosity and soil moisture content, and u depends on moisture content, and, perhaps, frequency. The range of earth conductivity covers about three orders of magnitude (excluding the rice paddy) and it is highly dependent on the presence of ground water. Yet the plants depending on this same water had, en masse, effective conductivities bounded within one-fifth that range.

Thus, knowledge of soil alone does not tell us enough about plants that will grow there, though soils with similar conductivities (Muen Chit, Chumphon CII, Satun) seem to support living plants with similar intrinsic conductivities (see Appendix A). But stem spacing, which can be related to stem number density (see Appendix B) may provide, together with soil conductivity, the key to dielectric behavior of groups of plants or forests.

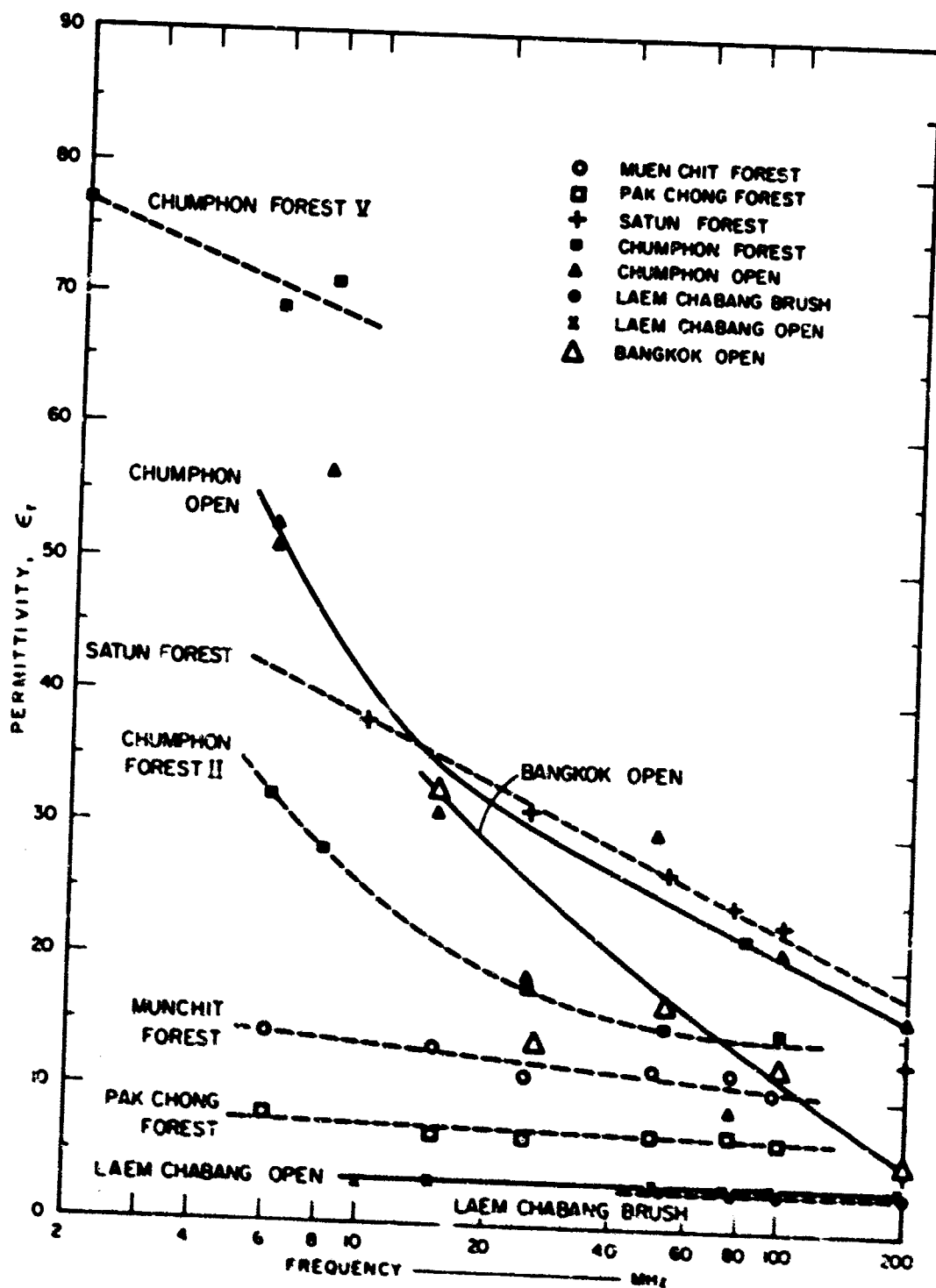


FIG 35 MEDIAN SURFACE GROUND PERMITTIVITY MEASURED AT SIX PLACES IN THAILAND

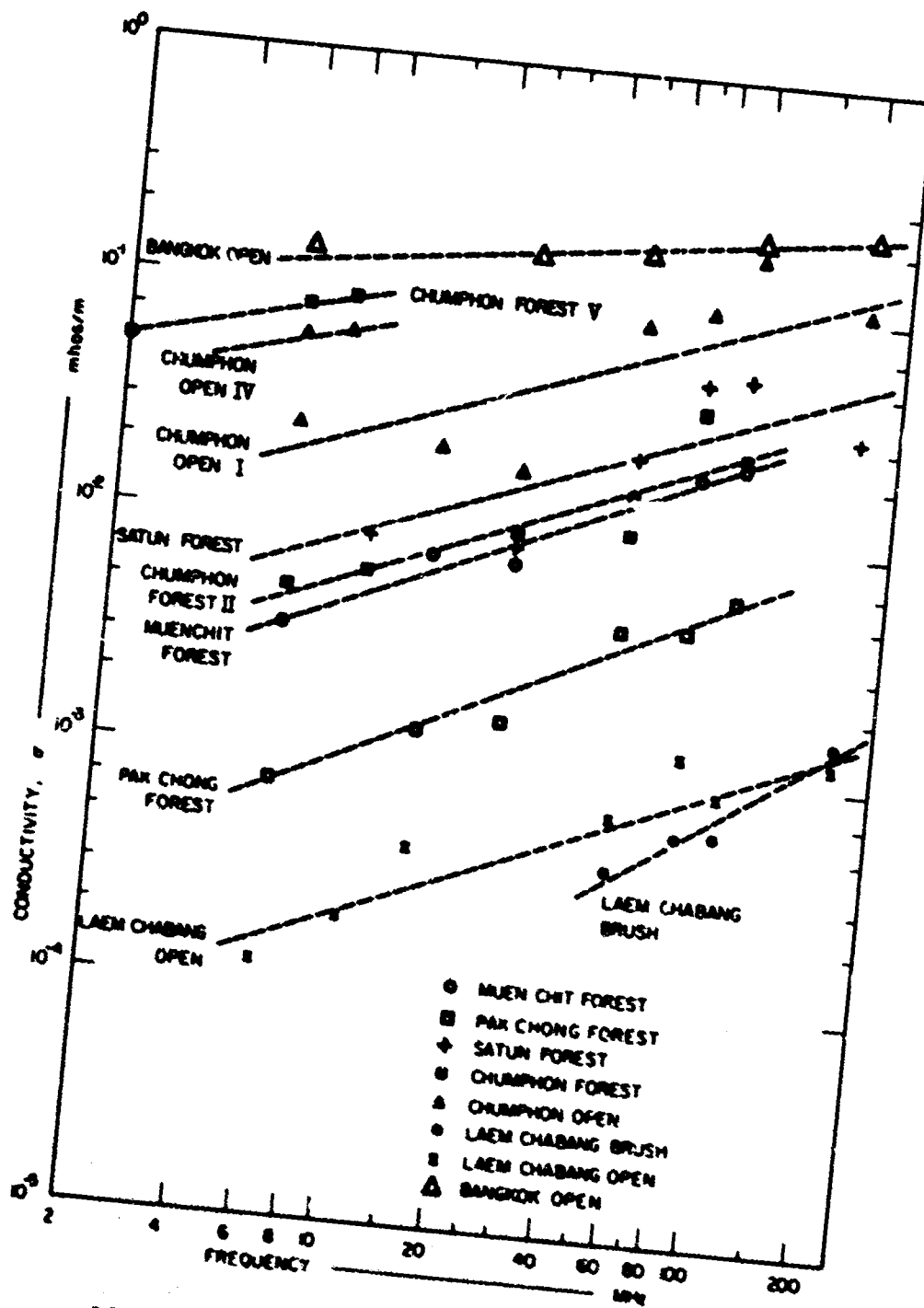


FIG 34 MEDIAN SURFACE GROUND CONDUCTIVITY MEASURED AT SIX PLACES IN THAILAND

RECOMMENDATIONS

1. Future sampling of the electric constants of vegetation should be done on a more random basis to reduce the bias that arises from the tendency of the field crew to orient the probes to the more dense growth. We suggest that a regular array of stations be chosen throughout the volume to be studied,^{*} each assigned a number in a set, and then n choices of numbers from that set be made from a table of random numbers based on that set. The interval between stations should be less than half the probe conductor spacing. The sample size n will be greatest for the least dense growth, but should always be made greater than 30. With this sample size, there is a 90 percent probability that the true median is within 20 percent of the observed median.
2. The vegetation probe should be used primarily to obtain electric constants as a function of height. The wire probe is best used for this, unless foliage is extremely dense, when pipe is simpler to use; but wire can be strung in fairly dense growth by using long bamboos to pull it through. However, when using the large-scale probes, care must be taken to obtain a large number of independent samples, just as with the small probe. It is not true that since the large probe senses more vegetation it measures more accurately, for we are then dealing with mature trees, and the problems of small probe work are just scaled up, in a simplified sense. The reason results with the wire and pipe probes often indicate more loss is that these large probes sense mostly trees, which act more like scatterers at any given frequency than does undergrowth. The small probe will never be bothered by this; it cannot be used with a large tree nearby unbalancing it.

* If the study is to represent a forest well, the volume should be large, and include the tree canopies.

3. If a gross study of the electric constants of vegetation in large areas or several forests is desired, the probes should be used only at random check-points for height profile. The main body of data could be obtained by making path-loss measurements and inverting the Sachs/Wyatt model. This technique would have the advantage, besides ease, of providing polarized information not available from the probe results. It would not, however, provide information on undergrowth beneath the trees.
4. The connection between stem number density and electric properties of vegetation should be established for different types of forest. A study composed of the first three recommendations plus an intensive vegetation survey and aerial photo-mosaic analysis at a convenient forest site would be more than adequate to estimate the accuracy with which vegetation electric constants can be predicted from aircraft or satellite reconnaissance data.
5. The ideas of Founds and LaGrone²⁸ should be extended from leaves to stems. Trees seem to be conductors even at VHF,^{16,29} though their quality as radiators may be in dispute, and an array of trees should probably be treated as a conductive artificial dielectric, at least for HF and lower frequencies. This implies that effective μ_r of the forest may be somewhat less than unity, contrary to all current assumptions.
6. The effect of varying μ_r in the model equations for radiowave propagation in the forest should be checked. The propagation constant is proportional to $\mu_r^{1/2}$.
7. The use of the assumption that effective ϵ_r of the vegetation medium must always be greater than unity should be discontinued.
8. Whenever we do work in the field we should measure the electric constants of earth as a function of depth to about 2 meters and take a core sample of the soil at each depth. In this way, we can investigate whether the conductivity of soil has much influence on that of the plants growing there. Furthermore, such data at radio frequency, so scarce in the literature, are of great importance

to the antenna engineer and of some importance to the models.
The probe technique is recommended.

9. When measuring ground constants at RF by the approximate method (see Sec. II-A), the connections from probe to impedance bridge should be made as short as possible to improve accuracy. This means using an unbalanced cable, not coax balun.
10. Environmental surveys in support of forest radio propagation studies should concentrate on the following parameters in addition to species identification:

Nearest-neighbor-distance statistical distribution

Stem-diameter statistical distribution *

Stem-height statistical distribution

Number of stems per square meter

Description of canopy coverage and layering

Estimate of undergrowth height and number of stems per square meter that reach breast height (1.3m)

Stem conductivity measured at audio frequency or at dc [†]
(This will probably require a statistical distribution)

Soil moisture by weight and by volume

Soil conductivity [†] at surface and below, for each type of soil found

Soil pH, salinity, and type.

* If stem height and diameter distributions can be empirically related for classes of forest, then only height need be specified.

[†] This measurement can be made using techniques similar to those of geophysical electric prospecting. The polar dipole array³⁰ operated at audio frequency is recommended.

Appendix A

BIODENSITY EXPERIMENTS

Appendix A

BIODENSITY EXPERIMENTS

We attempted to relate the mass density or biodensity of undergrowth in two of our samples to the electrical properties as measured with the small probe at 50 MHz. The procedure, involving cutting, packing the cuttings in a hopper, weighing, and probing as the weight changed, was similar to that described in the appendix to Ref. 4. The weight change of the Muen Chit sample (MII) was 25% in the first 24 hours after cutting, but there was a weight gain after 38 hours, and puzzling fluctuation thereafter. Moreover, the weight did not change during the hours of darkness although several powerful sun lamps were focused on the sample. By the 55th hour it was plain that the sample was infested with insect life that was rapidly reducing it to a more elementary state, and the experiment was discontinued. We were able to correlate the changes in sample effective permittivity measured by the probe with the fluctuation of air moisture, however. We measured the effect of air moisture on wood (the sample was sheltered from rain) by periodically weighing standard oven-dried wooden sticks* hung beside the cut foliage. This gave us an index of wood moisture absorbed from the air in percent by weight, for the vicinity of our experiment. The results are shown in Fig. A-1. There is a general slight trend of decreasing ϵ_r with decreasing weight, but the most significant feature of the graph is the correlation of ϵ_r with wood moisture. The effect of humidity on the dried sticks peaked between 0900 and 1000 local time; the peak in effective ϵ_r of the cut sample was at 1000 on the first two days. Moreover, there is a general slightly decreasing trend in fuel moisture over the period of the experiment that may be correlated with the same trend in ϵ_r . Thus

* Part of a forestry fuel-moisture kit purchased in California. These moisture readings depend on air humidity but reflect the time lag inherent in absorption by the wood.

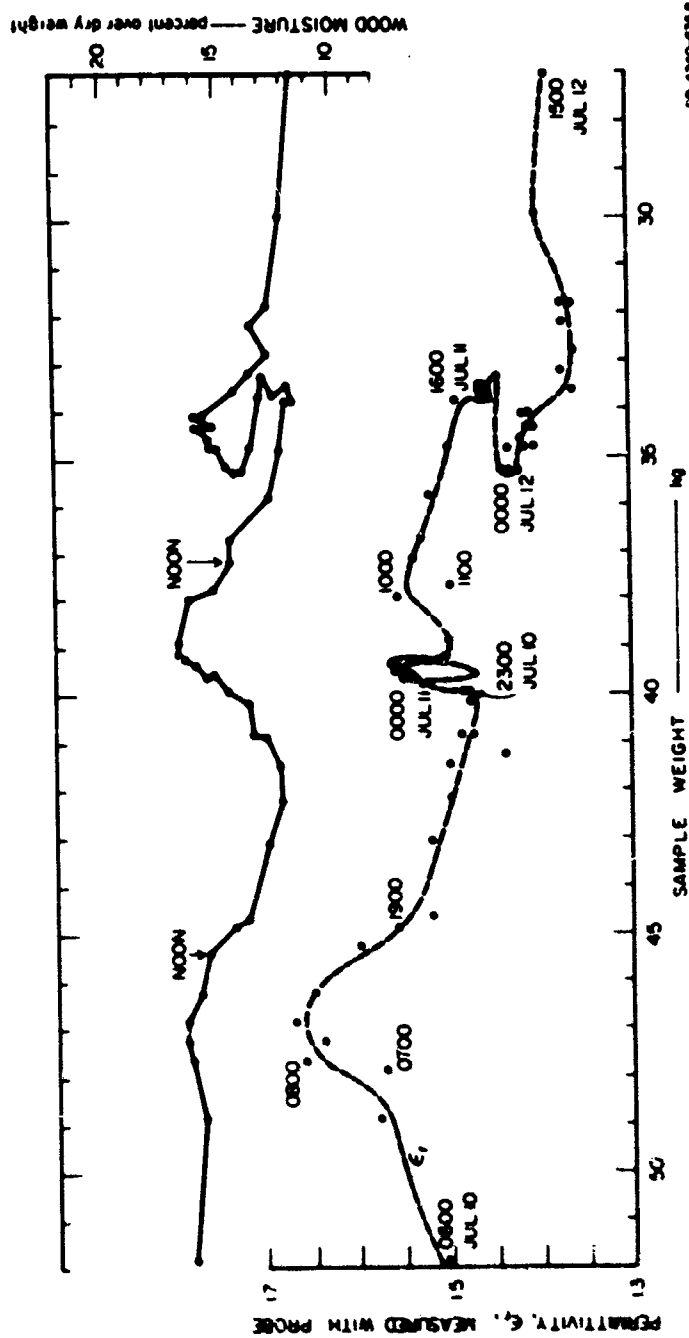


FIG. A.1 RESULTS OF BIODENSITY EXPERIMENT PERFORMED ON FRESHLY CUT UNDERGROWTH OF MUEN CHIT SAMPLE MII

we concluded that we would not be able to relate sample weight and water content in this case. The most probable explanation for the failure of the experiment in that sense is that the weight changes were owing largely to the presence of insects, notably ants, who preyed on the cut vegetation in large numbers and were immune to our insecticides. We decided that such experiments are not suited to field conditions in Thailand and did not repeat the attempt to air-dry cut vegetation.

However, we can obtain an upper bound on the intrinsic conductivity (σ_1) of the vegetation by using the relation⁴ between effective conductivity (σ) of a mixture of air and one other constituent, the fraction (F) of that constituent in the mixture, and the constituent's intrinsic conductivity:

$$\sigma \leq \sigma_1 F$$

We have made measurements of effective conductivity for two samples of vegetation that were subsequently weighed: Muen Chit MII and Chumphon CII. We are safe in assuming that the intrinsic conductivities of these two samples did not change within several hours after cutting.^{4,20,31} Then, if the subscripts 1 and 2 refer to conditions before and after the vegetation was cut, we may write:

$$F_1 \approx F_2 \sigma_1 \sigma_2$$

in order to estimate the fraction of vegetation in the living sample. We can estimate F_2 by assuming that the vegetation weight is essentially that of its water content, whose density is 10^3 kg m^{-3} , so that the initial weight of the cut sample is directly related to its volume. Then, dividing this volume by the volume of the hopper occupied by foliage, we obtain F_2 , and can compute σ_1 and F_1 . We can also obtain F_1 approximately by using the mean height of the living vegetation times the plot area as the normalizing volume.

The results of such an analysis, as applied to the Muen Chit and Chumphon undergrowth samples, are given in Table A-1. The values for F_1 and σ_1 (primed) were obtained based on mean growth height

Table A-1

DATA FOR DERIVATION OF INTRINSIC CONDUCTIVITY OF VEGETATION
AT 50 MHz ESTIMATED USING WEIGHT OF CUT UNDERGROWTH

Sample	Muen Chit MII	Chumphon CII
Area cut, m ²	12.25	17.5
Mean height, m	1	2.5
Upper decile height, m	3	4.5
Hopper vol., m ³	1.3	1.57
Initial weight, kg	51.8	61.2
F ₂	0.04 (0.029)*	0.04 (0.029)
σ ₂ , mmho/m	0.98	1.31
σ ₁ , mmho/m	25 (35)	33 (46)
σ ₁ , μmho/m	140	65
F ₁	0.006 (0.0043)	0.002 (0.0014)
F' ₁	0.004 (0.0029)	0.0016 (0.0011)
σ' ₁ mmho/m	35 (49)	41 (57)

* See text for explanation of numbers in parentheses.

We assumed, for the initial calculation of results, that the plants were 100% water. But if we use the lower saturation limit of moisture content for angiosperms (MC ≥ 75%), then the basic wood density is³¹

$$D = \frac{1}{0.65 + MC/100} = 0.715 \times 10^3 \text{ kg/m}^3$$

and we must decrease our values of F₂, F₁, and F'₁ by 28.5%, and increase σ₁ and σ'₁ by 40% as shown in parentheses in Table A-1. On this basis, the intrinsic conductivity of vegetation may be of the order 0.03 to 0.06

mmho/m. When we compare this range with the estimate obtained in the same way for California willow cuttings (0.03 mho/m) in the fall of 1965⁴ we begin to suspect that σ_1 does not vary greatly* from one vegetation sample to another.

The fractional volumes obtained in this way, being of the order 1-to- 5×10^{-3} , seem reasonable for very dense vegetation. But it was noted that the Chumphon undergrowth seemed more dense to the eye than that of Sample MII, and their respective stem densities were 5.25 and 4.9 stems/m². Moreover, the mean stem diameter[†] in Sample CII (1.2 cm) was twice that in Sample MII, so that we should expect the fractional volume of vegetation obtained from weighing, etc., to be greatest for Sample CII. That it was not, points up a basic problem in dealing with biodensity. Biodensity does not represent an average growth tendency unless the variance in vegetation height and diameter is quite small, but depends mostly on the largest and/or heaviest members of the sample; furthermore, it is quite dependent on plant species present.

It is probable that our σ_1 estimates based on biodensity are somewhat low for general application, especially since non-porous angiosperms are the most dense of all plants. We can form another estimate of F_1 based on the stem surveys done in our samples to see what the highest probable values of σ_1 might be. To do this, we ignore branches and leaves, and form a model of the sample having ρ stems per m² whose dimensions are equal to the median stem diameters[‡] and heights

* By another indirect and more approximate method, Dickinson et al.¹² estimate RF conductivity of California Eucalyptus stems at 0.24 mho m.

† Stem diameter of undergrowth plants was measured by caliper at a height of 0.3 meter above ground, since diameter at breast height could not always be measured (see Appendices B through G).

‡ If there is upward taper along the stems, this use of the diameter measured 0.3 m above their base tends to compensate for the neglect of branches and leaves.

surveyed. Then define F as the ratio of the sum of all ρ identical stem volumes (cylindrical) to the mean height on a square meter of the sample. That is,

$$F \approx \frac{\rho \pi a^2 h}{h} \approx \rho \pi a^2$$

where a is the mean radius of stems in the sample. The value of ρ is taken from the stem count. The results of this analysis are shown in Table A-2.

Table A-2

DATA FOR DERIVATION OF INTRINSIC CONDUCTIVITY OF
VEGETATION AT 50 MHz ESTIMATED USING ONLY GEOMETRY

Sample	Muen Chit MII	Chumphon CII
Number density ρ , m^{-2}	4.9	5.25
Mean radius, m	0.003	0.006
F	1.32×10^{-4}	5.94×10^{-4}
σ_1 , mho/m	1.0	0.11

There is not a grave difference between the intrinsic conductivities of the two samples obtained in this way, even though they represent widely varying species and growth conditions (see Appendices B and F). Indeed, we may choose $\bar{\sigma}_1 = 0.35$ mho/m and calculate σ_1 and σ_2 within about one-half order of magnitude using

$$\sigma = \bar{\sigma}_1 F \approx \bar{\sigma}_1 \rho \pi a^2$$

It is tempting to apply this formula to predict the effective conductivity of the Satun undergrowth sample (SI). Sample SI was on a 12.25 m^2 plot, having only 29 stems whose mean radius was 0.5 cm. Thus,

$$\rho = 2.37 \text{ stems/m}^2$$

and

$$\sigma \approx 0.35\pi 2.37 (0.005)^2 \text{ mho/m}$$

$$\approx 65 \text{ } \mu\text{mho/m}$$

at 50 MHz. This compares unfavorably with the median measured value (Fig. 19) of 40 $\mu\text{mho/m}$, but is within 20% of the probable value indicated by the dashed line.*

This "prediction" must be regarded as fortuitous, for it says nothing about the effect of spacing or diameter in terms of wavelength. It may be that the effects of wavelength, diameter, and stem spacing are compensating in the case of dense undergrowth viewed at 50 MHz. Clearly, the approximation is useless for large-diameter stems. More important, we should have to specify the effect of stem orientation in any useful model (i.e., anisotropic model). Only the mass of the stems does not seem directly relevant.

We can conclude, then that the intrinsic conductivities of many different types of plants probably lie within the decade 0.05 to 0.5 mho/m at VHF and that if these may be represented over a given region by a single value, then the effective conductivity of that vegetation should be predictable in terms of stem count, diameter, orientation, and the radio wavelength for which a conductivity estimate is desired. A study should be made toward this end.

* It may be significant that the conductivities of the soils beneath MII, CII and SI were similar (see Fig. 36).

Appendix D

ENVIRONMENTAL SURVEYS

Appendix B

ENVIRONMENTAL SURVEYS

1. Survey Techniques

The basic method of forestry survey involves identifying and measuring trees on a 10 by 40-meter sample plot. Several of these are chosen, usually at random, in a forest, but at SRI sites they were often located near antennas being studied. Each tree having a breast-height* diameter (DBH) greater than 5 cm was identified in these surveys. Its height was measured, in addition to DBH, and its position in the plot recorded. From this position information, the nearest-neighbor distance (NND) between trees could be measured on a plot map. The envelope height of any undergrowth present was usually estimated, and its dominant members identified.

Tree heights were measured using the Haga altimeter, which is similar to a bubble-sextant. The height of a tree is defined as the vertical distance from the top of its canopy envelope to the ground. It is not necessarily perpendicular to the ground slope since the Haga altimeter, like a spirit level, uses the earth's gravitational field as reference. If ground slope is appreciable, it too is measured with an altimeter, and a correction made. Identification of the top of a tree in a dense forest is, of course, a subjective problem, and tree height depends somewhat on the ability of the observer to get an advantageous view of the tree crown.

Tree diameter (at 1.3 meters above ground) is usually measured by taping the circumference and calculating, but a caliper has been used for small, regular-shaped trees and shrubs.

* Standard breast height is 1.3 meters.

The NND is often found by simply taping the distance between trees at breast height, but it is sometimes easier to map a dense growth and make measurements on the map. Only trees actually within the plots are given nearest neighbors in this way, so that a tree outside the border, though it may determine the NND for a tree in the sample, will not give rise to a reciprocal NND. But reciprocity in NND often occurs for close trees within the plot.

Because of our interest in undergrowth, and in the possibility of using it as a scale model for any nearby forest, we requested special detailed surveys of small (usually 3 by 3 meter) plots containing only undergrowth. This was done for us by the MRDC-ES at Chumphon (CII), Satun (SI), Muen Chit (MII), and Pak Chong (PI). The usual measurements were made, except that all stems and vines growing in the plots, above 30 cm high, were studied; since DBH had little significance, stem diameters and spacings were measured at 30 cm above ground.

Visibility in a forest is measured by counting dots painted on three 30-cm-diameter targets as the target array is withdrawn from the observer. The observer uses supported binoculars at 1.20 meters high. The center target is also 1.20 meters high; the others are at 0.5 and 1.90 m. The count is usually made for 5-meter increments of target distance and for 8 radials of equal spacing.

Soil core samples were also taken each 15 or 30 cm to a depth of 2 meters at the forestry plot corners. These were tested in situ for grain size, penetration (cone index), and pH (hydrogen ion content); but sealed samples were sent to the SEATO laboratory in Bangkok for determination of specific gravity, plasticity, etc., and mineralogical analysis where required. Moisture content analysis was done at the MRCD-ES laboratory. The moisture content was found in percent by weight, using a drying process. The Troug soil-reaction kit and lime color chart are used to measure pH. Soil color is assessed by comparison with Munsell soil-color charts. Cone-index (penetrability) values are measured with a cone penetrometer. Water-table height is noted if it is within 2 meters of the surface. Permeability to water (or compactness) is

estimated as "rapid," "moderate," or "poor;" another subjective evaluation is that of soil texture, which is done by manual touch.

Some or all of these environmental parameters were obtained at the five sites described in this report, and are presented in detail in reports published or in preparation by the MRDC-ES.^{18,19,33,34,35} But the most important of these parameters for the radio physicist, in order of significance, are:

NND given by statistical distribution, and/or tree density

Height and DBH given by statistical distribution (these two parameters can often be related)

Soil moisture content

General soil type.

In addition, the botanist-physicist probably has a great interest in vegetation species classes and soil pH. We present in the following appendices only the most important of these environmental parameters, with the exception of species listings, related to our studies of the electric properties of the environment at Chumphon, Pak Chong, Laem Chabang, Satun, and Muen Chit, Thailand.

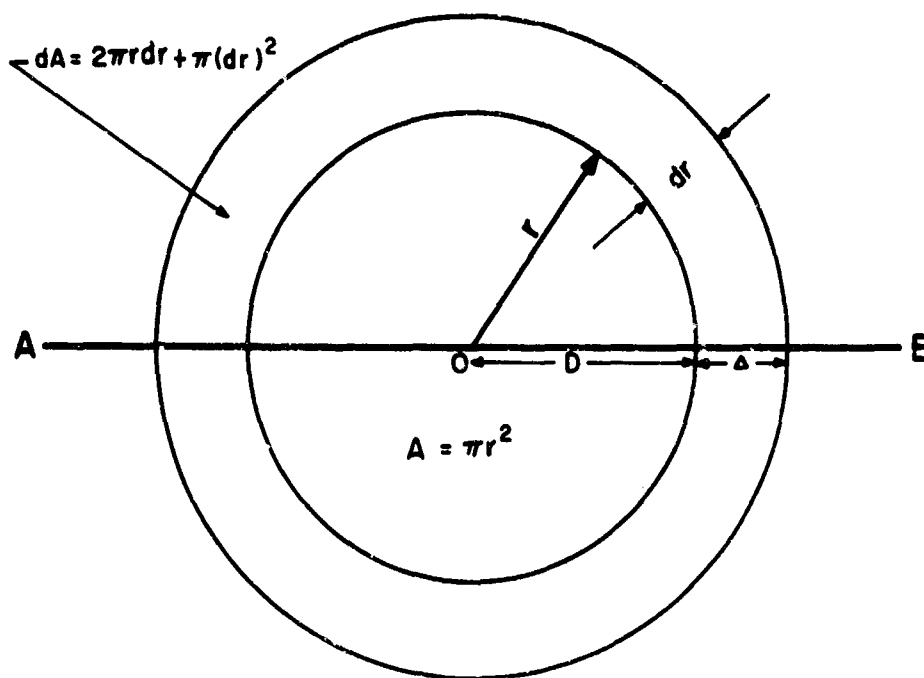
2. Theoretical NND Distribution

We wish to establish a model for the underlying distribution of trees spaced in a forest that gives rise to our nearest-neighbor distance samples. We shall refer to Fig. B-1, and base the development on a random* growth distribution.

Since, along a radial from the center of any tree, O, no other significant tree[†] can grow within some distance D, which might correspond to the canopy projection in a high-latitude forest, or to the surface root complex in a rain forest, the probability of finding a tree growing

* Random growth does not often occur naturally, but the assumption of random distribution is a good approximation, usually providing averages that describe true growth characteristics within a 10% margin of error. See Ref. 20.

† The MRDC-ES Survey Teams use only trees larger than 5 cm diameter at breast height.



DB-4240-651R

FIG. B-1 SAMPLE DESCRIPTION SPACES FOR NEAREST-NEIGHBOR-DISTANCE PROBABILITY MODEL

at distance $D + \Delta$ on any radial line depends on the probability that no tree is within D and at least one tree is within Δ . If we assume that D and Δ are variable parameters defined between zero and infinity on the line OB , and construct circles as shown in Fig. B-1, of radius r and $r + dr$ defining areas A and dA , we will enclose ρ trees per unit area. Thus, statistical ecologists^{20,36} have been able to postulate that the probability of finding T trees randomly distributed in some area A should be given by Poisson's Distribution with parameter ρA :

$$P [T; A] = \frac{(\rho A)^T \exp(-\rho A)}{T!} \quad (B-1)$$

where ρ is the mean rate of occurrence of trees per unit area. That is, ρ is the mean tree number density, and ρA represents the number of trees in any area A . The probability that A has no trees (we are neglecting the reference tree at O) is:

$$\begin{aligned}
 P [0; A] &= \exp(-\rho A) \\
 &= \exp(-\rho \pi r^2) \quad . \quad (B-2)
 \end{aligned}$$

The probability that A has at least one tree is the complement* of Eq. (B-2):

$$1 - P [0; A] = 1 - \exp(-\rho \pi r^2) \quad . \quad (B-3)$$

We can define this as the cumulative distribution function for the nearest-neighbor distance, since NND will $\leq r$ if and only if there is at least one tree in area A. But it may be clearer to make a complete development; we define the probability that there is at least one tree in A as (refer again to Fig. B-1):

$$P [r < \text{NND} < r + dr] = P [0; A] (1 - P[0; A + dA]) \quad .$$

That is, the probability that r is the NND is the probability of the intersection of the two events (no tree in A) and (complement of no tree in a). The latter is the probability of finding at least one tree at r--that is, the element of area dA. It is found similarly to Eq. (B-3), as:

$$1 - \exp[-\rho \pi dr(2r + dr)] \quad . \quad (B-4)$$

Thus,

$$P(r < \text{NND} < r + dr) = f(r) = e^{-\rho \pi r^2} \left[1 - e^{-\rho \pi dr(2r + dr)} \right] \quad . \quad (B-5)$$

But since $dr \rightarrow 0$, we can, by expanding the second factor in an infinite series and neglecting terms not of first order, write the density

* That is, one set of events in the description space is the complement of the other (see Ref. 37).

function* as:

$$f(r) = F'(r) = e^{-\rho\pi r^2} 2\rho\pi r dr \quad (B-6)$$

Thus the cumulative distribution function by integration of (B-6) is:

$$F(r) = \int_0^r e^{-\rho\pi r^2} d(\rho r^2) = e^{-\rho\pi r^2} \Big|_0^r \quad (B-7)$$

and the nearest-neighbor-distance distribution has the same form as Eq. (B-3):

$$P(NND \leq r) = 1 - \exp(-\rho\pi r^2) \quad (B-8)$$

Neal²⁶ of the MRDC-ES used the following artifice in order to graph $P(NND > r)$ as a straight line, and we will adopt his method of presentation for the Rayleigh distribution since we are using MRDC statistical growth parameters:

Rewrite Eq. (B-8): in terms of its complement, as follows:

$$\begin{aligned} P(NND > r) &= 1 - P(NND \leq r) \\ &= \exp(-\rho\pi r^2) \end{aligned} \quad (B-9)$$

Take the logarithm to base 10:

$$\begin{aligned} \log P(NND > r) &= -\rho\pi r^2 \log e \\ &= -0.4343 r^2 / S^2 \end{aligned} \quad (B-10)$$

where $S = 1/\sqrt{2\rho\pi}$ is the standard deviation of the distribution. In terms of percentiles and the number of trees ρ per unit area, we can write the relation below, which is linear in $(r = NND)^2$:

$$\log 100 P(NND > r) = 2 - 1.36\rho r^2 \quad (B-11)$$

* This may be recognized as the Rayleigh density function with variance $1/2\rho\pi$.

We have thus graphed the square of the radius r (in this case it is nearest-neighbor-distance) as a function of the logarithm of percentile for all Rayleigh distributions in this report.

We can develop several useful relations based on Eq. (B-10) that may be applied for any Rayleigh distribution. We list them below, with their counterparts written in terms of tree number density ρ as well.

$$\text{Median } M_r \approx 1.18 S \quad ; \quad \text{Median NND} \approx 0.47/\sqrt{\rho} \quad . \quad (\text{B-12})$$

Upper quartile of the cumulative distribution is

$$UQ \approx 1.67 S \quad \text{or} \quad 0.666/\sqrt{\rho} \quad (\text{B-13})$$

and the lower quartile is

$$LQ \approx 0.758 S \quad \text{or} \quad 0.325/\sqrt{\rho} \quad . \quad (\text{B-14})$$

For the inverse cumulative distribution, these quartiles are interchanged.

The mean can be obtained from Eq. (B-6) as the first moment of density:

$$\bar{r} = \int_0^{\infty} r f(r) dr \quad (\text{B-15})$$

$$= \int_0^{\infty} r 2\pi\rho r \exp(-\pi\rho r^2) dr \quad (\text{B-16})$$

$$= \int_0^{\infty} \frac{r^2}{S^2} \exp(-r^2/2S^2) dr \quad (\text{B-17})$$

Let

$$u = r^2/2S^2$$

$$du = r dr / S^2 \quad .$$

Then

$$\bar{r} = S\sqrt{2} \int_0^{\infty} u^{1/2} e^{-u} du \quad (B-18)$$

$$= \frac{S\sqrt{2}}{2} \Gamma(1/2)$$

$$= S\sqrt{\pi/2} \approx 1.253 S \quad \text{or} \quad \text{NND} = 1/2\sqrt{\rho} \quad (B-19)$$

Finally, we may relate the mean, standard deviation, and quartiles of a Rayleigh distribution to its median M_r :

$$\bar{r} \approx 1.062 M_r \quad (B-20)$$

$$S \approx 0.847 M_r \quad (B-21)$$

$$UQ \approx 1.415 M_r \quad (B-22)$$

$$LQ \approx 0.643 M_r \quad (B-23)$$

By using the survey done at the Chumphon undergrowth sample 454B (CII in this report), we may test on a small scale whether we can generate NND distributions based on a number density, or stem count. The entire growth of stems higher than one foot on an 8 by 3.5-meter plot was counted and mapped. The total number of these, which includes climbing vines, was 147. This gives a number density $\rho = 5.25 \text{ stems/m}^2$, from which we can predict an NND Rayleigh distribution as shown by the dashed line on Fig. B-2. The predicted median $0.47/\sqrt{\rho} = 20.55 \text{ cm}$ is larger than the median NND measured from the vegetation plot map, but the prediction does seem reasonable for 40 percent of the total NND distribution, especially the larger spacings.

The actual shape of the total NND distribution is more nearly Chi-Square than Rayleigh, suggesting that the occurrence of stem-doubling, root-suckers, and twining climbers may be causing the departure from the prediction.

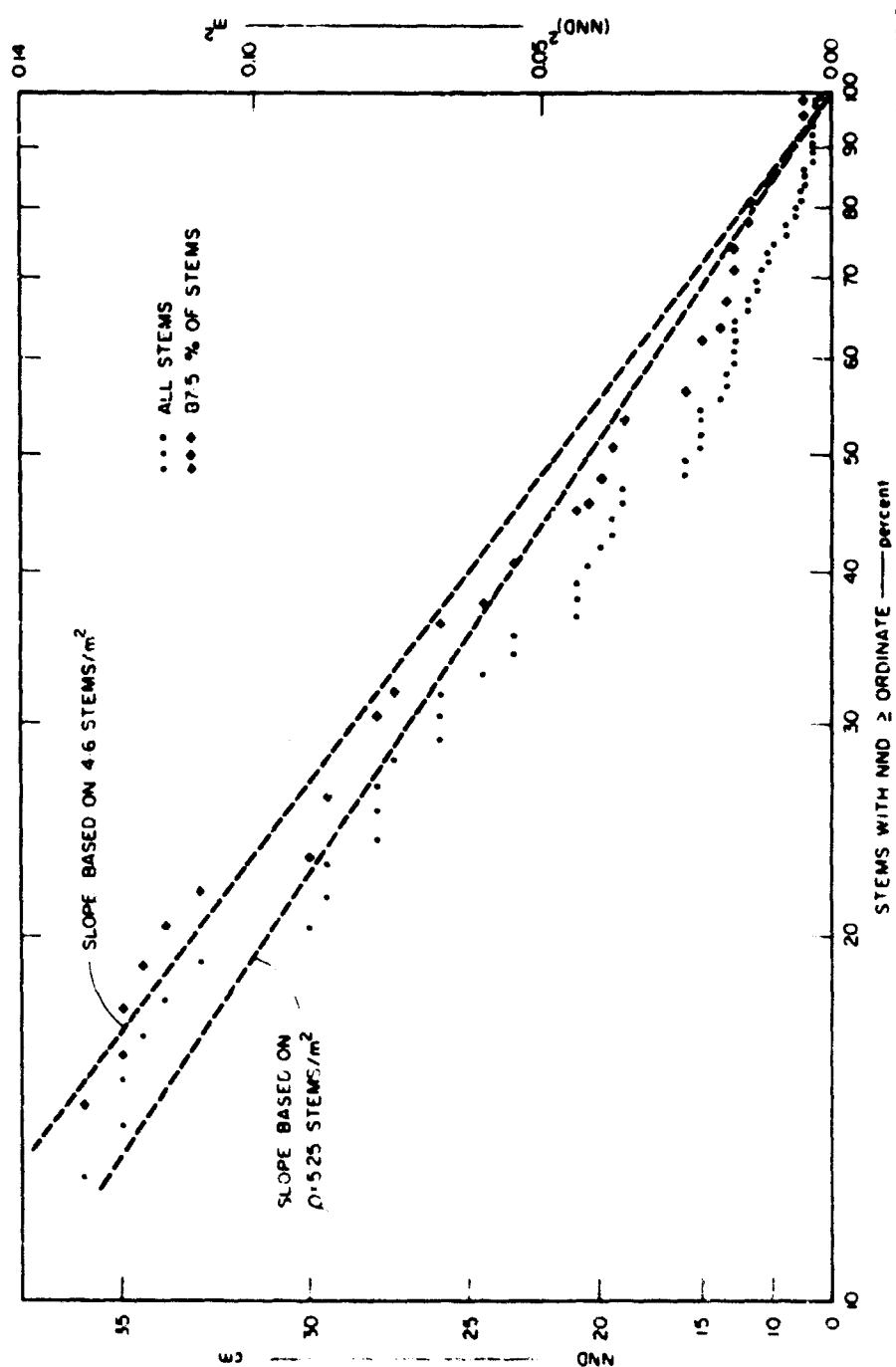


FIG. B.2 INVERSE CUMULATIVE DISTRIBUTION OF NEAREST-NEIGHBOR DISTANCES FOR UNDERGROWTH
 SAMPLE CII

If we ignore all $NND < 7$ cm, we can remove the bias, which results mostly from stems that will never grow higher than 1.5 meters, or man-pack antenna height. When we thus re-form the NND distribution, based on 87.5 percent of the former total, we have only $\rho = 4.6 \text{ stems/m}^2$, but these are the most significant ones. The fit of prediction to measured NND is better (Fig. B-2) now, and we can use the predicted median 21.9 cm rather than the measured 19.8 cm.

Appendix C

ENVIRONMENTAL DESCRIPTION FOR CHUMPHON

Appendix C

ENVIRONMENTAL DESCRIPTION FOR CHUMPHON

Chumphon forest is classified as fresh water swamp forest. Its structure and density are nearly uniform throughout the test area. Except near the midpoint (Mark 31 to Mark 33) of Xeledop Test Trail A, where the land is raised about 1.5 m above water level, most of the trees are stilt-rooted and straight-stemmed. The top (crown) canopy is continuous throughout the forest, causing suppression of lower trees and undergrowth. The undergrowth is uniform, and grows about 4 m high.

A forestry survey of trees having DBH greater than 5 cm was made for the vicinities of Xeledop Test Trails A and B (see Fig. 21). The survey located 644 trees, using 17 standard plots. Their mean density is about 0.095 trees/m². The summary statistical distributions are given for height, diameter, and NND in Figs. C-1 through C-3. Nine of the standard plots were in a region without undergrowth. Two of these, Plots 439 and 440, were very near the OWL height profile sample (CV). The distributions of tree height, diameter, and NND for those two plots are given in Figs. C-4 through C-6.

In addition to the standard large plots, a special small vegetation plot (454B) was surveyed to include undergrowth Sample CII. Here, all plants growing higher than 30 cm were located; their diameters were measured at that height. This plot was near the northwestern edge of the forest on the raised land, but its vegetation growth was very much like that surveyed in two similar plots (454A and C) in the interior swamp. The density in Sample CII was 5.25 stems/m² (147 plants on an 8-by-3.5-m base). Statistical distributions of growth parameters for this plot are given in Figs. C-7 through C-9.

Even though the vegetation in this forest stand is evergreen there is an accumulation of leaf litter on the forest floor in a thick layer 2-4 cm deep, decomposing into humus. The soil underneath, mostly clay, is thus rich in nutrient. Soil characteristics inside and outside Chumphon forest are summarized in Tables C-I and C-II.

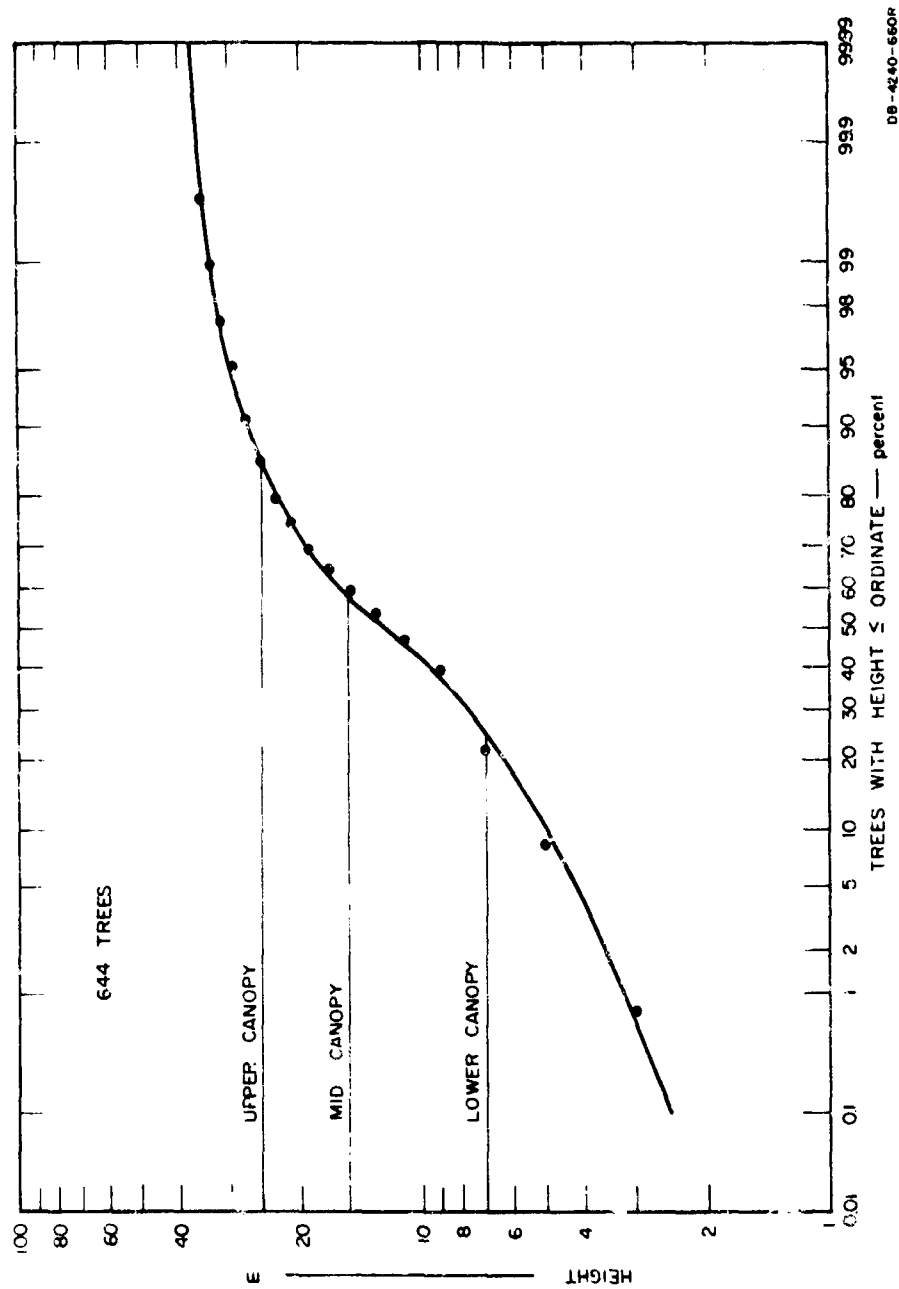


FIG. C-1 HEIGHT DISTRIBUTION FOR ALL TREES SURVEYED AT CHUMPHON SITE

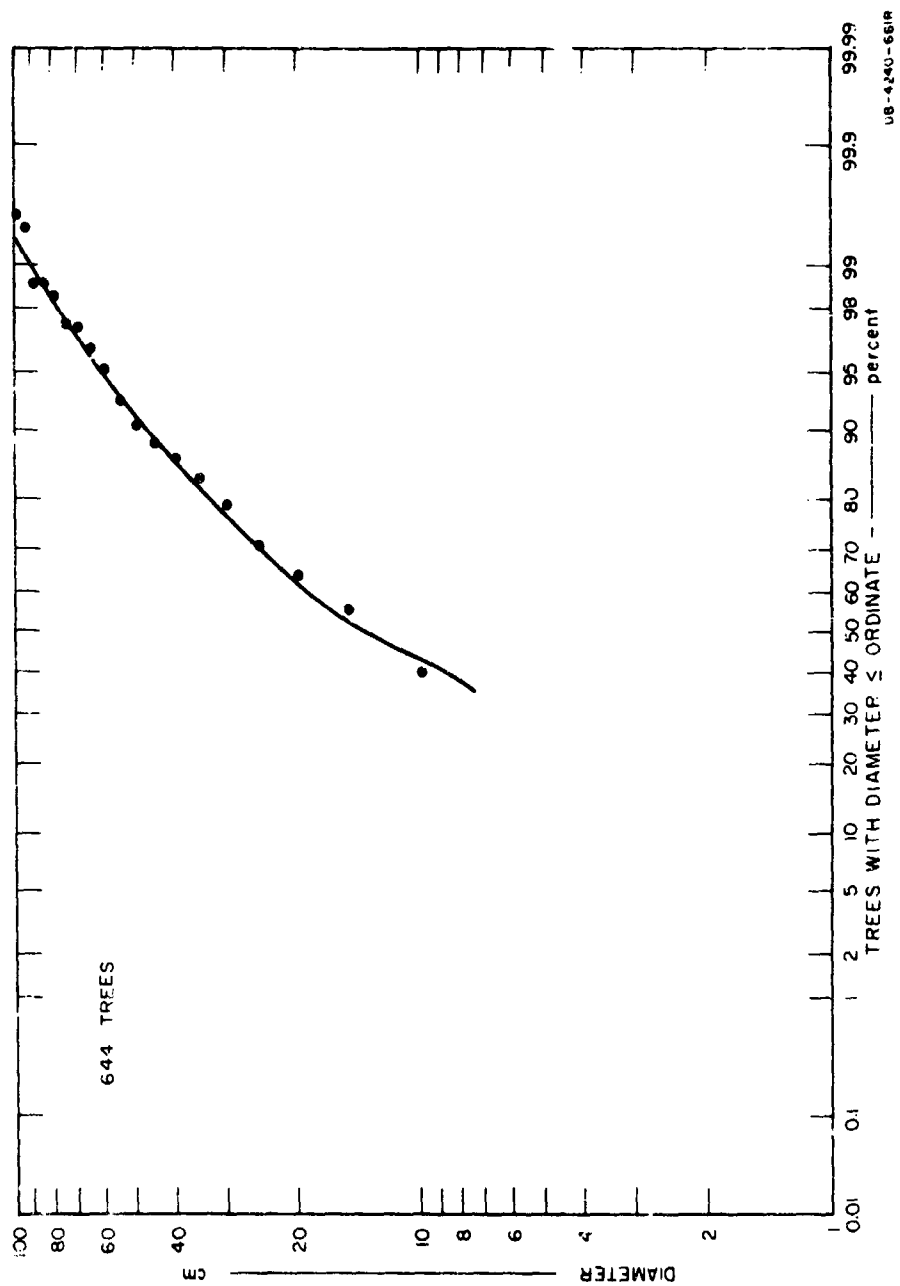


FIG. C-2 DIAMETER DISTRIBUTION FOR ALL TREES SURVEYED AT CHUMPHON SITE

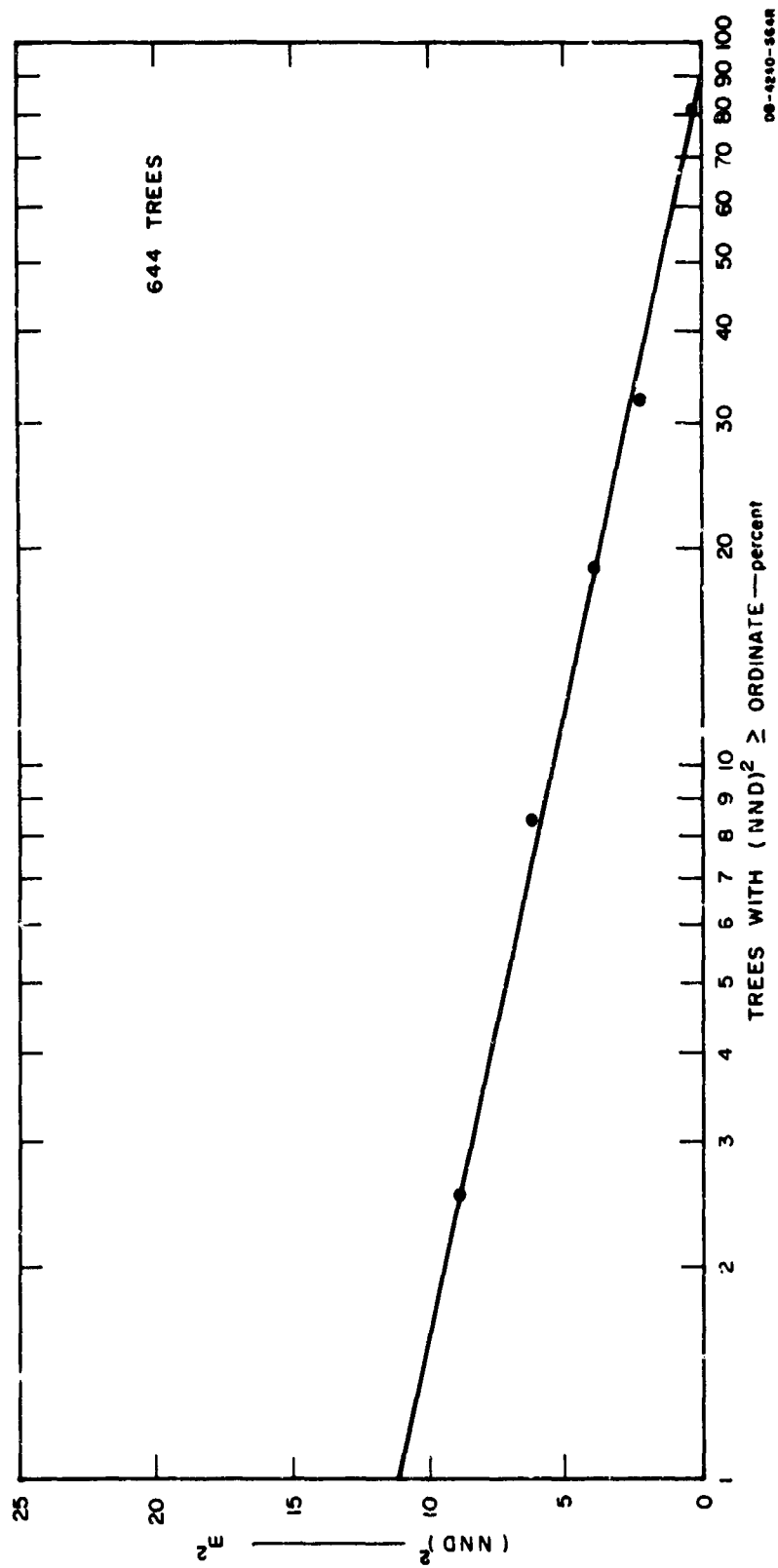
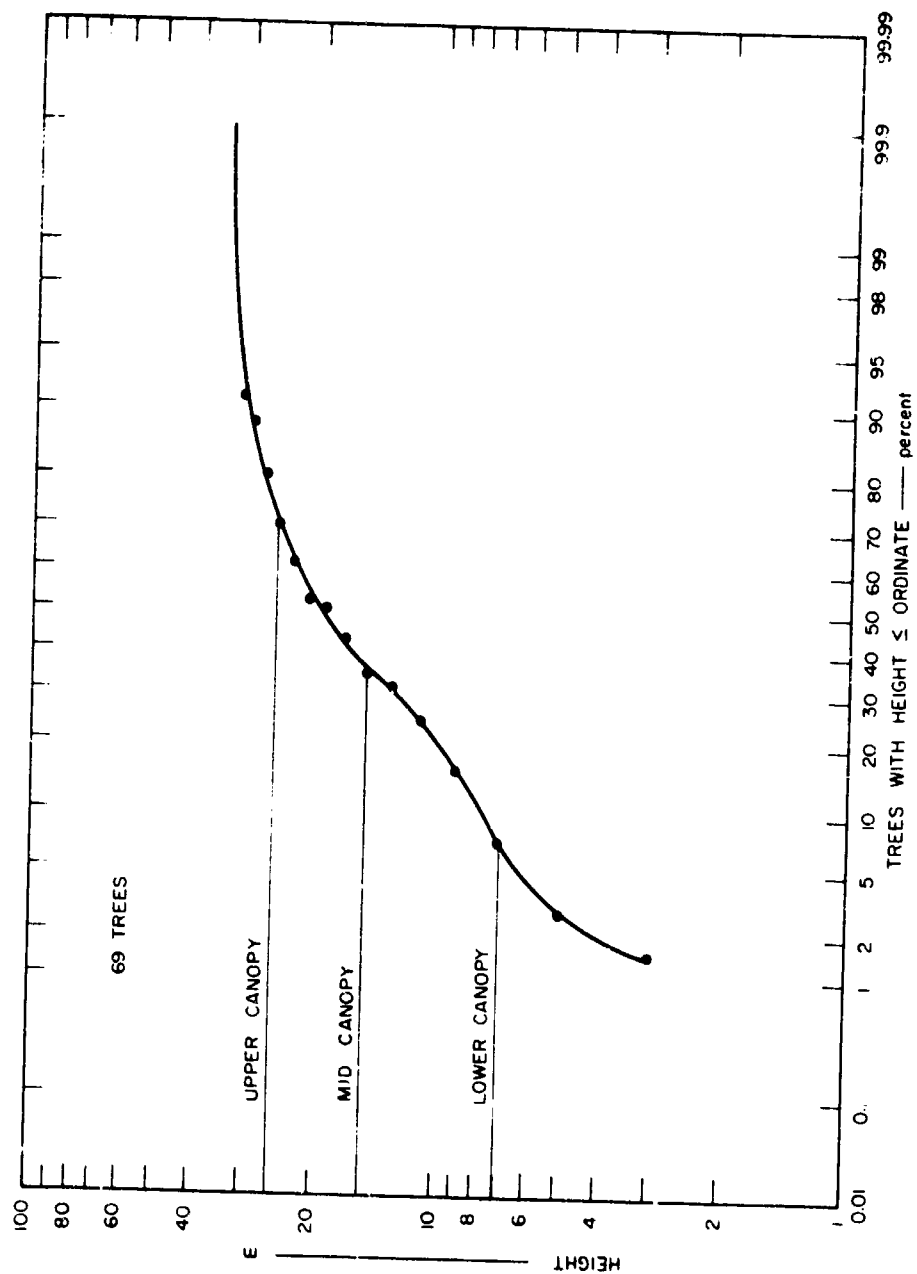


FIG. C-3 NND DISTRIBUTION FOR ALL TREES SURVEYED AT CHUMPHON SITE



DB-4240-658R

FIG. C-4 HEIGHT DISTRIBUTION FOR TREES IN CHUMPHON SAMPLE CV

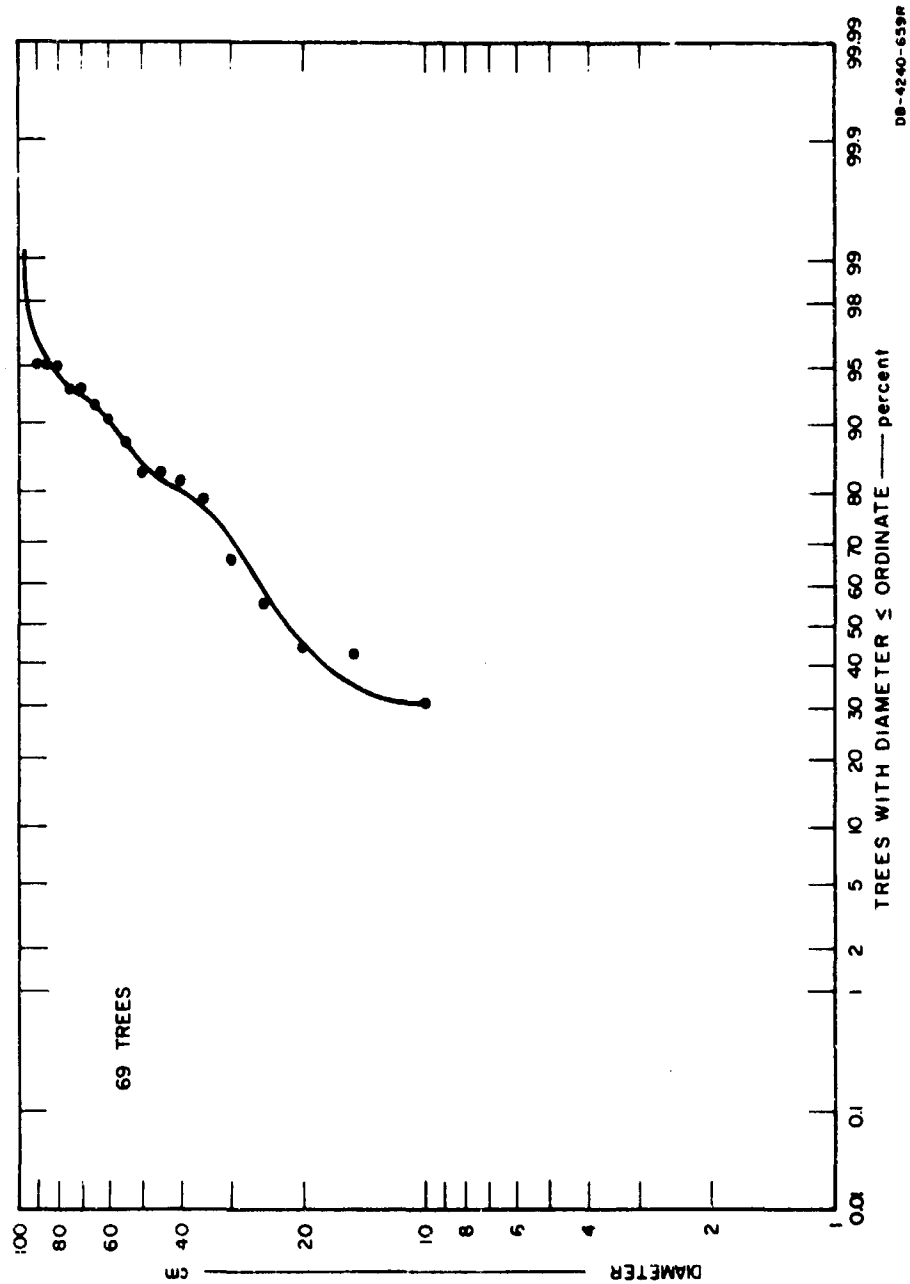


FIG. C-5 DIAMETER DISTRIBUTION FOR TREES IN CHUMPHON SAMPLE CV

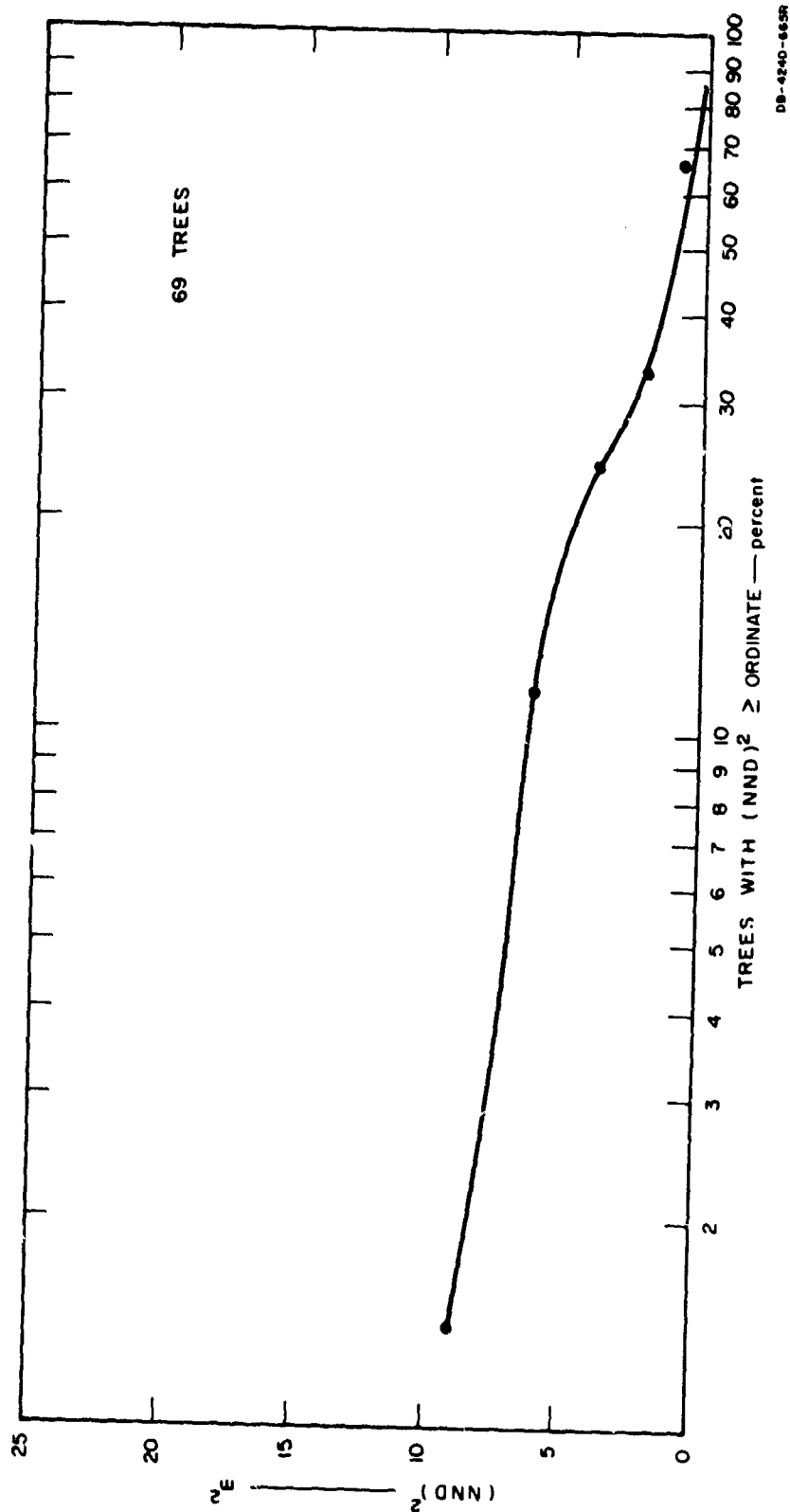


FIG. C-6 NND DISTRIBUTION FOR TREES IN CHUMPHON SAMPLE CV

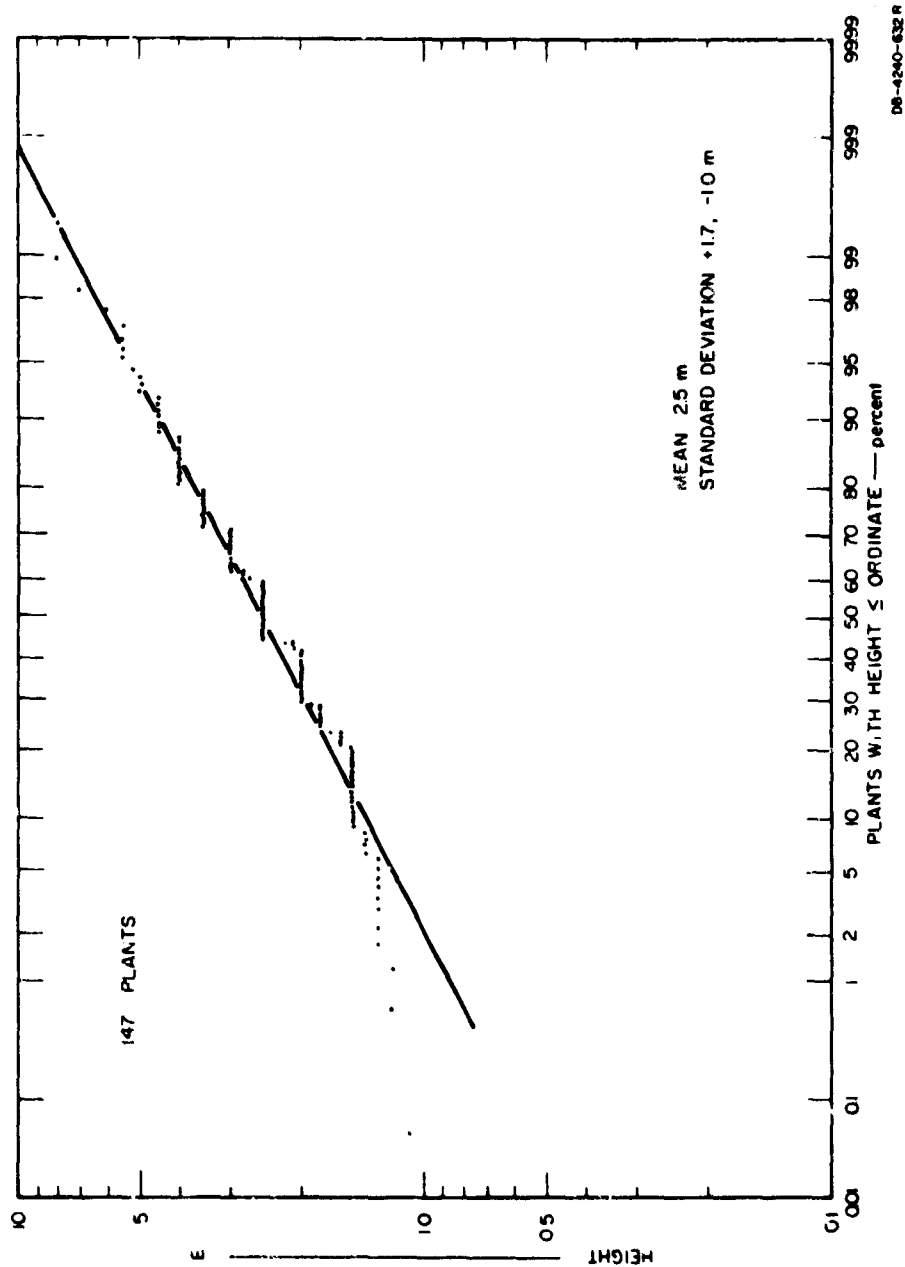
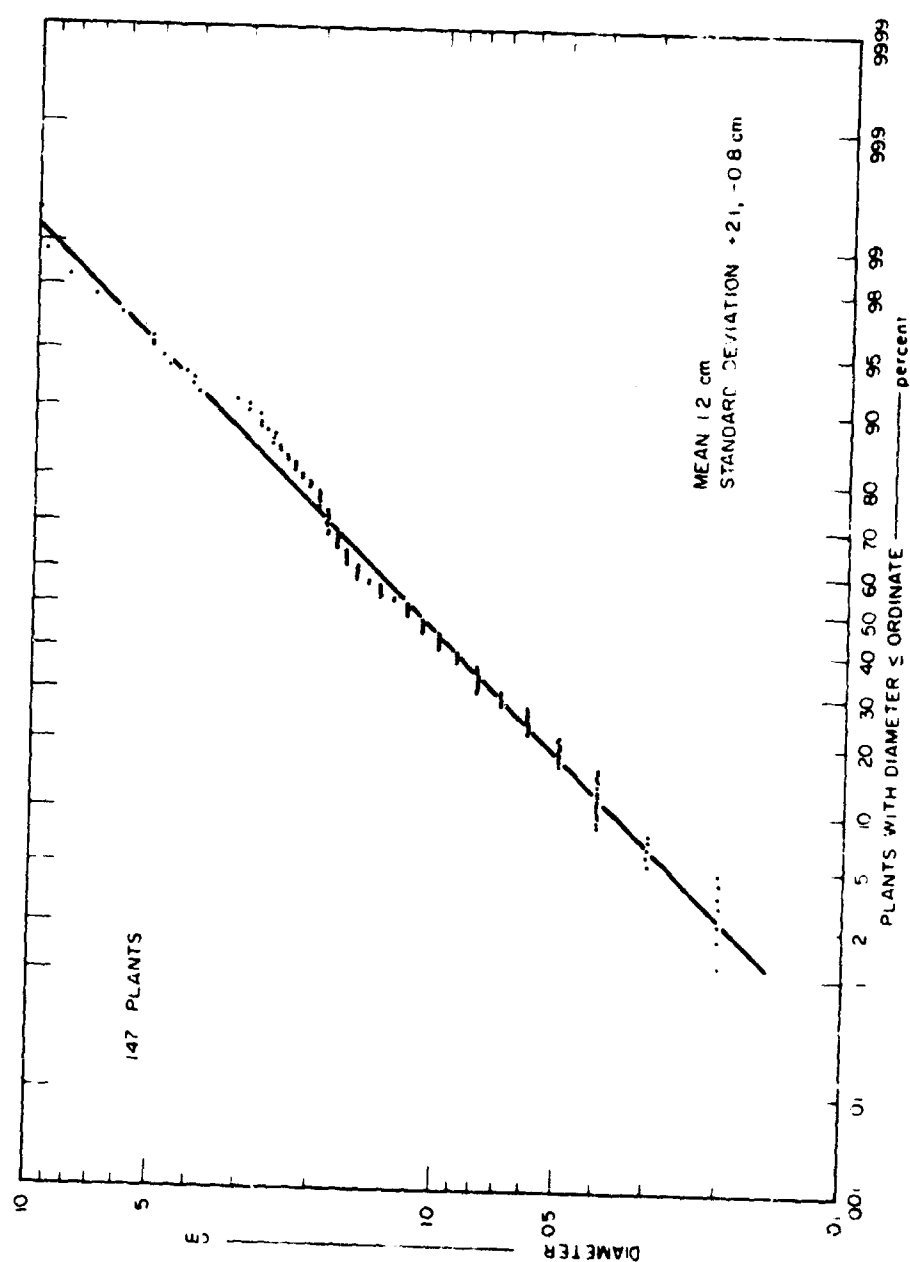


FIG. C-7 HEIGHT DISTRIBUTION FOR ALL PLANTS IN UNDERGROWTH SAMPLE CII



DB-4240-633 R

FIG. C-8 DIAMETER DISTRIBUTION FOR ALL PLANTS IN UNDERGROWTH SAMPLE CII

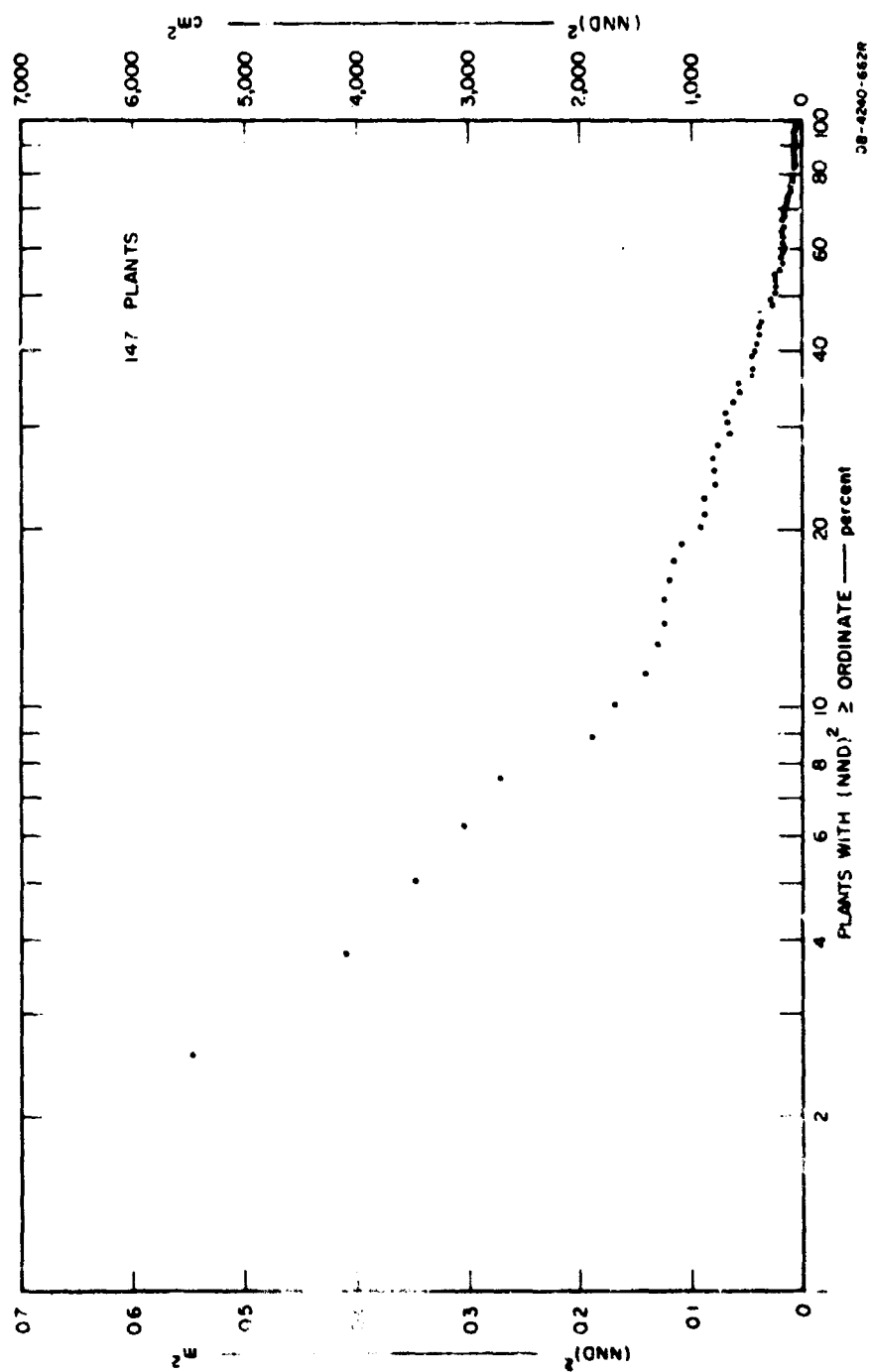


FIG. C-9 NND DISTRIBUTION FOR ALL PLANTS IN UNDERGROWTH SAMPLE CII

Table C-1

CHUMPHON SOIL SUMMARY--OPEN TERRAIN

MRDC Plot No.	Texture		Color		pH Value	Moisture Content (% by weight)	Depth (inches)	Remarks
	USDA	USCS	Surface	Subsoil				
PCL (10 m west of Point O, MPX Trail)	SIL	CL	Dark greyish brown owing to humus to depth of about 3 inches	Light brownish grey	8.0	35.4	0 - 6	Water table was found at 6-inch depth
	SIL	CL		Mottled color of light grey to pale yellow	8.0	19.7 - 24.2	6 - 40	Soil contained very fine-grain gravel
	SIL	CL		Mottled color of yellowish brown	7.9		40 - 60	
	SIL	ML-CL	Dark greyish brown to dark brown owing to humus to depth of about 3 inches		6.0 - 6.5	27.0	0 - 5	Gravel layer began at 21 inches and varied to 30 inches
PCL-2 (at OWL Sample C-1)	SIL-L	CL		Yellowish brown to light yellowish brown	5.9 - 6.2	20.8 - 22.5	5 - 30	
	GL	SC		Mottled color of yellowish brown to brown	6.2 - 6.5	21.2	30 - 60	

Table C-2
CHUMPHON SOIL SUMMARY--INSIDE FOREST

NRDC Plot No.	Texture		Color		pH Value	Moisture Content (% by weight)	Depth (inches)	Remark
	USDA	USCS	Surface	Subsoil				
OWL C-II (about 200 m from lime- stone mountain)	GSL	SN-SC	Dark brown owing to humus to depth about 2 inches		5.8 - 6.4	13.8	0 - 6	Soil contained very high stone fragment about 60-80% gravel size, of subrounded and irregular shape of stone fragments
	VGSL	GW-GC		Yellowish brown to light yel- lowish brown	5.6 - 5.8	12.7 - 13.0	6 - 16	
	VGSil	GC		Light grey	6.2		18 - 30	
	Sil	OL-ML	Very dark grey owing to humus and litter to depth about 6 inches		8.0 - 8.2	94.5	0 - 6	
437 and 438 (near forest edge, Trail A marker number 15)	Sil	ML		Light grey with stripes of yellow	7.8 - 8.2	29.8 - 38.8	6 - 48	Soil contained about 13-19% gravel size, 6 mm maximum
	GI,	SC		Light grey with stripes of yellow	7.8		48 - 60	

Table C-2 (Concluded)
CHUMPHON SOIL SUMMARY--INSIDE FOREST

MRDC Plot No.	Texture		Color		pH Value	Moisture Content (% by weight)	Depth (inches)	Remarks
	USDA	USCS	Surface	Subsoil				
439 and 440 (OWL C-V)	SiL	OL-NL	Very dark grey owing to humus and litter to depth about 6 inches		8.2	100	0 - 4	Water table at ground surface. Soil contained 13-30% subrounded gravel, 6 mm maximum
	SiL	NL		Light grey with stripes of yellow	8.2	44.1 - 47.1	4 - 30	
	SiL	NL		Light grey to light brownish	8.2	41.5	30 - 59	

Appendix D

ENVIRONMENTAL DESCRIPTION FOR PAK CHONG

Appendix D

ENVIRONMENTAL DESCRIPTION FOR PAK CHONG

The forest in the Pak Chong test area is classified as dry or semi-evergreen forest. Its canopy is generally divided into two stories, the upper from 6 to 41 meters and the lower from 1.5 to 18 meters. The crown canopy covers about 60 percent of the ground. The average density of the lower story is about 0.04 trees per m^2 . The average density of the upper story is about 0.06 trees per m^2 .

The undergrowth is fairly dense and lumped in many open spaces among the canopy; there, penetrability on foot is poor. The height of undergrowth varies from 2 to 6 meters.

The forestry survey at this site was made during the first half of 1964. The results are published in Refs. 18 and 19. Twelve plots of 10 by 40 meters, four plots of 10 by 50 meters and 2 plots of 10 by 60 meters were surveyed. They contained 670 classifiable trees. The average density is 0.08 trees per m^2 . Summaries of statistical distributions of tree height, diameter and NND are given in Figs. D-1 through D-3.

A second survey trip was made during November 1966 and a special undergrowth plot (Sample P-I) was surveyed in detail. All plants inside the sample were located, and their diameters were measured at 30-cm height. This plot is in the standard plot 43 which was surveyed in 1964. The density in the test undergrowth sample is 6.8 stems/ m^2 (62 plants on 3-by-3-meter basal area). The statistical distributions of vegetation parameters for this plot are given in Figs. D-4 through D-6.

The terrain elevation varied from 290 m to 720 m throughout the forest. At the location of the OWL sample, the elevation is about 380 m. Soil data obtained at the site in 1964 are summarized in Tabled D-I.

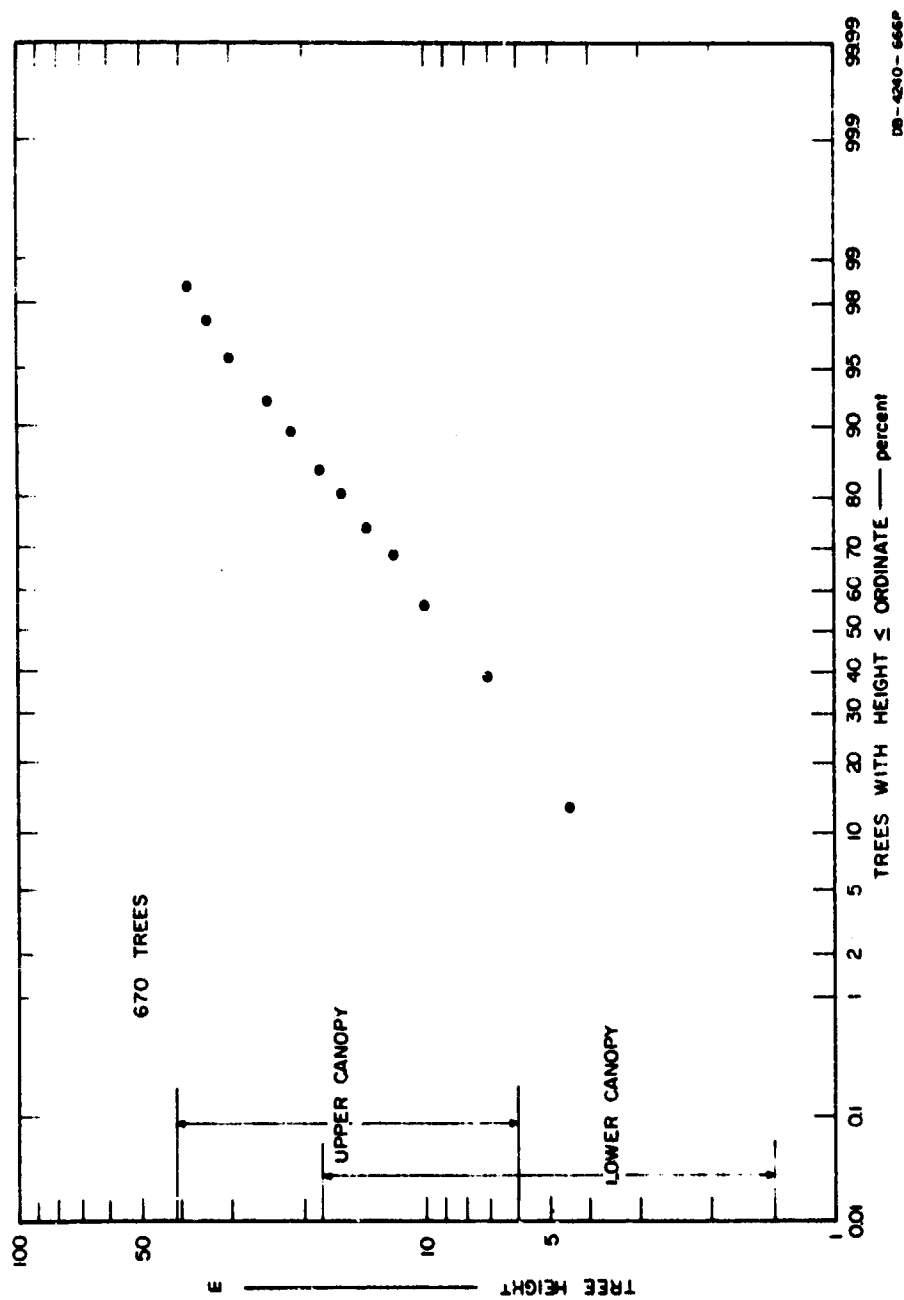
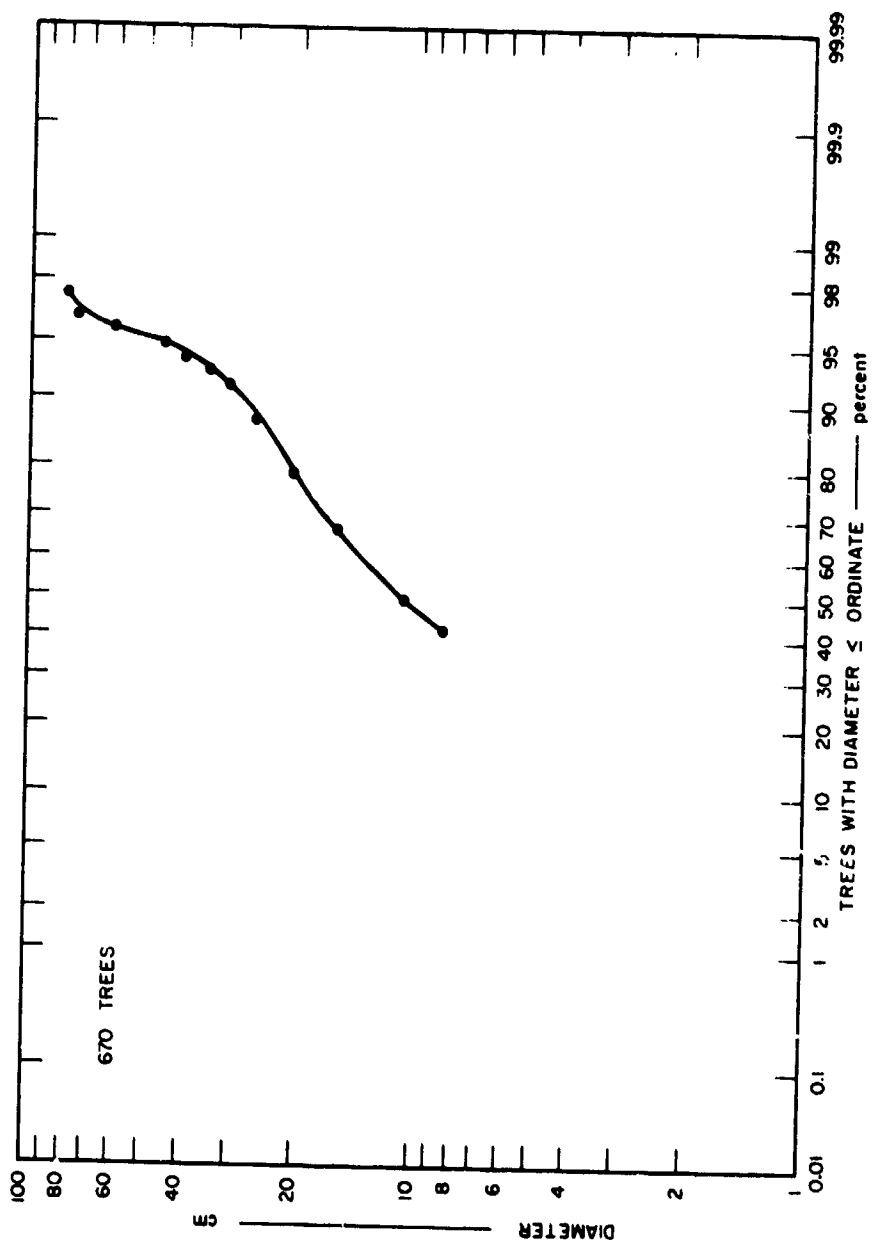


FIG. D-1 HEIGHT DISTRIBUTION FOR ALL TREES SURVEYED AT PAK CHONG SITE



DB-4240-637R

FIG. D-2 DIAMETER DISTRIBUTION FOR ALL TREES SURVEYED AT PAK CHONG SITE

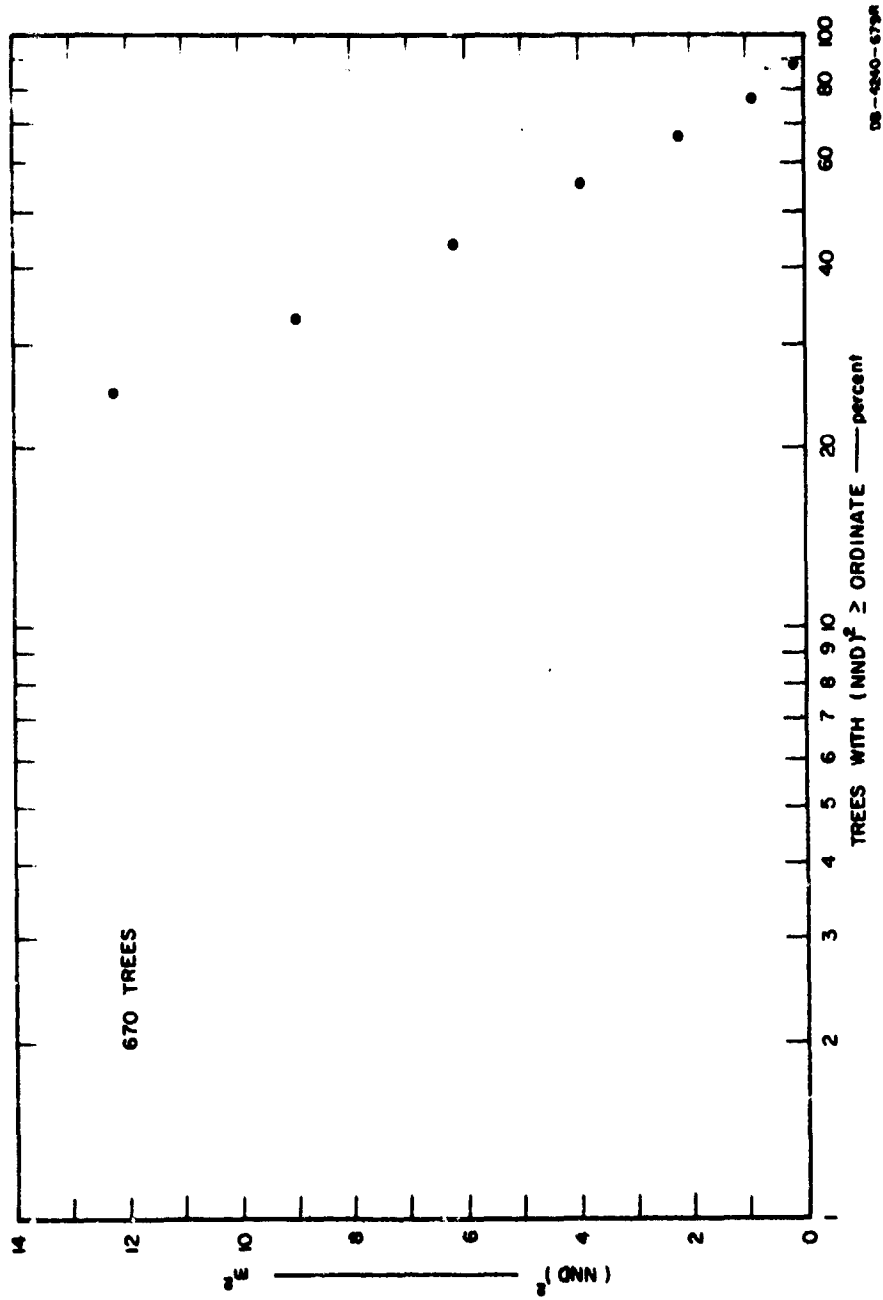


FIG. D-3 NND DISTRIBUTION FOR ALL TREES SURVEYED AT PAK CHONG SITE

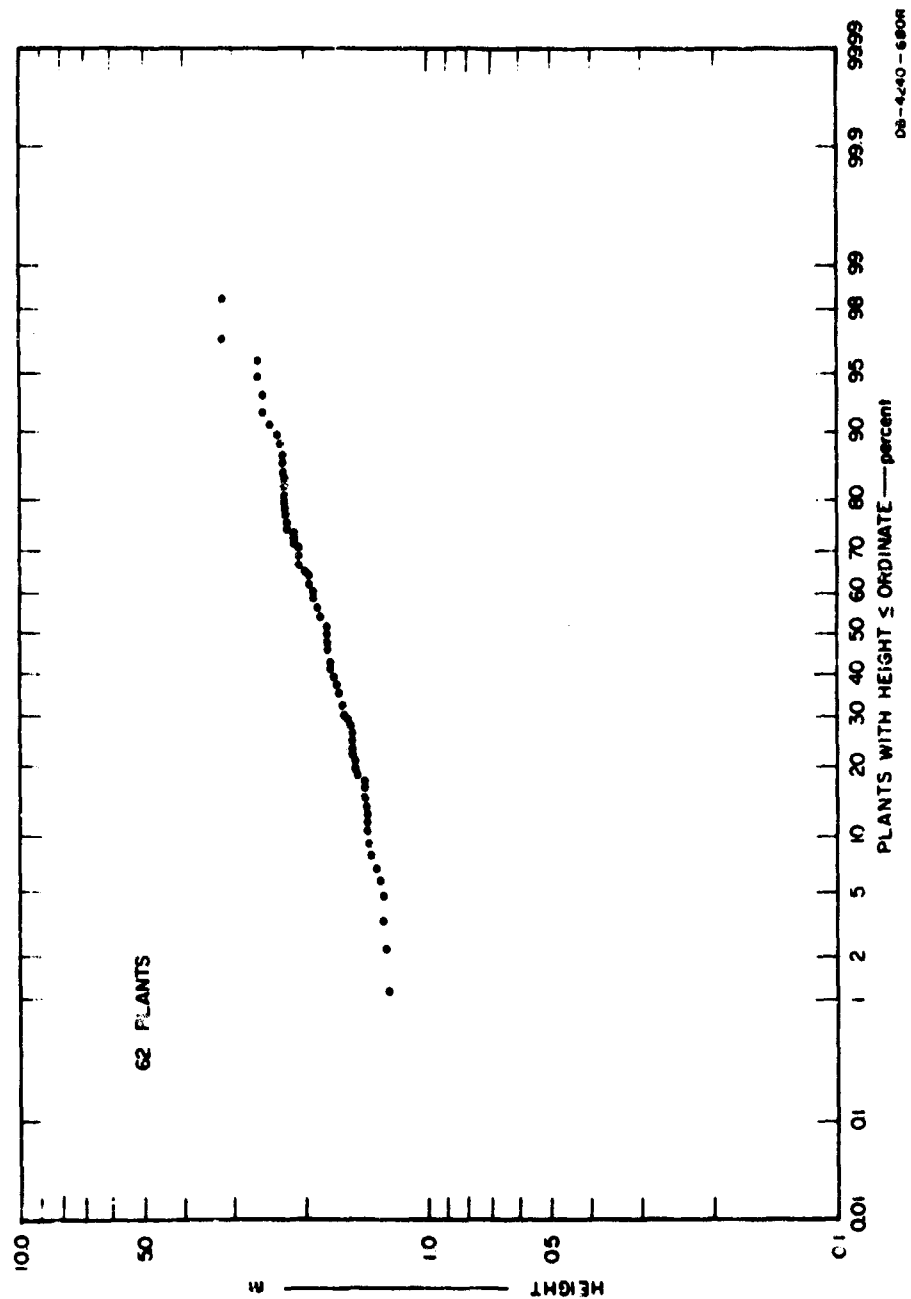


FIG. D-4 HEIGHT DISTRIBUTION FOR ALL PLANTS IN UNDERGROWTH SAMPLE PI

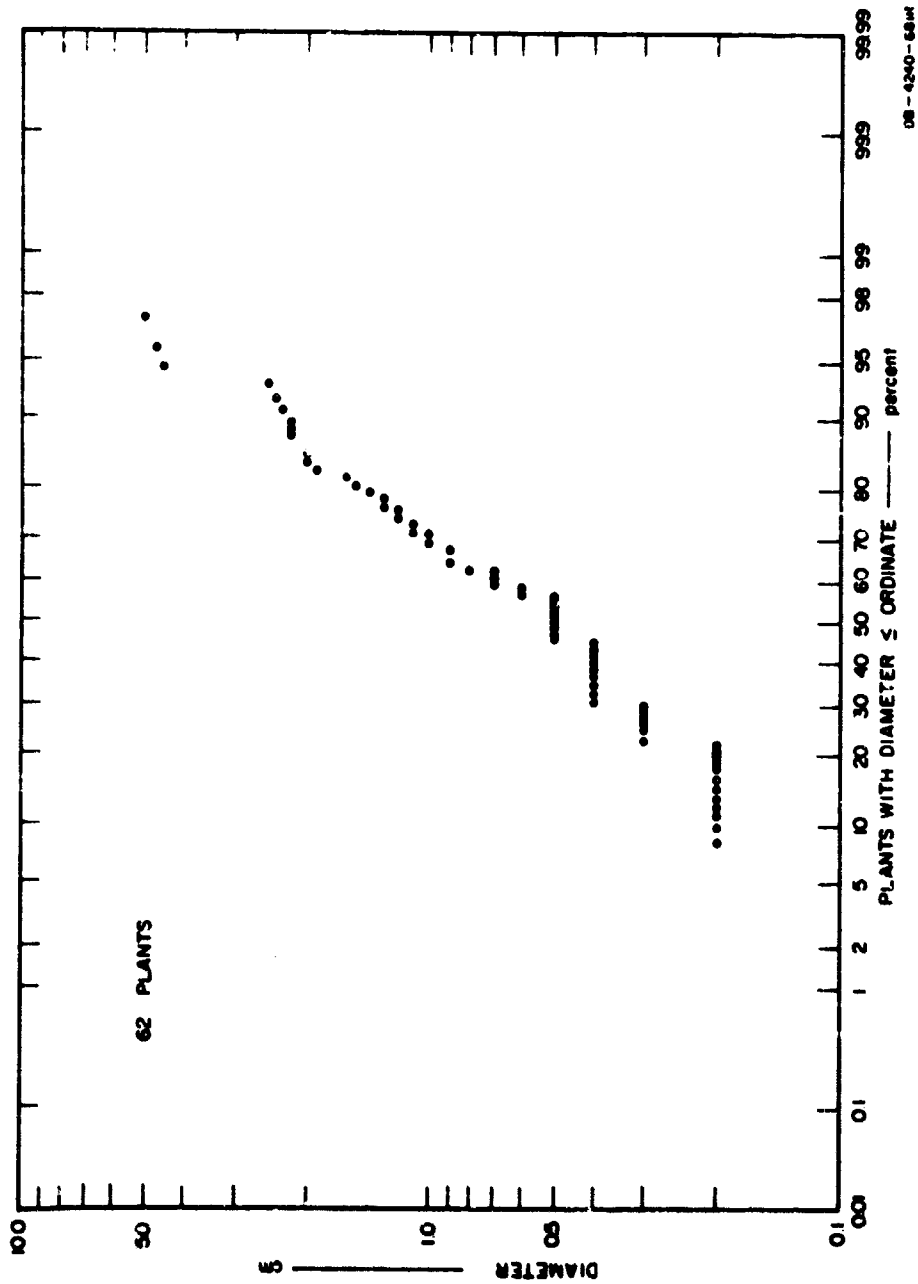


FIG. D-5 DIAMETER DISTRIBUTION FOR ALL PLANTS IN UNDERGROWTH SAMPLE P1

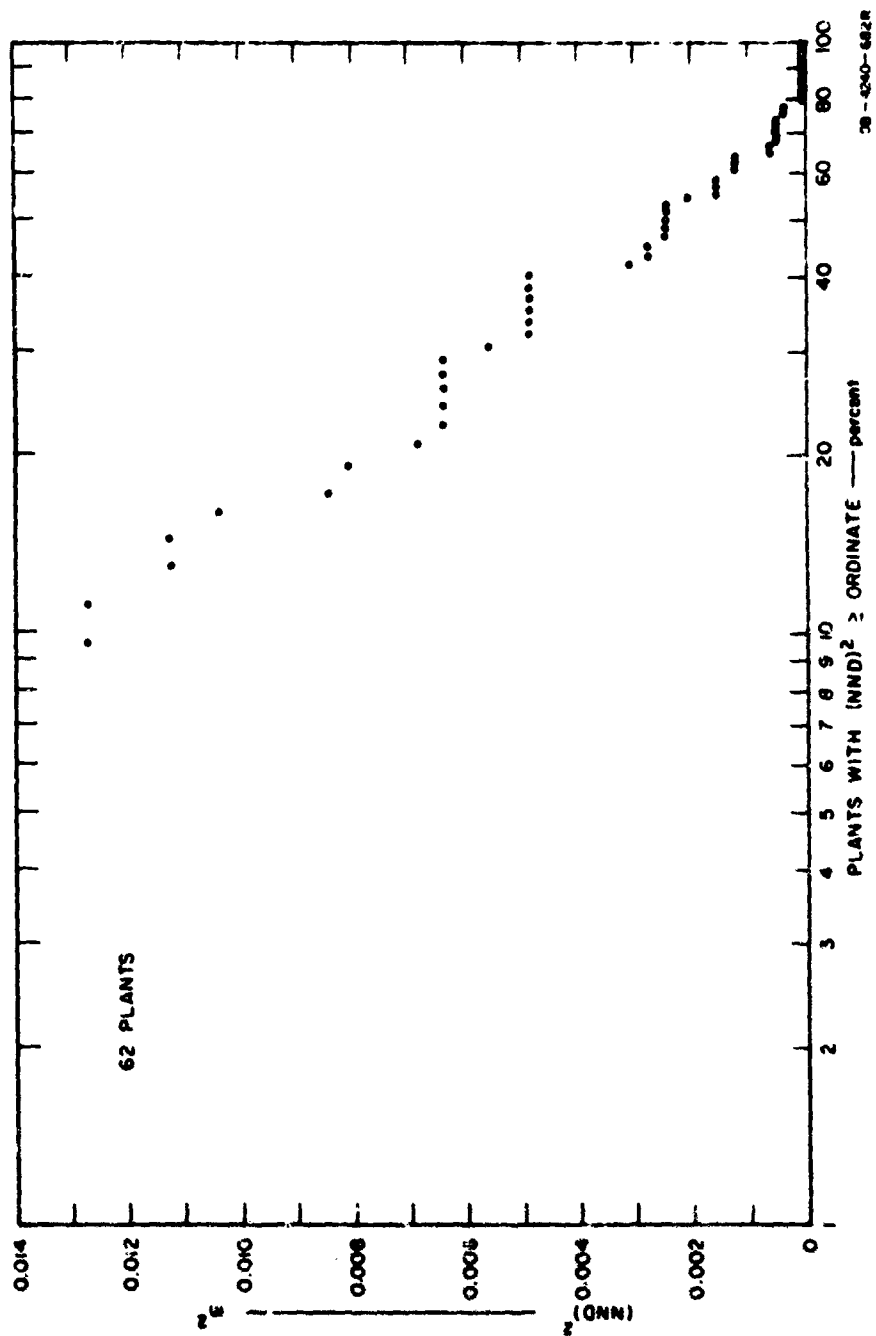


FIG. D-6 NNND DISTRIBUTION FOR ALL PLANTS IN UNDERGROWTH SAMPLE PI

Table D-1

SOIL SUMMARY FOR PAK CHONG FOREST NEAR XOPAT (DECEMBER 1966)

MADC No.	Texture		Color		pH value	Moisture Content (% by weight)	Depth (inches)	Remarks
	USDA	USCS	Surface	Subsoil				
401 (OWL site)	CL-ML	SIL	Brown	Brown	4.8 - 5.8	17.2	0 - 6	Some litter at surface to 1/4
	CL	SIL		Reddish brown	4.8 - 5.0	16.4 - 17.4	6 - 58	
	SC	GSIL		Reddish brown	4.9 - 5.0	12.2	58 - 62	Hit stone at 62 inches
43	CL sandy clay	Silt loam	Dark brown	Yellowish red	5.5	24 - 32	72	
44	CL, silty clay	Loam		Dark red		33	60	
45	CL-ML, silty clay	Loam		Dark red	5.0	25.6	72	
62	CL, silty clay	Loam to silt loam		Dark brown Yellowish red	5.0 4.5	11.4 - 11.6	0 - 30 30 - 60	

Appendix E

ENVIRONMENTAL DESCRIPTION FOR LAEM CHABANG

Appendix E

ENVIRONMENTAL DESCRIPTION FOR LAEM CHABANG

The evergreen beach forest at the SRI Laem Chabang site is composed mainly of shrubs, bushes, climbers, and thorny succulen herbs. Few trees taller than 10 meters can be found in the test area. The undergrowth there is a dense, tangled mass that is difficult to penetrate or to see through, but there are many open spaces among the clumps of vegetation. The average height is between 2.5 and 6 meters. A mean undergrowth height for the entire area surveyed would be about 3.5 meters.

The OWL Sample LII was taken at a spot near the MRDC plot No. 307 where the ground was covered with uniformly dense shrubs, climbers, thorny scrubs with an average height about 3.5 meters. There is one costatus tree 11 m high near the OWL sample.

The Sample LII stands on a plain about 5 meters above sea level. The soil underneath is well-graded sand and was covered with dry leaves about 6 mm deep. Humus, very dark grey in color, was present in this layer. The characteristics of the soil are similar throughout the vegetated area. Soil data are summarized in Table E-1. The MRDC-ES plot numbers shown were used for inventory purposes only; no forestry survey was made.

Table E-1

SOIL SUMMARY FOR VEGETATED AREA NEAR LAEM CHABANG

MRDC Plot No.	Soil Type Texture		Color		pH Value	Moisture Content (% by weight)	Depth (inches)
	USCS	USDA	Surface	Subsoil			
304	SW	Well graded sand		Reddish brown	4.8 - 6.1	3.46 - 3.75	0 - 12
					4.9 - 5.8	3.84 - 4.10	18 - 48
					5.0 - 5.7	3.36 - 3.63	60 - 72
305	SW	Well graded sand		Reddish brown	4.8 - 6.4	3.72 - 4.87	0 - 12
					4.9 - 5.8	3.58 - 4.28	18 - 48
					5.0 - 5.7	3.66 - 3.87	60 - 72
306	SW	Well graded sand	Dark grey	Dark grey, brown	6.3 - 8.0	4.2 - 4.62	0 - 12
					5.9 - 8.0	4.0 -- 4.75	18 - 48
					5.5 - 8.0	5.82 - 6.20	60 - 72
307	SW	Well graded sand	Dark grey	Dark grey, brown	5.6 - 7.0	4.93 - 5.29	0 - 12
					5.5 - 6.0	3.74 - 4.53	18 - 48
					5.6 - 5.9	4.02 - 4.15	60 - 72

Appendix F

ENVIRONMENTAL DESCRIPTION FOR KUAN KARLONG FOREST IN SATUN

A forest survey was made during May-June 1967. The vegetation around the Jansky & Bailey radial test trails X, Y, Z, and W was examined. Twenty-five standard plots (10 by 40 m) were chosen at random around this area, and 1,031 trees having DBH larger than 5 cm were classified.

The forest in the test site was classified as tropical rain forest, formed by a number of evergreen trees, characteristic of the upper Malaysian flora. The forest is composed mainly of tall trees of various heights, and tree density is rather even throughout the forest; open gap is rarely to be found. The upper canopy density is about 80 percent crown cover. To the eye, the forest looks quite uniform.

The structure of this forest can be defined in three canopy stories, disregarding the undergrowth. The crown (top) canopy story is discontinuous, with a height of about 24-30 m. The average tree density in this story is about 0.02 stems/m^2 . The height of the middle story ranges from 15 to 23 meters. Trees in this story vary greatly in height and species. The average tree density is about 0.018 stems/m^2 . The lowest story is composed of a great number of trees with height ranging from about 8 to 14 meters, and the space between the lowest and middle story is irregularly filled up with trees of intermediate height. Therefore, the tree crowns of both stories form a continuous and closed foliage layer. The tree density in the lower story averages about 0.107 stems/m^2 .

The undergrowth is uneven in height and density throughout the forest; shrubs and climbers are individually scattered about the test area, and in certain localities they are almost absent. In the spaces where the sunlight can reach the ground, the undergrowth is chiefly composed of dense shrubs, climbers, and herbaceous plants. The height of this lumpy undergrowth is about 3 to 7 meters.

The statistical description of this forest is presented in Figs. F-1 through F-3 where the cumulative distribution of tree height, diameter, and nearest-neighbor distance was plotted.

An additional forestry survey was made on the OWL sample S-1, where all trees higher than one foot were described. The cumulative distribution of tree height, diameter, and nearest-neighbor distance is shown in Figs. F-4 through F-6. There were only 29 plants actually within the 3.5-by-3.5-m boundary of the sample (density $\rho = 2.4 \text{ stems/m}^2$). In order to get better statistical sample size, the 11 plants in the immediate vicinity of the S-1 plot were included in the distribution by MRDC-ES.

The test site area is on a peneplain of an average elevation of 50 meters above mean sea level. The soil there was surface clay over laterite or other rocky soil. A summary of the soil-analysis results is given in Table F-1.

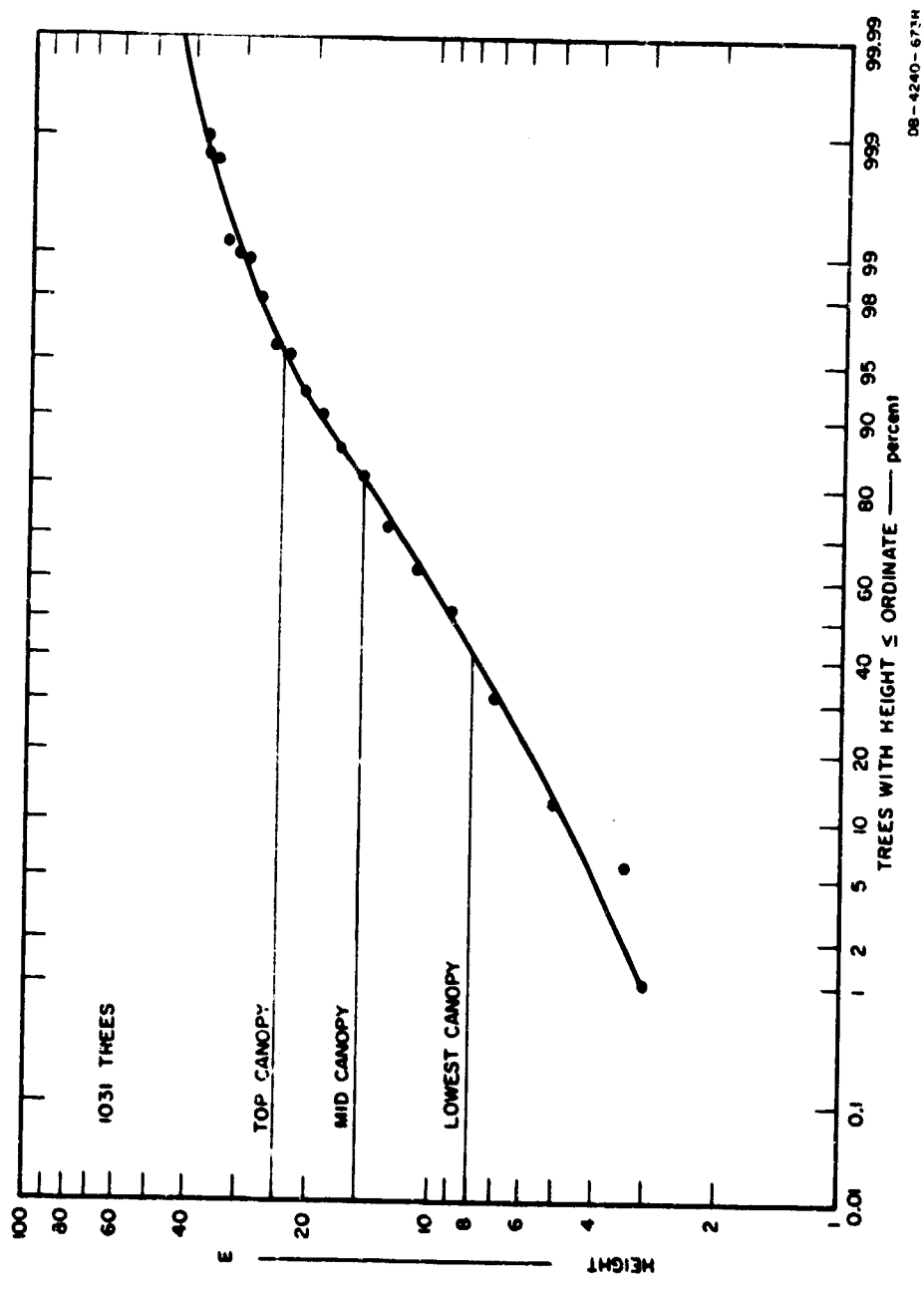


FIG. F.1 HEIGHT DISTRIBUTION FOR ALL TREES SURVEYED AT SATUN SITE

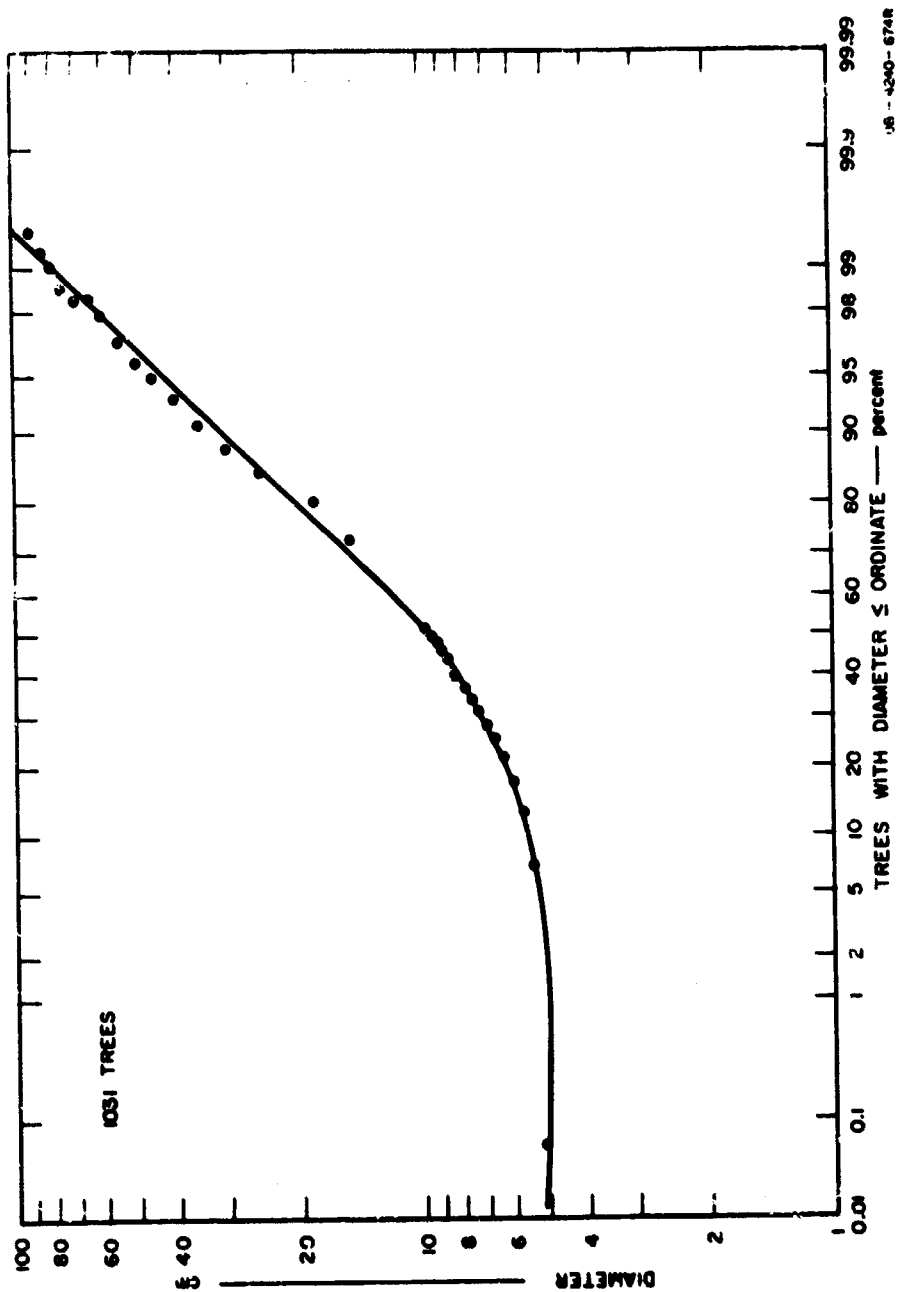


FIG. F-2 DIAMETER DISTRIBUTION FOR ALL TREES SURVEYED AT SATUN SITE

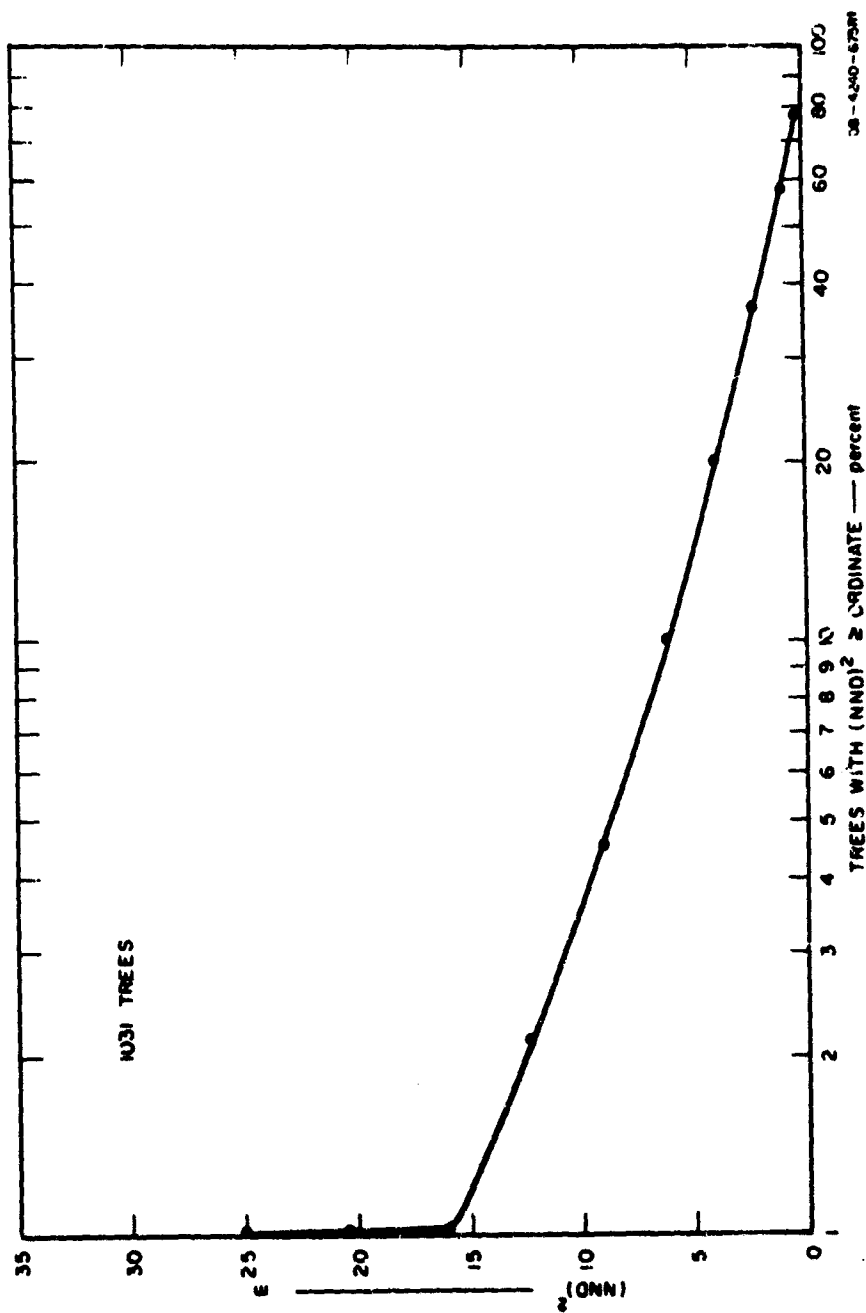


FIG. F-3 NND DISTRIBUTION FOR ALL TREES SURVEYED AT SATUN SITE

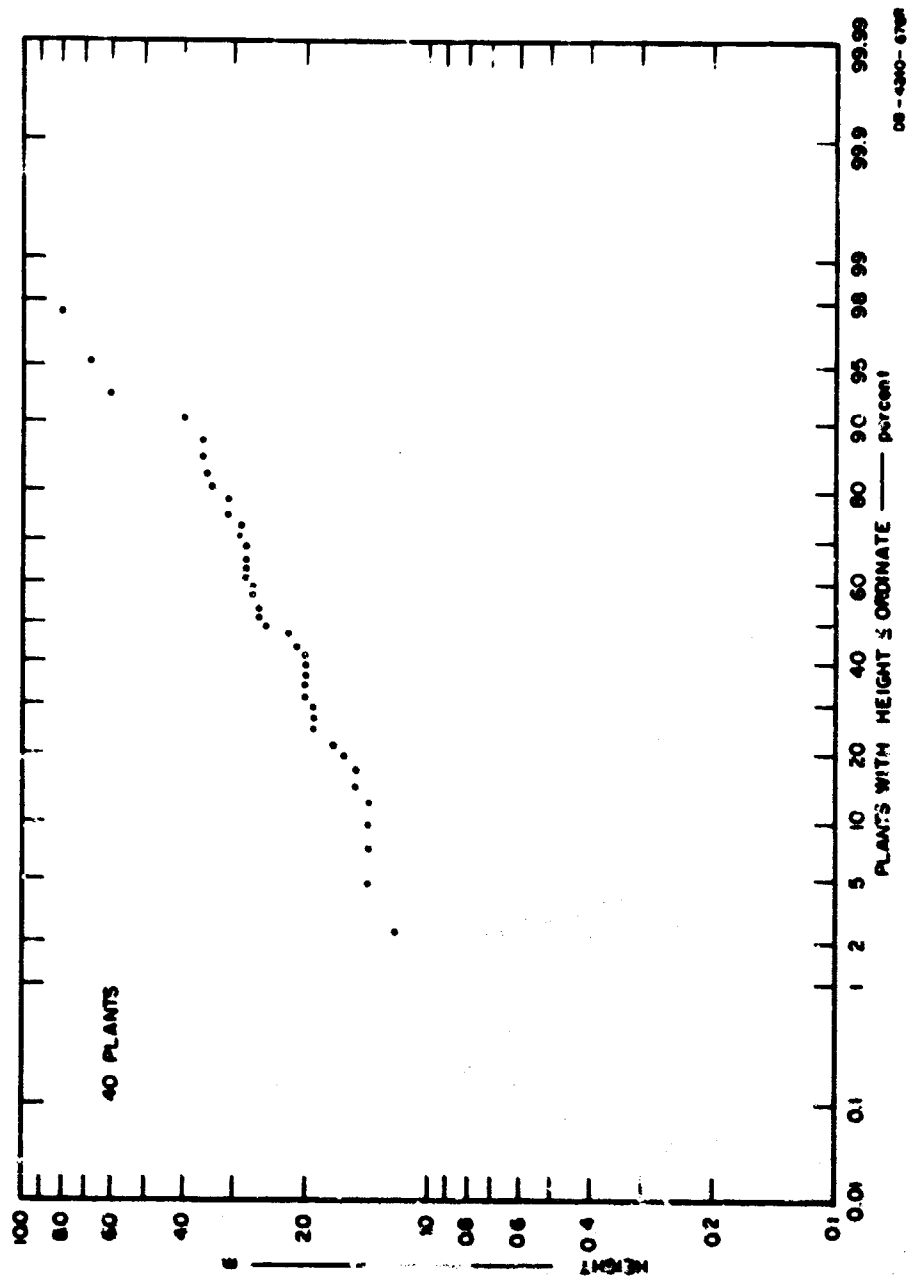


FIG. F-4 HEIGHT DISTRIBUTION FOR ALL PLANTS IN UNDERGROWTH SAMPLE S1

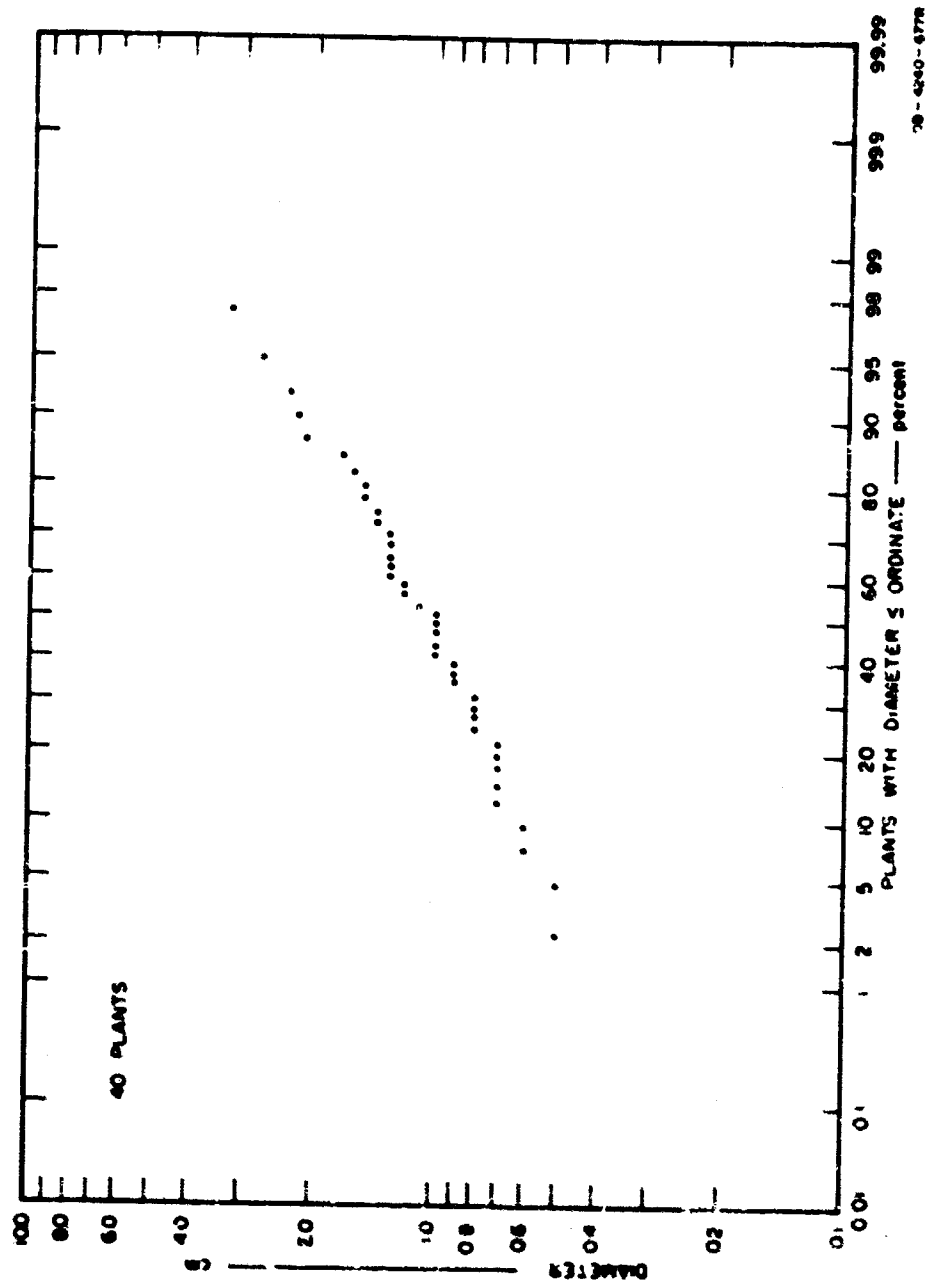


FIG. F.3 DIAMETER DISTRIBUTION FOR ALL PLANTS IN UNDERGROWTH SAMPLE 51

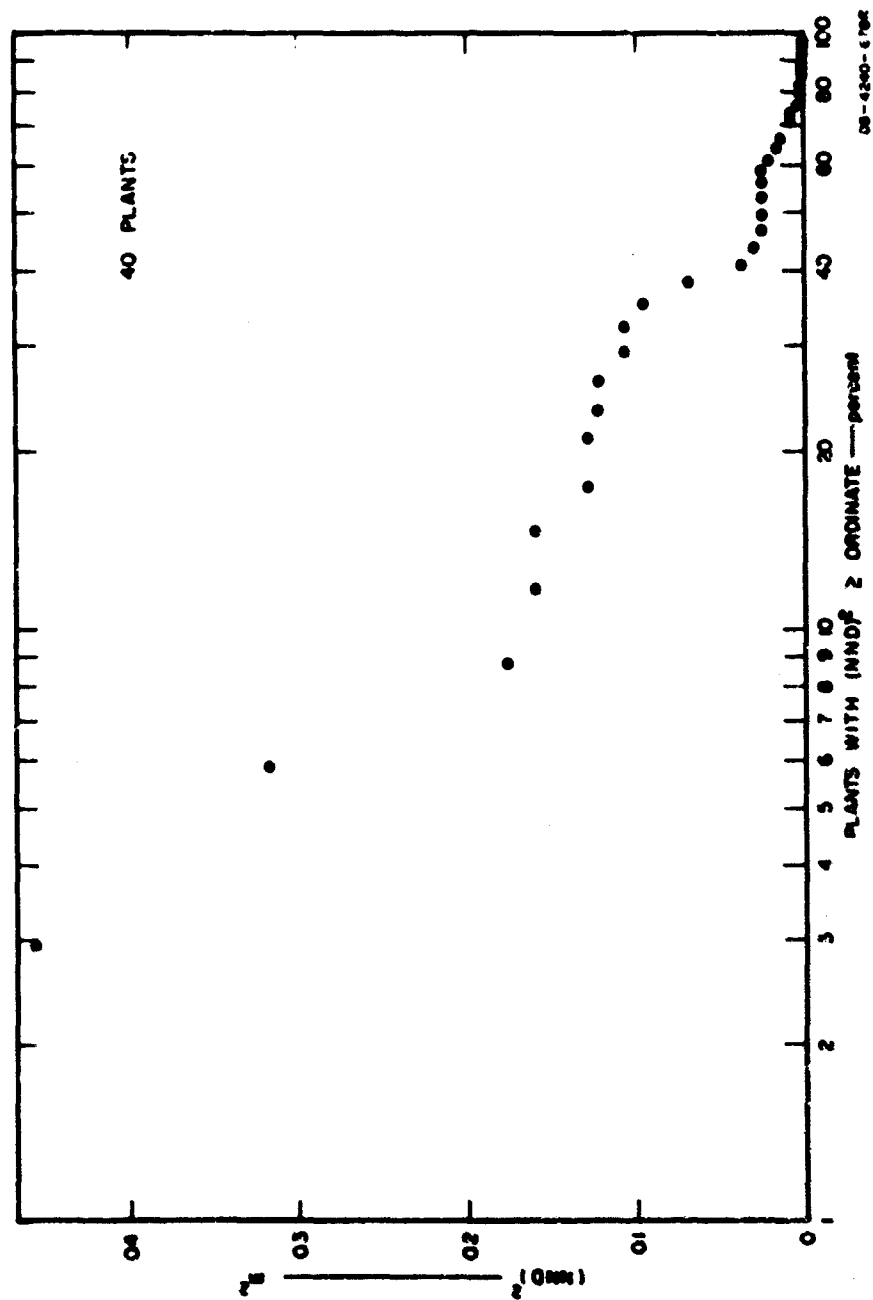


FIG. F-6 NND DISTRIBUTION FOR ALL PLANTS IN UNDERGROWTH SAMPLE SI

Table P-1
SATIN SOIL SUMMARY

WISC Plot No.	Texture		Color		pH Value	Moisture Content (% by weight)	Depth (inches)	Remarks
	LSM	USCS	Surface	Subsoil				
427	CSIL	ML	Brown	Brown to strong brown	5.0 - 5.5	34.6	0 - 9	Soil was developed from decomposed stone
	CSIL	ML		Strong brown	5.0 - 5.1	25.7 - 29.4	9 - 26	
	SL-SCl	ML		Mottled color of red to light red	5.1	31.6	26 - 60	
428	SL	SL-CL	Light yellowish brown	Strong brown to yellowish red		26.9 - 30.2	0 - 18	Soil contained very fine-grain sand
	SL	CL				28.1	18 - 30	
	SL-CL	CL				23.8	30 - 60	
429	SL	SL-CL	Dark greyish brown	Yellowish brown	5.0 - 6.2	27.4 - 30.8	0 - 12	Soil contained very fine-grain sand, no stone fragment
	SL	CL		Mottled color of very pale brown, strong brown	5.0	28.9	12 - 27	
	SL-CL	ML		Mottled color of light grey, strong brown	5.8 - 6.0	24.4	27 - 60	

Table F-1 (Concluded)

NRIC Plot No.	Texture		Color		pH Value	Moisture Content (% by weight)	Depth (inches)	Remarks
	USDA	USCS	Surface	Subsoil				
433 at J & B VHF Antenna Tower	SiL	CL	Brown to dark brown owing to litter and humus about 2 inches deep	Strong brown	5.0 - 5.3	26.2 - 28.6	0 - 12	The layer of weathered stone began from 3 inches and varied to 19 inches
	GSiL-GSiCL	MH-CH		Red	5.2 - 5.5	23.9 - 30.8	12 - 36	
	SiCL	MH-CH		Mottled color of red, reddish yellow	5.5		30 - 60	
44, 435	SiL	OL or HL	Brown to dark brown owing to litter and humus about 2 inches deep	Strong brown	4.8 - 5.5	29.7 - 32.0	0 - 12	
	GSiL	GM		Reddish yellow	5.2	22.3	12 - 18	
	GSiL-GSiCL	MH-CH		Red	5.2	31.5	18 - 42	
	SiL-SiCL	ML		Mottled color of reddish yellow, red	5.2		42 - 60	
436 (OWL Sample)	SiL	OL or ML	Brown	Light yellowish brown	4.8 - 5.0	32.1	0 - 6	Soil contained very fine-grain sand
	GSiL	GM		Reddish yellow	4.8 - 5.0	27.4 - 29.2	6 - 24	
	GSiL	ML		Reddish yellow	5.0 - 5.3		24 - 60	

Appendix G

ENVIRONMENTAL DESCRIPTION FOR MUEN CHIT

Appendix G

ENVIRONMENTAL DESCRIPTION FOR MUEN CHIT

The secondary dry evergreen forest here is quite non-uniform owing to logging. Tree canopy and height are discontinuous. The density of all trees surveyed averaged 0.07 stems/m^2 , and 88.7 percent are under 15 m high. Generally, the canopy was three-storied, although only two stories were discernible in certain areas. Trees in the top canopy are of an uneven height, averaging over 25 m. The density of trees in this story is only 0.0017 stems/m^2 . The density of middle-story trees is about 0.0021 stems/m^2 , and their height is about 15 to 24 m. The lowest story is composed of small trees between 6 and 14 m in height. Some trees are lower than undergrowth, and it is often hard to see the difference between these two layers. Vegetation in the lowest layer is usually grouped together and appears throughout the forest. About 60 percent of the trees are in this layer.

The ground is only 60 percent covered by canopy, and the dense undergrowth associated with the open canopy makes penetrability on foot very poor. The average height of undergrowth is about 3.6 meters throughout the site.

A forestry survey was conducted on twenty-six 10-by-40-meter plots, two 10-by-50-meter plots, and several 3-by-3-meter sample plots around the test antennas of the airborne Xeledop and ionospheric sounder program. The MRDC inventory numbers 384, 386, and 388 are near the OWL Sample M-I; and the inventory numbers 395 and 391 are near OWL Samples M-II and M-VI, respectively.

The statistical distributions of tree height, diameter, and NND for all 686 trees surveyed is shown in Figs. G-1 through G-3, where all trees having DBH larger than 5 cm are accounted.

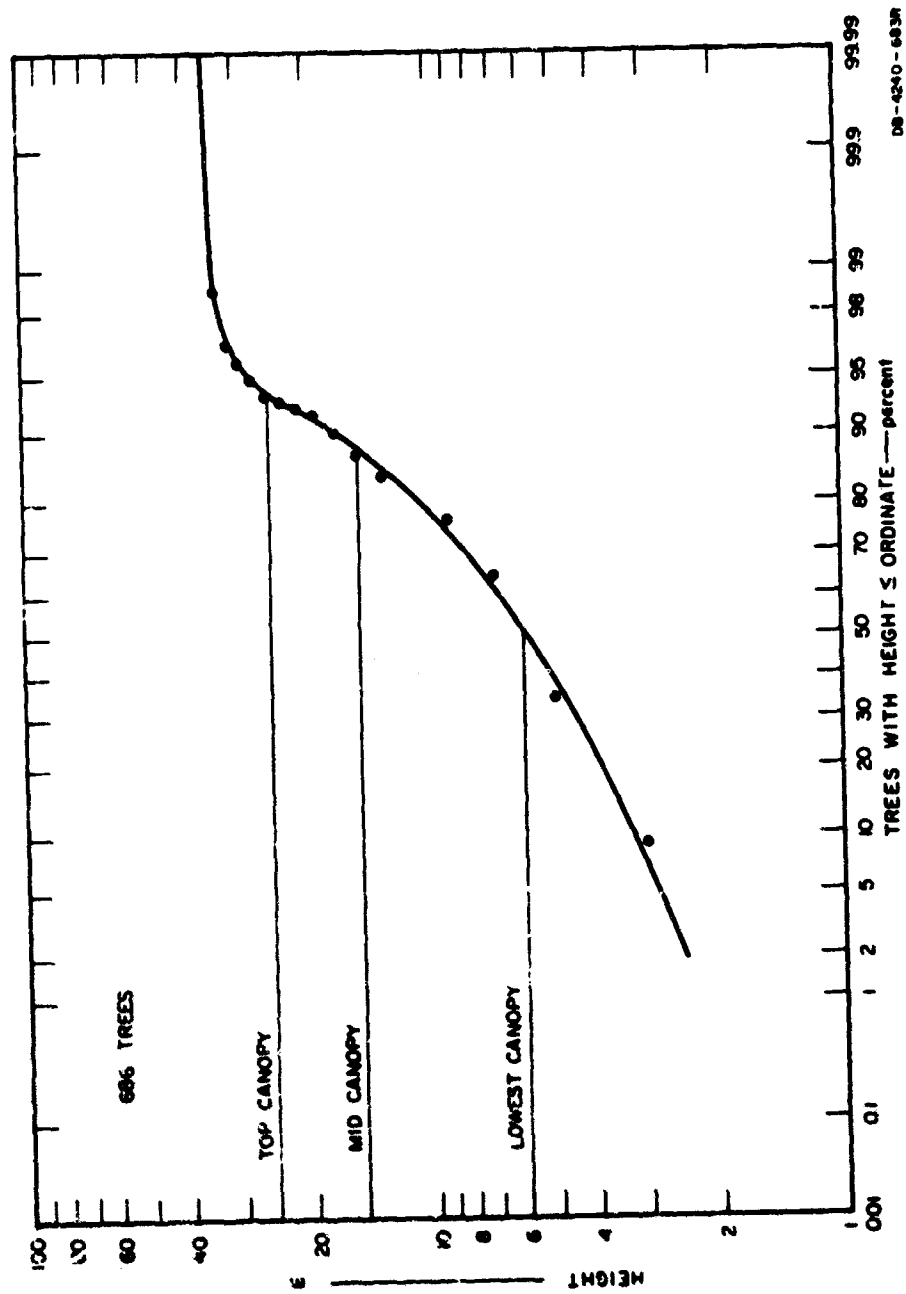


FIG. G-1 HEIGHT DISTRIBUTION FOR ALL TREES SURVEYED AT MUEN CHIT SITE

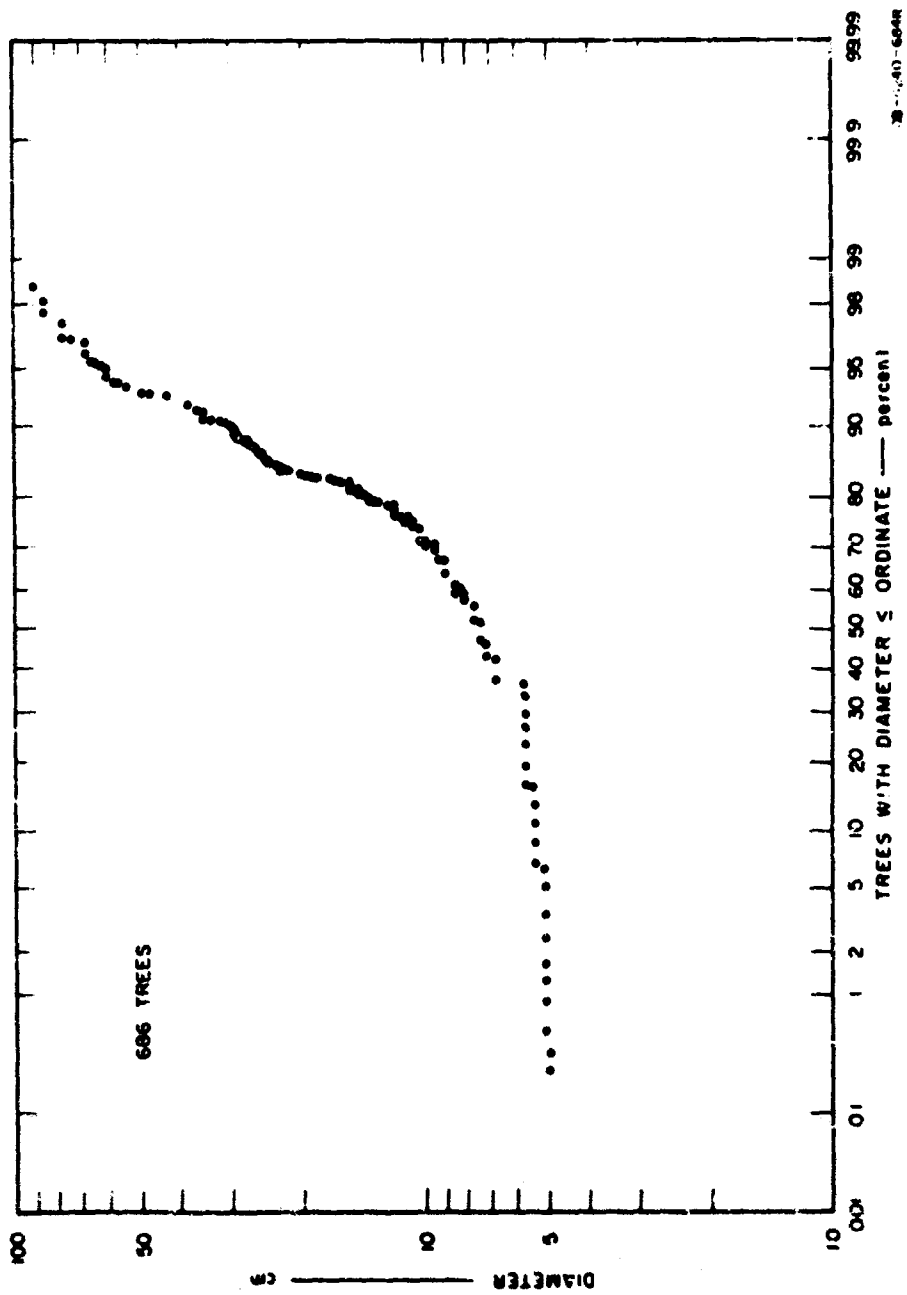


FIG. G-2 DIAMETER DISTRIBUTION FOR ALL TREES SURVEYED AT MUEN CHIT SITE

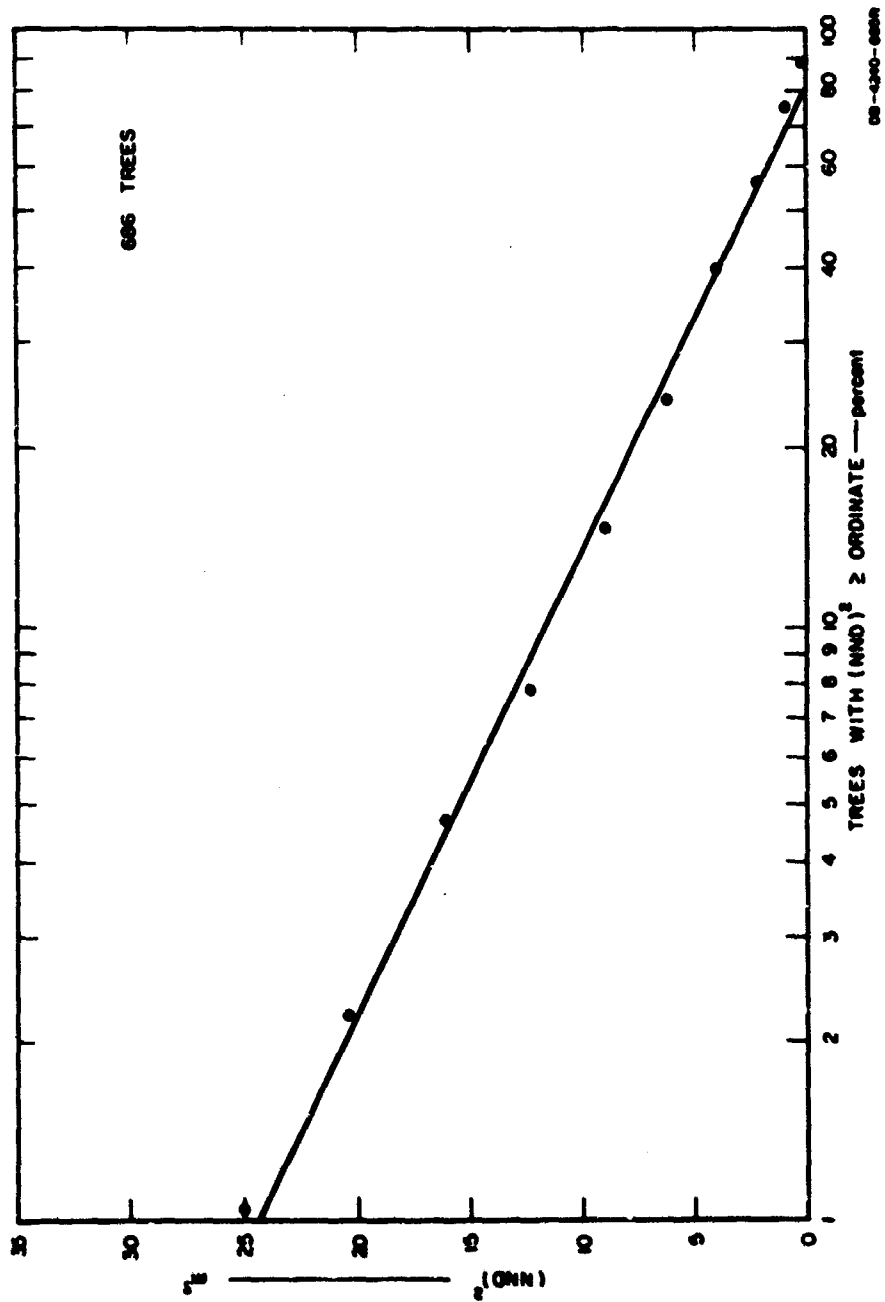


FIG. G-3 NND DISTRIBUTION FOR ALL TREES SURVEYED AT MUEN CHIT SITE

The survey of the OWL Sample MII is presented in the culmative distributions of height, diameter, and nearest-neighbor distance of all plants higher than 1 foot within the 3.5-by-3.5-m sample boundary (Figs. G-4 through G-6). There were 60 plants counted, giving a density of 4.9 stems/m².

A soil survey was made, indicating a surface composed of humus layer, leaf litter, and decomposed remains of trees. The results are summarized in Table G-1.

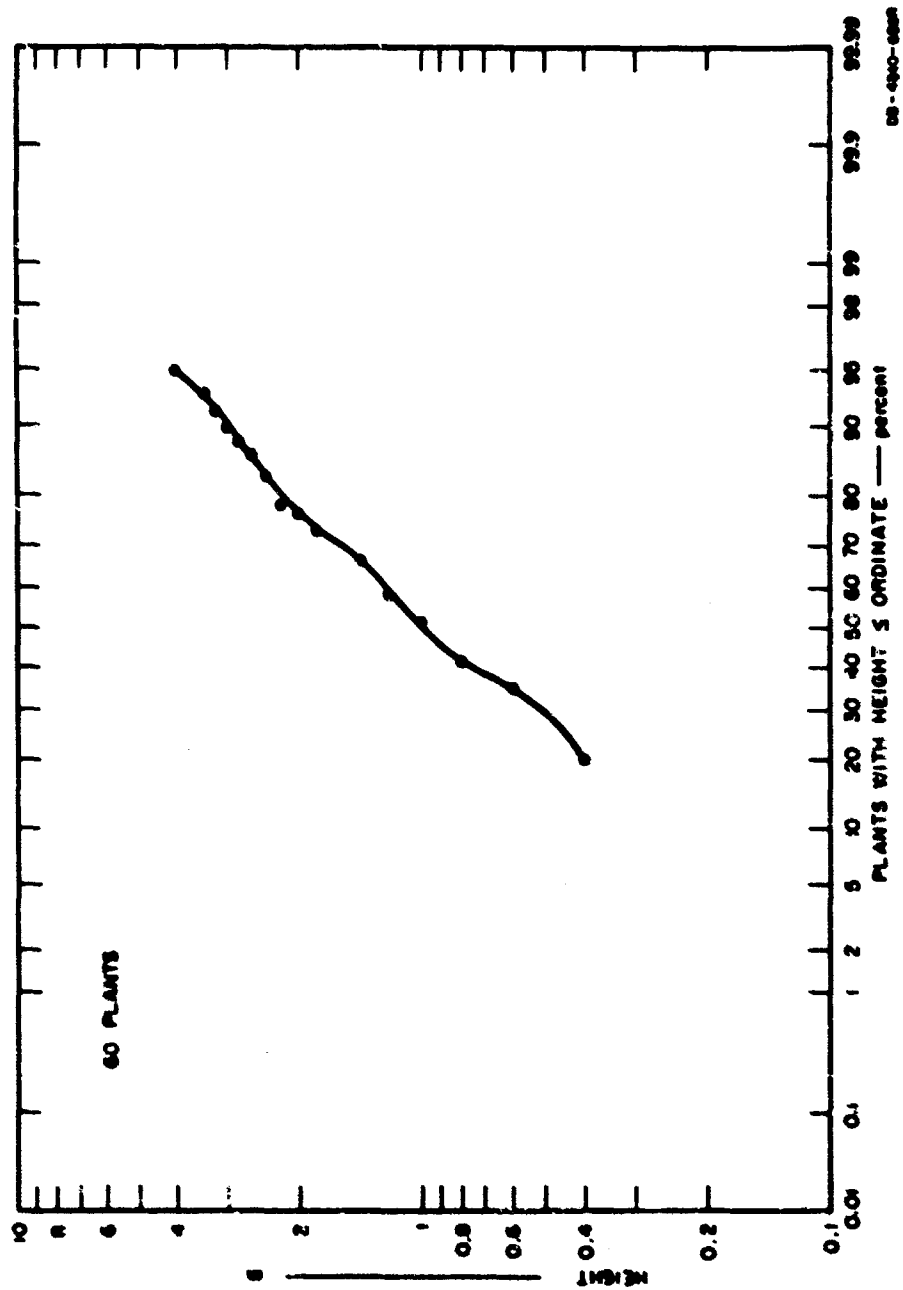


FIG. G-4 HEIGHT DISTRIBUTION FOR ALL PLANTS IN UNDERGROWTH SAMPLE MII

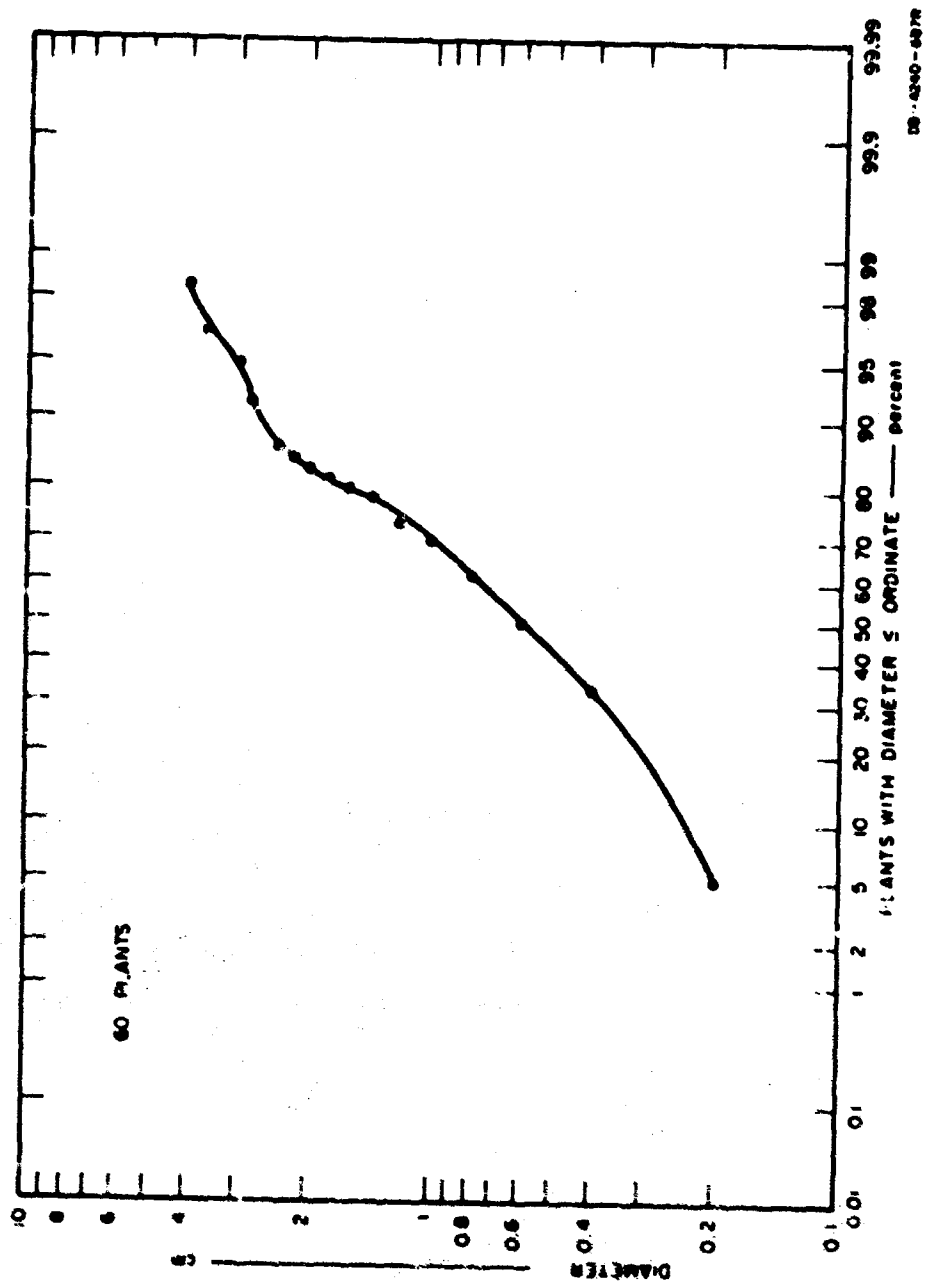


FIG. G-5 DIAMETER DISTRIBUTION FOR ALL PLANTS IN UNDERGROWTH SAMPLE MII

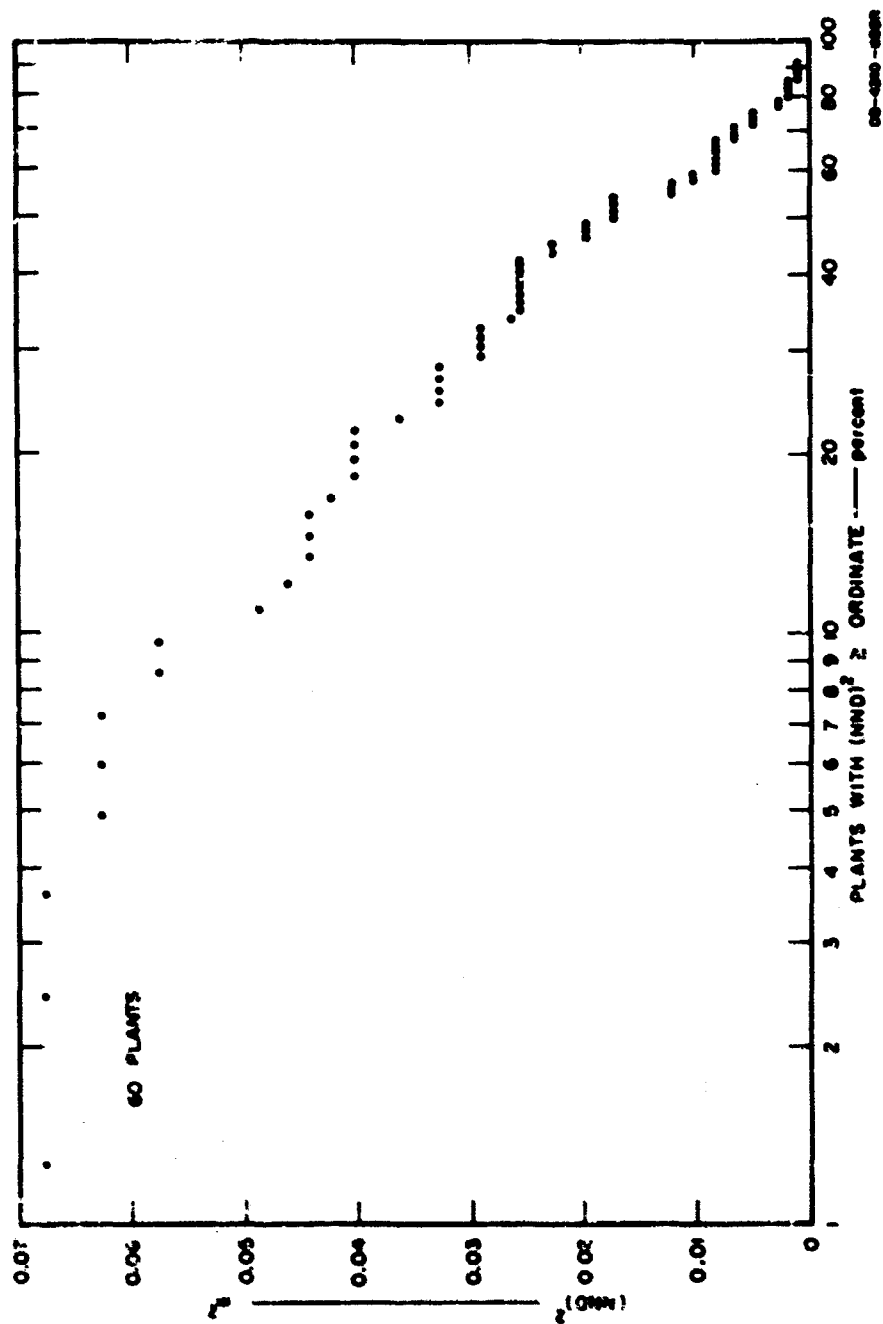


FIG. G-6 MND DISTRIBUTION FOR ALL PLANTS IN UNDERGROWTH SAMPLE MII

Table C-1
SOIL SUMMARY FOR MUEN (HIT FOREST NEAR CHONBURI
(June - July 1966)

WHIT Plot No.	Texture		Color		pH Value	Moisture Content (% by weight)	Depth (inches)	Remarks
	1-10A	1-10B	Surface	Subsoil				
100 & 109	1A-1L	SM	Brown	Light yellowish brown	5.0 - 6.7		0 - 15	Granite or its metamorphic rock
	1A-1L	SM		Light yellowish brown	5.0 - 5.3		15 - 42	
	6-1L	SC		Light reddish brown	5.5		42 - 72	
	1A-1L	SM	Brown	Light reddish brown	5.2 - 7.0		0 - 24	Granite or its metamorphic rock
	1A-1L	SM		Light reddish brown to reddish brown	5.2 - 5.4		24 - 72	
111, 112, & 113	1L	SM	Brown to dark brown	Brown	6.3 - 7.2		0 - 3	2-inch stone frag- ment was found in this profile at 6 inches depth. The bedrock or stone was found at 15-45 inches depth.
	1L	SM		Light yellowish brown	6.0		3 - 18	
	1L	SC		Light yellowish brown to very pale brown	5.8 - 6.0		18 - 36	
	1L	SC		Dark brown	5.8 - 6.0		36 - 45	

Table G-1 (continued)

MRDC /lot No.	Texture		Color		pH Value	Moisture Content (% by weight)	Depth (inches)	Remarks
	USDA	USC3	Surface	Subsoil				
314, 315 & 316	SL	SM	Brown	Light yellowish brown to very pale brown	4.9 - 6.5		0 - 18	
	(SL-GSCL)	SC		Reddish yellow	4.9		18 - 35	
	GSL	SC		Dark brown to reddish brown	4.9		35 - 60	
	LS	SM	Dark to dark brown		5.2 - 5.4		0 - 6	
317	LS	SM		Light reddish brown	5.2 - 5.4		6 - 18	Sand particles having gap of medium size
	GLS	SM		Light yellowish brown	5.3 - 5.7		18 - 40	
	LS	SM	Brown to dark brown		5.2 - 6.2		0 - 6	
	LS	SM		Light reddish brown	5.2 - 5.5		6 - 22	
318	LS-SL	SM		Pinkish grey	4.8		22 - 26	Hit stone or bedrock at 40- inch depth
	SCL	SC		Mottled color and strips of grey	4.8		26 - 40	
	LS	SM-d	Brown	Light yellowish brown	5.8 - 7.2	4.4	0 - 9	
	LS	SM-d		Brown	5.0 - 5.5	6.3 - 8.9	9 - 24	
383 & 385	LS	SM-d	Brown	Light yellowish brown	5.8 - 7.2	4.4	0 - 9	
	LS	SM-d		Brown	5.0 - 5.5	6.3 - 8.9	9 - 24	

Table G-1 (continued)

NRDC Plot No.	Texture		Color		pH Value	Moisture Content (% by weight)	Depth (inches)	Remarks
	USDA	USCS	Surface	Subsoil				
383 & 385 (cont'd.)	SL	SC		Brown to strong brown	4.8 - 5.0		24 - 50	
	GSL	SC		Brown to strong brown	4.9		50 - 60	
	LS	SM-d			5.0 - 6.5	7.5 - 8.6	0 - 18	
	LS	SM-d			4.9		18 - 28	
384 & 385	SL	SC		Brown to strong brown	5.0		28 - 42	
	GLS	SC		Mottled color of light yellowish brown	5.3		42 - 52	
	GLS	SC		Mottled color of strong brown	5.3		52 - 60	
	LS	SM-d		Brown	5.4 - 7.8	8.2 - 8.7	0 - 15	
387	LS	SM-d			5.3 - 5.4	8.6	15 - 30	
	SL	SC			5.0 - 5.3		30 - 45	
	GSL	SC		Mottled color of reddish brown to yellowish red	4.9		45 - 52	
	LS	SM-d	Brown	Light yellowish brown	4.8 - 6.5	6.2 - 6.3	0 - 12	
388	GLS	SM-d		Brown to strong brown	4.8 - 5.0	7.4	12 - 13	

Table G-1 (continued)

MRDC Plot No.	Texture		Color		pH Value	Moisture Content (% by weight)	Depth (inches)	Remarks
	USDA	USCS	Surface	Subsoil				
388 (cont'd.)	GSL	SC		Strong brown	5.0 - 5.1		18 - 36	
	GLS	SM-u		Mottled color of strong brown to brown	5.1 - 6.0			
389 & 390	LS-SL	SM-d	Brown	Brown to strong brown	5.4 - 7.2	8.8 - 12.8	0 - 15	
	GSL	SC		Strong brown	5.2 - 5.5	7.6	15 - 42	
	GSL	SC		Strong brown	5.5 - 5.7		42 - 60	
391	LS	SM-d	Surface to 1-inch depth was brown to dark brown	Brown	5.5 - 7.3	13 - 15.4	0 - 15	
	LS-SL	SC		Strong brown	5.0 - 5.2	9.7	15 - 42	
	GSL	SC			5.3 - 5.6		42 - 60	
392	LS	SM-d	Dark brown	Brown	4.8 - 7.3	5.6 - 10.4	0 - 33	Very dense layer of laterite concretions 58 inches below surface
	GLS	SM-d		rown to light brown	5.0		33 - 45	
	GLS	SM-d		Mottled color of reddish brown	5.5 - 5.7		45 - 58	
393 & 394	SL	SM-SC	Dark brown to 1-inch depth	Brown	5.8 - 6.5	9.0 - 15.4	0 - 15	
	GSL	SC		Strong brown	5.9	9.4	15 - 27	

Table G-1 (concluded)

NRDC Plot No.	Texture		Color		pH Value	Moisture Content (% by weight)	Depth (inches)	Remarks
	USDA	USCS	Surface	Subsoil				
393 & 394 (cont'd.)	GSL	SC		Yellow red to reddish yellow	5.9		27 - 40	
	GSL	SM-u		Mottled color of yellowish red	5.7 - 5.9		40 - 60	
396	SL	SH-d	Dark brown of humus layer to 2- inch depth	Brown to light brown	5.5 - 6.7	12.4 - 18.2	0 - 24	
	LS	SC		Yellowish red to reddish yellow	5.5		24 - 60	
397	SL	SM-d	Dark brown of humus layer to 2- inch depth	Brown to light brown	5.0 - 6.5	12.6 - 17.3	0 - 20	
	LS	SC		Yellowish red to reddish yellow	5.0 - 5.1		20 - 40	
	SL-SIL	SM-SC		Strong brown	5.0		40 - 51	

Appendix H

THE OWL COMPUTER PROGRAM

Appendix H

THE OWL COMPUTER PROGRAM

The calculation of electrical parameters from results of impedance measurements made on the OWL probes is separated into two programs. Program I contains four steps of calculation as follows: (1) conversion of impedance bridge dial readings to polar form; (2) impedance transformation through a network connecting bridge to probe, following the method for calculating Z_0 (OC-SC or L-2L) as instructed; (3) sorting air and sample data, and (4) calculating air (control) parameters. The logical flow of these computations is shown in Fig. H-1. The program accepts direct dial readings of the Boonton 250A RX meter; or dial readings of the GR 1606, GR 1601, or HP 803A bridges normalized to frequency and zero setting; or it will accept conductance and normalized susceptance inputs from the GR 1602B admittance meter. The bridge dial readings are coded in the computer as to real and imaginary parts X and Y, with subscripts according to the type of bridge termination. (For example, when we measure the open-ended impedance of a coax balun we code the bridge readings as X_B , Y_B). These bridge readings, together with the balun (or other input network) impedances and the other parameters shown in Table H-1, are given as the input of Program I. Air and sample data are input to the computer at the same time and sorted as part of the program. The user must, however, make sure the control data he inputs do correspond, for site, data, probe size, etc., with the sample data. The output of Program I is a sorted sequence of air and sample cards having the parameters shown in Table H-2. There is also a printed listing of all Program I outputs.

Computer Program II makes the calculation of electrical parameters shown in Table H-3, based on the input data that are the output of Program I. The mathematical equations used in both programs are presented in Tables H-4 and H-5. The logical flow chart of Program II is shown in Fig. H-2.

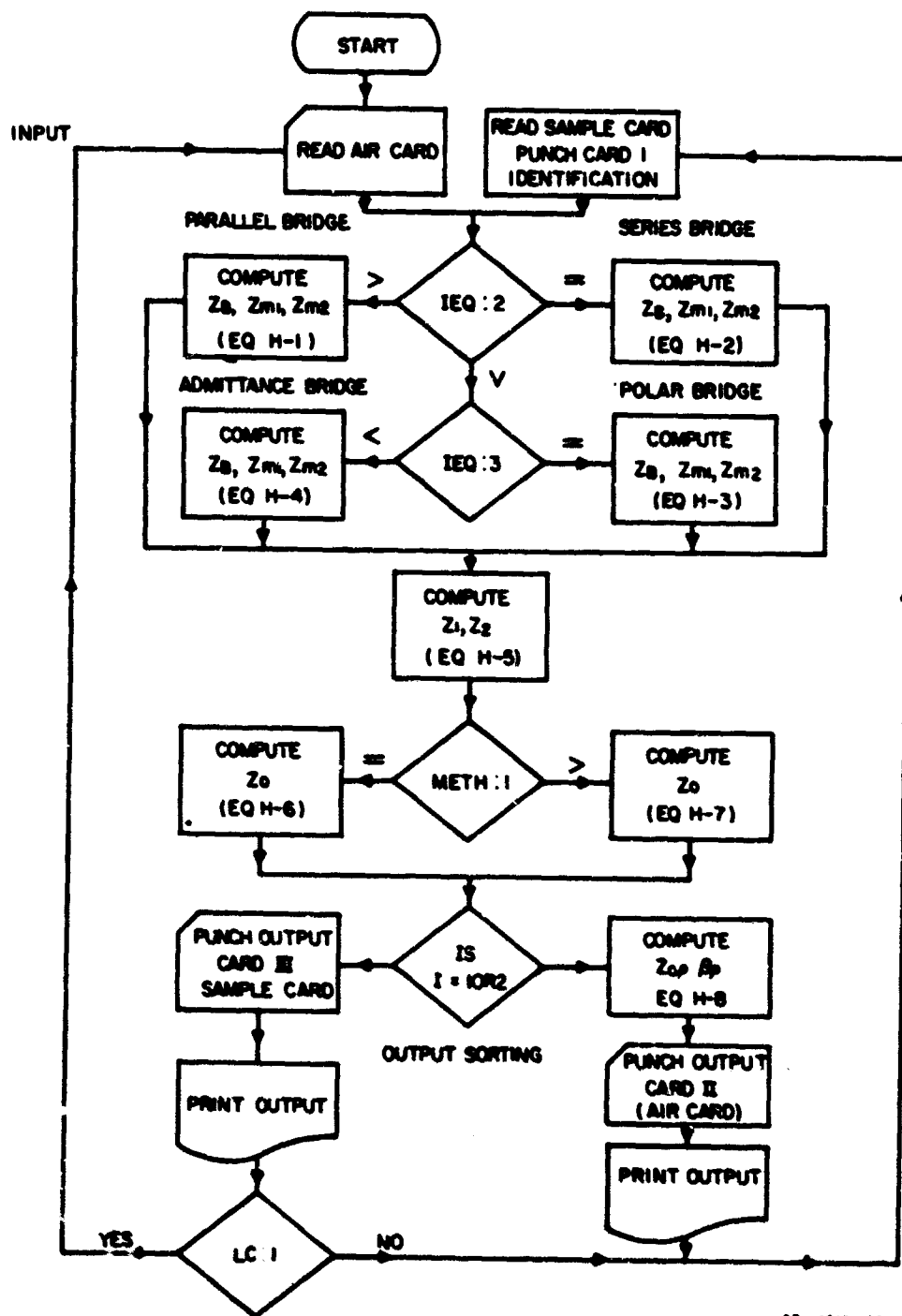


FIG H-1 FLOW DIAGRAM FOR PROGRAM 1

Table H-1

INPUT PROGRAM I

Air Card Only	F_p = Frequency in MHz, p indicates OWL is placed in air.
Air Card	I = Card Index--identifies air or sample medium (1 = air, 2 = sample).
and	IEQ = Alphanumeric code to indicate type of equipment used where 1 = Parallel Bridge, as Boonton 250A RX meter.
Sample	2 = Series Bridge, as GR 1606 RF or 1601 VHF
Medium	3 = Polar Bridge, as HP 803A VHF
Card	4 = Admittance Bridge, as GR 1602-B admittance meter.
	METH = Sampling method for calculation of Z_o : where 1 = OC-SC method 2 = L-2L method.
	L = Basic OWL probe length in meters.
	N = Number of half wavelengths contained in OWL length.
	T = Network transformation ratio (for half-wave coax balun $T = 4 < 0^\circ$).
	X_B, Y_B = Bridge impedance reading of open ended coaxial balun or similar input network.
Air Card and Sample	X_{m1}, Y_{m1} = Bridge impedance reading of input network with open-ended probe connected.
Medium	X_{m2}, Y_{m2} = Bridge impedance reading of input network connected to probe shorted at L or open-ended at 2L, depending on whether METH = 1 or 2. X and Y denote the quantities tabulated below, according to the type of bridge used.
Card	

	<u>IEQ</u>	<u>X</u>	<u>Y</u>
Air Card and	1	Resistance in kilohm	Capacitance in picofarad
Sample	2	Resistance in ohm	Reactance in ohm
Medium	3	Magnitude of impedance in ohm	Argument of impedance degree
Card	4	Conductance in mho	Suscept. ce in mho

Sample
Medium
Card
Only

Identification = Date and time, site, sample (FS =
vegetation GCS = ground); probe spacing,
diameter, and station.

F = Measured frequency in sample in MHz.

LC = Computing index: to indicate the last
card of a normalizing process, LC = 1.

Table H-2

OUTPUT PROGRAM I/INPUT PROGRAM II

Card Output I
and
Input to II

Identification (as in Table H-1)

L = Basic probe length.

F_p = Control frequency* in MHz.

F = Sample measurement frequency in MHz.

Z_{1p} = Control input impedance of open-ended probe.

Z_1 = Sample input impedance of open-ended probe.

Z_{op} = Control characteristic impedance of probe.

Z_o = Sample characteristic impedance of probe.

Listing Output
I Only

Z_{2p} = Control input-impedance of short-ended probe
(at length L) or open-ended probe (at length $2L$).

Z_2 = Sample input impedance of short-ended probe
(at length L) or open-ended probe (at length $2L$).

β_p = Control phase constant.

* F_p should equal F , but will not quite owing to thermal effects, etc.

Table H-3

OUTPUT OF PROGRAM II

Identification (as in Table H-1)

EPS (ϵ_r) = Permittivity of the sample relative to air.

SIGMA (σ) = Conductivity of the sample relative to air.

DELTA (δ) = Loss tangent of the sample.

ALPHA (A) = Attenuation rate for TEM waves in the sample.

BETA (B) = Phase constant for TEM waves in the sample.

MU (μ_r) = Magnetic permeability of the sample relative to air.

GAMMA (γ) = Complex propagation constant of TEM waves in the sample.

Table H-4

EQUATIONS IN PROGRAM I

I IMPEDANCE CONVERSION TO POLAR FORM

A. Parallel Bridge:

$$Z_m = 1000[(1/X)^2 + (2\pi FY/1000)^2]^{-1/2} / \tan^{-1}(2\pi FYX/1000) \text{ ohms.} \quad (H-1)$$

B. Series Bridge:

$$Z_m = (X^2 + Y^2)^{1/2} / \tan^{-1}(Y/X) \text{ ohms.} \quad (H-2)$$

C. Polar Bridge:

$$Z_m = X/Y \text{ ohms.} \quad (H-3)$$

D. Admittance Bridge:

$$Z_m = 1000 (X^2 + Y^2)^{-1/2} / -\tan^{-1}(Y/X) \text{ ohms.} \quad (H-4)$$

II IMPEDANCE TRANSFORMATION

$$Z = \frac{TZ_B Z_m}{Z_B - Z_m} = Z_1 \text{ or } Z_2 \text{ ohms.} \quad (H-5)$$

III Z_o CALCULATED, METHODS

A. OC-SC Method:

$$Z_o = (Z_1 X_2)^{1/2} \text{ ohms.} \quad (H-6)$$

B. L - 2L Method:

$$Z_o = [Z_1 (2Z_2 - Z_1)]^{1/2} \text{ ohms.} \quad (H-7)$$

Table H-5

EQUATIONS IN PROGRAM II

I CONSTANTS OF THE MEDIUM FROM PROBE PARAMETERS

$$\epsilon_r = \frac{F_P}{F} \cdot \frac{\text{Im}[\Gamma/Z_o]}{\text{Im}[\Gamma_p/Z_{op}]} \quad (\text{H-8})$$

$$\delta = \text{Re}[\Gamma/Z_o] / \text{Im}[\Gamma/Z_o] \quad (\text{H-9})$$

$$\sigma = 55.63 F \epsilon_r \delta \times 10^{-6} \text{ mhos/m} \quad (\text{H-10})$$

$$A = \frac{2\pi F}{C} \left(\mu_r \epsilon_r \frac{-1 + \sqrt{1 + \delta^2}}{2} \right)^{1/2} \quad (\text{H-11})$$

$$B = \frac{2\pi F}{C} \left(\mu_r \epsilon_r \frac{1 + \sqrt{1 + \delta^2}}{2} \right)^{1/2} \quad (\text{H-12})$$

$$\gamma = A + jB \quad (\text{H-13})$$

$$\mu_r = \frac{F_P}{F} \frac{\text{Im}[\Gamma/Z_o]}{\text{Im}[\Gamma_p/Z_{op}]} \quad (\text{H-14})$$

II THE PROBE PARAMETERS ARE

$$\Gamma = \alpha + j\beta$$

$$\alpha = -\frac{1}{4L} \left[\ln \frac{(1-a)^2 + b^2}{(1+a)^2 + b^2} \right]$$

$$\beta = \frac{1}{2L} \left[(2N-1)\pi - \tan^{-1} \left(\frac{1-a}{b} \right) - \tan^{-1} \left(\frac{1+a}{b} \right) \right]$$

$$a = \text{Re}[Z_c/Z_1]$$

$$b = \text{Im}[Z_c/Z_1]$$

$$\Gamma_p = \Gamma \text{ for probe in air}$$

c = Velocity of light in vacuum.

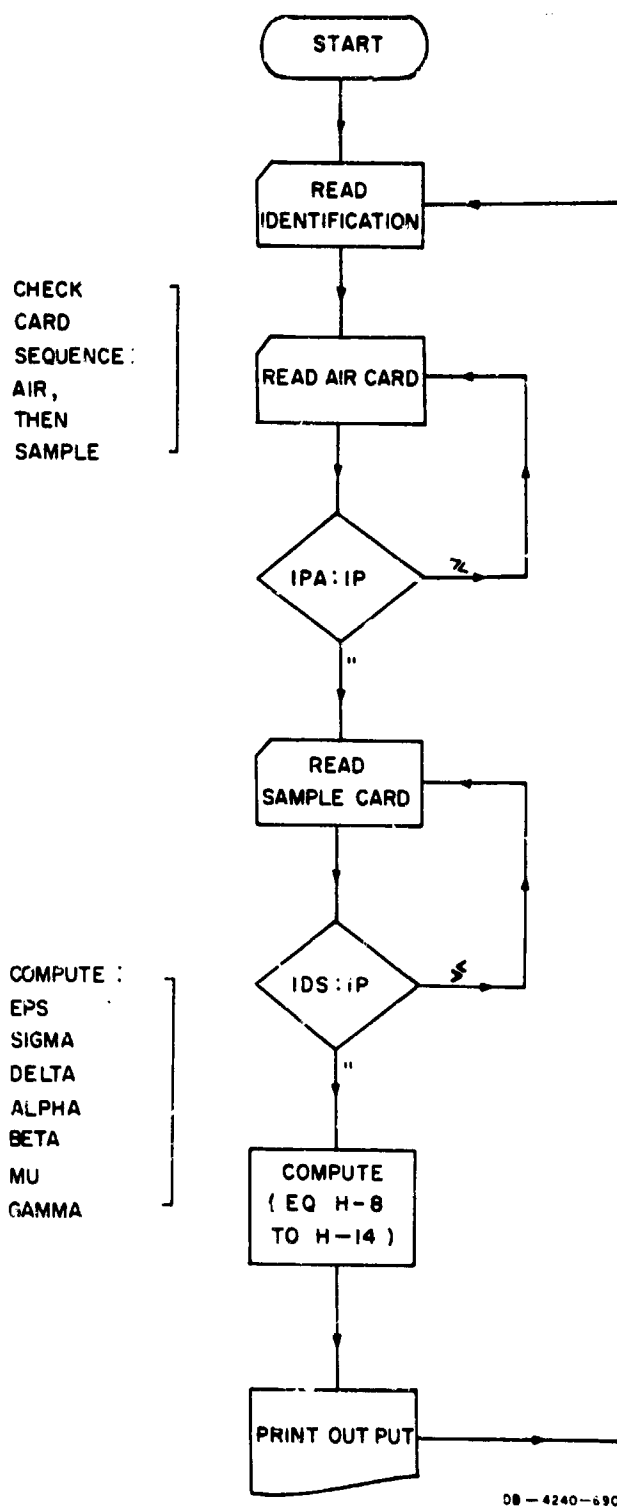


FIG. H-2 FLOW DIAGRAM FOR PROGRAM II

REFERENCES

1. J. W. Herbstreit and W. Q. Crichlow, "Measurement of the Attenuation of Radio Signals by Jungle," J. Res. NBS, Radio Science, Vol. 68D, No. 8, pp. 903-906 (August 1964).
2. J. R. Shirley, "Radio Within the Infantry Battalion in the Jungle," Project Doughboy, Technical Memorandum ORO-T-277, Operations Research Office, The Johns Hopkins University, Chevy Chase, Maryland (August 1954).
3. E. J. Kirkscether, "Ground Constant Measurements Using a Section of Balanced Two-Wire Transmission Line," IRE Trans., AP-8, No. 3, p. 307 (May 1960).
4. H. W. Parker and G. H. Hagn, "Feasibility Study on the Use of Open-Wire Transmission Lines, Cavities and Capacitors to Measure the Electrical Properties of Vegetation," Special Technical Report 13, SRI Project 4240, Contract DA 36-039 AMC-00040(E), Stanford Research Institute, Menlo Park, California (August 1966).
5. D. L. Sachs, "A Conducting Slab Model for Electromagnetic Propagation Within a Jungle Medium II," Internal Memorandum IMR-471, Defense Research Corporation, Santa Barbara, California (30 September 1966).
6. D. L. Sachs and P. J. Wyatt, "A Conducting Slab Model for Electromagnetic Propagation Within a Jungle Medium," Radio Science, Vol. 3 (New Series), No. 2, pp. 125-134 (February 1968).
7. T. Tamir, "The Role of the Skywave and Lateral Waves on Propagation in Forest Environments," paper presented at ARPA/AGILE Communications Colloquium at Atlantic Research Corporation, Alexandria, Virginia (1 March 1967).
8. J. Taylor, "A Note on the Computed Radiation Patterns of Dipole Antennas in Dense Vegetation," Special Technical Report 16, SRI Project 4240, Contract DA 36-039 AMC-00040(E), Stanford Research Institute, Menlo Park, California (February 1966).
9. N. E. Goldstein, H. W. Parker, and G. H. Hagn, "Three Techniques for Measurement of Ground Constants in the Presence of Vegetation," Special Technical Report 30, SRI Project 4240, Contract DA 36-039 AMC-00040(E), Stanford Research Institute, Menlo Park, California, (March 1967).
10. C. Barnes, "Transmitters Towed Through Air Test Antenna's Radiation Pattern," Electronics, pp. 96-101 (October 1965).

11. C. Barnes, "Xeledop Antenna Pattern Measuring Equipment, 2 to 50 MHz," Communication Lab., Stanford Research Institute, Menlo Park, California (January 1965).
12. C. Barnes, "Xeledop Antenna Pattern Measuring Equipment, 50 to 100 MHz," Communication Lab., Stanford Research Institute, Menlo Park, California (April 1966).
13. G. E. Barker and G. D. Koehrsen, "Full-Scale Pattern Measurements of Simple HF Field Antennas in a Thailand Tropical Forest," Special Technical Report 35, SRI Project 4240, Contract DA 36-039 AMC-00040(E), Stanford Research Institute, Menlo Park, California (February 1968).
14. Jansky and Bailey, "Tropical Propagation Research," Semiannual Report 6, Contract DA 36-039 SC-90889, Atlantic Research Corporation, Alexandria, Virginia (1 January - 30 June 1965).
15. N. K. Shrauger and K. L. Taylor, "Initial VHF Propagation Results Using Xeledop Techniques and Low Antenna Heights," Special Technical Report 26, SRI Project 4240, Contract DA 36-039 AMC-00040(E), Stanford Research Institute, Menlo Park, California (December 1966).
16. G. H. Hagn, G. E. Barker, H. W. Parker, J. D. Hice, and W. A. Ray, "Preliminary Results of Full-Scale Pattern Measurements of Simple VHF Antennas in a Eucalyptus Grove," Special Technical Report 19, SRI Project 4240, Contract DA 36-039 AMC-00040(E) (January 1966), AD 484-239.
17. G. H. Hagn, "The Use of Ground Wave Transmission Loss and Intelligibility Data to Predict the Effective Range and Performance of VHF Man-Pack Radios in Forest," Special Technical Report 11, SRI Project 4240, Contract DA 36-039 AMC-00040(E), Stanford Research Institute, Menlo Park, California (September 1966).
18. K. Christensen, J. W. Kelley, A. Nalampoon, and S. Sukhawong, "Environmental Description I of the Jansky & Bailey Test Site at Khao Yai, Thailand," MRDC Report 66-015, Military Research and Development Center, Bangkok, Thailand (January 1966).
19. K. Christensen and D. G. Neal, "Environmental Description II of Jansky & Bailey Test Site at Khao Yai, Thailand," MRDC Report 66-026, Military Research and Development Center, Bangkok, Thailand (July 1966).
20. H. L. Mills and S. E. Clagg, "The Physiognomy of Vegetation: A Quantitative Approach to Vegetation Geometry Based upon the Structural Cell Concept as the Minimum Sample Size," available from Marshall University, Huntington, West Virginia (1964).
21. F. J. Massey, Jr., "A Note on the Estimation of a Distribution Function by Confidence Limits," Ann. Math. Stat., Vol. 21, pp. 116-119 (1950).

22. A. N. Kolmogorov, Limit Distribution for Sums of Independent Random Variables (Addison-Wesley, Cambridge, Massachusetts, 1954).
23. A. H. Bowker and G. J. Lieberman, Engineering Statistics, p. 65 (Prentice-Hall, Englewood Cliffs, New Jersey, May 1961).
24. A. M. Mood and F. A. Graybill, Introduction to the Theory of Statistics, p. 252 (McGraw-Hill/Kogakusha 2nd Edition, Tokyo, 1963).
25. S. B. Cohn, "The Electric and Magnetic Constants of Metallic Delay Media Containing Obstacles of Arbitrary Shape and Thickness," J. App. Phys., Vol. 22, pp. 628-634 (May 1951).
26. D. G. Neal, "Statistical Descripor of the Forests of Thailand," MRDC Report 67-019, Military Research and Development Center, Bangkok, Thailand (May 1967).
27. H. W. Parker and G. H. Hagn, "Electrical Properties of Forests," paper presented at ARPA/AGILE Communications Colloquim at Atlantic Research Corporation, Alexandria, Virginia (1 March 1967).
28. D. J. Pounds and A. H. La Grone, "Considering Forest Vegetation as an Imperfect Dielectric Slab," Report No. 6-53, Electric Engineering Research Laboratory, University of Texas, Austin, Texas (31 May 1963).
29. G. H. Hagn, E. L. Younker, and H. W. Parker, "Research-Engineering and Support for Tropical Communications," p. 46, Semiannual Report 6, Covering the Period 1 October 1965 through 31 March 1966, SRI Project 4240, Contract DA 36-039 AMC-00040(E), Stanford Research Institute, Menlo Park, California (June 1966).
30. G. V. Keller and F. C. Frischknecht, Electrical Methods in Geophysical Prospecting, pp. 97-100 (Pergamon Press, London 1966).
31. C. M. Stewart, "Moisture Content of Living Trees," Nature, Vol. 214, pp. 138-140 (8 April 1967).
32. R. M. Dickinson, P. D. Potter, and W. J. Schimandle, "Tree Antennas," Space Technology Applications Report 33-1, Jet Propulsion Laboratory, California Institute of Technology, Pasadena, California (10 May 1967).
33. S. Pongpangan and D. V. Vanek, "Environmental Description of Stanford Research Institute Communication Test Site near Ban Muen Chit, Thailand," Joint Thai-U.S. Military Research and Development Center, Environmental Sciences Division Report, Bangkok, Thailand (to be published in 1968).
34. S. Pongpangan and D. V. Vanek, "Environmental Description of Stanford Research Institute Communication Test Site near Chumphon, Thailand," Joint Thai-U.S. Military Research and Development Center, Environmental Sciences Division Report, Bangkok, Thailand (to be published in 1968).

35. D. V. Vanek, and S. Pongpangan, "Environmental Description of the Jansky & Bailey Test Site at Satun," Joint Thai-U.S. Military Research and Development Center, Environmental Sciences Division Report, Bangkok, Thailand (in preparation 1968).
36. J. G. Skellam, "Random Dispersion in Theoretical Populations," Biometrika, Vol. 38, pp. 196-218 (1951).
37. E. Parzen, Modern Probability Theory and Its Applications, pp. 17-22 (Wiley/Toppan International Edition, Tokyo, 1960).
38. J. Taylor, Ching Chun Han, Chung Lien Tien, and G. H. Hagn, "Open-Wire Transmission Line Techniques for Measuring the Macroscopic Electrical Properties of a Forest Region," Special Technical Report 42, SRI Project 4240, Contract DA 36-039 AMC-00040(E), Stanford Research Institute, Menlo Park, California (in preparation).

UNCLASSIFIED

Security Classification

DOCUMENT CONTROL DATA - R & D

(Security classification of title, body of abstract and indexing annotation must be entered when the overall report is classified)

1. ORIGINATING ACTIVITY (Corporate author) Stanford Research Institute 333 Ravenswood Avenue Menlo Park, California 94025		2a. REPORT SECURITY CLASSIFICATION UNCLASSIFIED	
		2b. GROUP N/A	
3. REPORT TITLE ELECTRIC CONSTANTS MEASURED IN VEGETATION AND IN EARTH AT FIVE SITES IN THAILAND			
4. DESCRIPTIVE NOTES (Type of report and inclusive dates) Special Technical Report 43			
5. AUTHOR(S) (First name, middle initial, last name) H. W. Parker Withan Makarabhiromya			
6. REPORT DATE December 1967		7a. TOTAL NO OF PAGES 198	7b. NO OF REFS 38
8a. CONTRACT OR GRANT NO. Contract DA 36-039 AMC-00040(E)		9a. ORIGINATOR'S REPORT NUMBER(S) Special Technical Report 43 SRI Project 4240	
8b. PROJECT NO. Order No. 5384-PM-63-91			
c. ARPA Order 371		9b. OTHER REPORT NO(S) (Any other numbers that may be assigned this report)	
d.			
10. DISTRIBUTION STATEMENT Distribution of this document is unlimited			
11. SUPPLEMENTARY NOTES		12. SPONSORING MILITARY ACTIVITY Advanced Research Projects Agency Washington, D.C.	
13. ABSTRACT <p>Balanced two-conductor open transmission line probes were used to measure effective electric constants in vegetation and in the earth. Effective relative permittivity, ϵ_r, and permeability, μ_r, in undergrowth at five dispersed sites were practically unity. The ranges of variation in all results were $0.9 < \epsilon_r < 1.2$ and $0.8 < \mu_r < 1.1$. On the average, ϵ_r was about 1.05. μ_r was about 0.98. Median effective conductivity of the undergrowth varied insignificantly between sites, but showed distinctive variation with frequency, from about $20 \pm 30\%$ at 6 MHz to $300 \pm 30\%$ ($\mu\text{mho/m}$) at 100 MHz. In the few instances where measurements were made among mature trees the results were similar to those obtained for undergrowth.</p> <p>The most important parameters influencing vegetation constants were stem spacing (related to stem number density) and intrinsic stem conductivity (estimated to be between 0.05 and 0.5 mho/m).</p> <p>Ground-constant values varied greatly between sites, in a manner consistent with the variation of soil moisture content.</p> <p>Environmental forestry and soil surveys, summarized in the appendices to this report, are useful in explaining or applying the electric-constant results.</p>			

DD FORM 1473

(PAGE 1)

57N 0101-807-6801

UNCLASSIFIED

Security Classification

UNCLASSIFIED

Security Classification

14 KEY WORDS	LINK A		LINK B		LINK C	
	ROLE	WT	ROLE	WT	ROLE	WT
Vegetation electric constants Electric ground constants Conductivity Attenuation by foliage Dielectric permittivity Magnetic permeability Thailand jungle: forest growth parameters tree nearest neighbor distances tree height distributions tree diameter distributions soil characteristics Thailand SEACORE						